Downloaded from https://www.lyellcollection.org by Imperial College of Science, Technology and Medicine on Mar 27, 2026

JGS
Journal of the Geological Society

Review article

https://doi.org/10.1144/jgs2025-099 | Vol. 183 | 2026 | jgs2025-099

A review of multi-scale sedimentological heterogeneities in the Ormskirk Sandstone Formation of the East Irish Sea Basin and their impact on the injection and migration of CO_2

Daniel Breeze[1]*, Nicola Scarselli[1], Gary J. Hampson[2] and Domenico Chiarella[1,3]

[1] Clastic Sedimentological Investigation (CSI), Department of Earth Sciences, Royal Holloway, University of London, Egham, Surrey TW20 0EX, UK
[2] Department of Earth Science and Engineering, Imperial College, London SW7 2AZ, UK
[3] Biological, Geological and Environmental Sciences Department, Alma Mater Studiorum University of Bologna, Bologna, Italy

DB, 0009-0004-1489-3177; NS, 0000-0002-6477-6866; GJH, 0000-0003-2047-8469; DC, 0000-0003-2482-0081
* Correspondence: daniel.breeze.2014@live.rhul.ac.uk

Abstract: Heterogeneities in siliciclastic sedimentary rocks manifest as variations in physical properties, composition and fabric. Depositional environments control primary heterogeneity, with transport mechanisms and sequence stratigraphic context also playing key roles. Secondary (diagenetic) heterogeneity develops post-deposition via compaction, dissolution and cementation. Understanding how these heterogeneities influence CO_2 injection and migration within siliciclastic reservoirs is essential for carbon capture and storage (CCS) planning. The Ormskirk Sandstone Formation (OSF), the target reservoir for the HyNet North West CCS project, contains depositional, diagenetic and structural heterogeneities. This paper presents a comprehensive review of these features, focusing on heterogeneities of depositional and diagenetic origin; structural heterogeneities are acknowledged but lie beyond the scope of this review. Heterogeneities in the OSF occur at multiple scales. At the smallest scale, diagenetic processes such as cementation, compaction and grain coatings alter reservoir quality and contribute to heterogeneity at the pore and facies scale. At the facies scale, depositional fabrics such as laminae and cross-stratification, along with the spatial arrangement of depositional elements, reflect shifting palaeoenvironmental conditions and sedimentological processes. These controls give rise to complex architectures, including porous, highly permeable aeolian sandsheets interbedded with heterolithic and often cemented interdune facies associations, and multilateral, stacked fluvial channel deposits. At the reservoir-zone and reservoir scales, the stacking and lateral interfingering of architectural elements, such as bars, channels, dune sets and overbank deposits, generates stratigraphic heterogeneity that governs CO_2 plume geometry, flow pathways and storage efficiency.

Received 1 May 2025; **revised** 10 November 2025; **accepted** 11 December 2025

Elevated atmospheric levels of CO_2 due to anthropogenic activity have resulted in growing instability in the Earth's climate and biosphere systems (Rockström *et al.* 2023). To mitigate rising CO_2 atmospheric concentrations, many countries have recognized the urgent need to reduce the carbon intensity of their economies. One proposed strategy is carbon capture and storage (CCS), whereby CO_2 emissions are captured and permanently sequestered within geological formations, either in subsurface saline aquifers (Ringrose *et al.* 2021) or in depleted hydrocarbon reservoirs (Hannis *et al.* 2017). The HyNet North West project (HNNWp), situated in the Liverpool Bay area of the East Irish Sea Basin (EISB) (Fig. 1), is one such initiative (BEIS 2020). This decarbonization project is targeting three offshore depleted hydrocarbon reservoirs for CO_2 storage: the Hamilton, Hamilton North and Lennox fields (English *et al.* 2024), operated by ENI at the time of writing (ENI UK Limited 2024).

The Ormskirk Sandstone Formation (OSF), part of the Sherwood Sandstone Group (SSG), is the targeted reservoir for the long-term storage of CO_2 within these Liverpool Bay fields. A wide range of depositional and diagenetic heterogeneities has been documented in the aeolian, heterolithic and fluvial sandstones of the OSF (Meadows and Beach 1993*a*; Herries and Cowan 1997; Cowan *et al.* 1999; Yaliz and Chapman 2003; Yaliz and Taylor 2003; Meadows 2006; Bunce 2018; Scorgie *et al.* 2021; Chedburn *et al.* 2022). The objective of this review is to synthesize previous work on the characterization and quantification of depositional and diagenetic heterogeneities to better understand their impact on CO_2 migration and long-term storage performance. Sedimentological heterogeneities occur across multiple scales, from the pore scale of cements and grain contacts to the facies scale of laminae and bedding planes, reservoir-zone scale of stacked architectural elements in fluvial channel belts, and reservoir scale of intercalated fluvial, aeolian and sabkha deposits (Fig. 2) (Morrow 1971; Lasseter *et al.* 1986; Miall 1988; Jordan and Pryor 1992; Medici *et al.* 2019*b*; Yeste *et al.* 2020; Chiarella *et al.* 2025).

Outcrop studies, alongside petrographic, petrophysical and geophysical data, are widely represented in the literature relating to the OSF (Burley 1987; Jones and Ambrose 1994; Meadows 2006; Scorgie *et al.* 2021; Chedburn *et al.* 2022). Many of these data have historically been used to model and characterize the Liverpool Bay reservoirs for hydrocarbon production (Colter and Ebbern 1978; Meadows and Beach 1993*a*; Stuart 1993; Yaliz and Chapman 2003; Yaliz and Taylor 2003). The insights gained from these studies can now be applied to better understand reservoir properties and heterogeneities when modelling the migration of injected CO_2 into depleted hydrocarbon sandstone reservoirs for long-term storage (Williams *et al.* 2013; Newell and Shariatipour 2016; Onoja and Shariatipour 2018; Medici *et al.* 2019*a*; Onoja *et al.* 2019; Jackson *et al.* 2022; Alshakri *et al.* 2023). Although structural heterogeneities, such as fracture networks and reservoir-bounding fault systems, are recognized in the OSF (Coward 1995; Needham and Morgan 1997; Bunce 2018; Williams *et al.* 2018; Chedburn

© 2026 The Author(s). This is an Open Access article distributed under the terms of the Creative Commons Attribution License (http://creativecommons.org/licenses/by/4.0/). Published by The Geological Society of London. Publishing disclaimer: https://www.lyellcollection.org/publishing-hub/publishing-ethics

Downloaded from https://www.lyellcollection.org by Imperial College of Science, Technology and Medicine on Mar 27, 2026

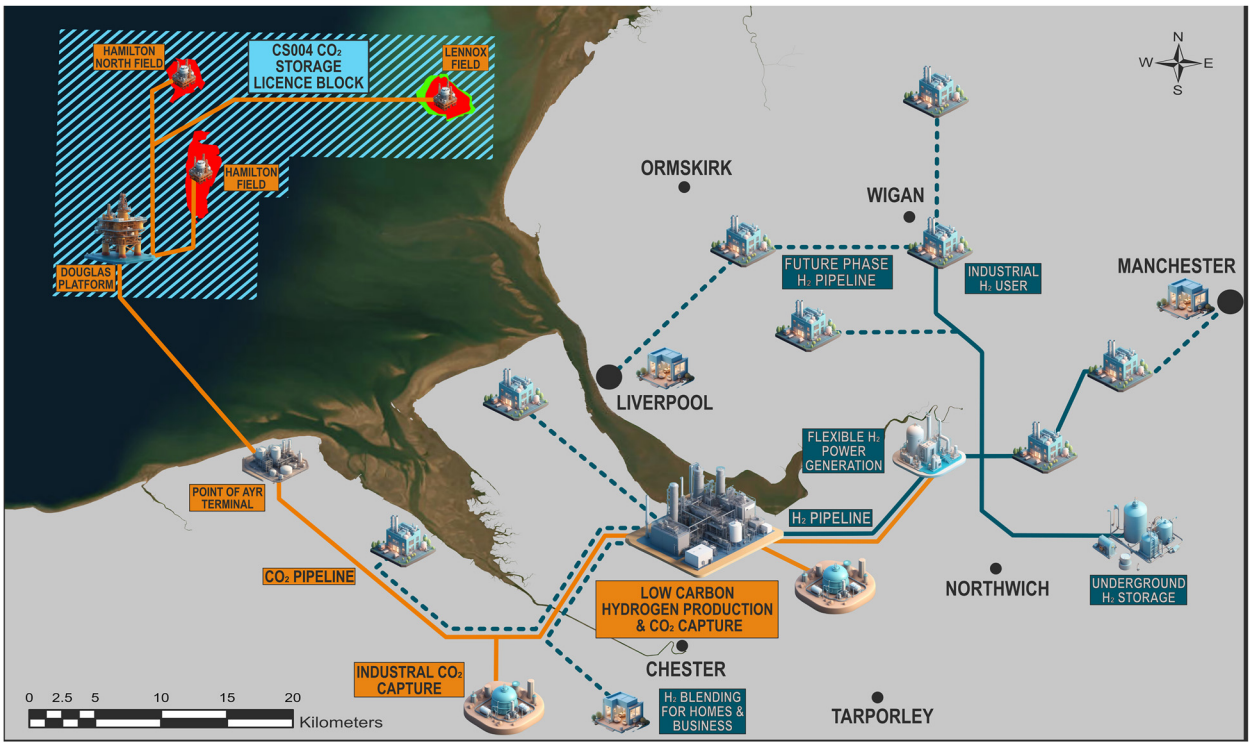


Fig. 1. Schematic diagram of the HyNet North West project, showing current (solid lines) and planned (dashed lines) infrastructure, including the location of the CO_2 storage licence block (light blue polygon) in Liverpool Bay and the three carbon capture and storage target reservoirs in the Hamilton, Hamilton North and Lennox fields. Source: basemap and reference data: Esri, Maxar, Earthstar Geographics, Esri UK, Garmin, FAO, NOAA, USGS, © OpenStreetMap contributors, and the GIS User Community. Contains information from the North Sea Transition Authority © Crown copyright 2025. Licensed under the NSTA Open User Licence (equivalent to the UK Open Government Licence v3.0).

et al. 2022), this review focuses exclusively on diagenetic and depositional heterogeneities, as they represent the primary controls on fluid flow and storage performance within the target reservoirs.

Nomenclature and stratigraphy

The SSG is a term first introduced in the literature in a Geological Society of London Special Report (Warrington *et al.* 1980), in which a lithostratigraphic framework was favoured, as chronostratigraphic correlation and subdivision of the SSG was limited by a paucity of diagnostic marker fossils (Ambrose *et al.* 2014). Magnetostratigraphy has been used in an attempt to circumvent this issue (Fig. 3) (Mange *et al.* 1999; Hounslow and Muttoni 2010).

The British Geological Survey's (BGS) comprehensive lithostratigraphic review of the UK SSG (Ambrose *et al.* 2014) recommended that the term Ormskirk Sandstone Formation be replaced by the Helsby Sandstone Formation (HSF). The new HSF also encompasses several other formations, including the Otter Sandstone in the Wessex Basin and the Kirklinton Sandstone in the Carlisle Basin (Fig. 4a). The HSF takes its name from the SSG succession in the Cheshire Basin, and the three members there, Frodsham, Delamere and Thurstaston (Fig. 3) (Thompson 1970), are correlatable with the SSG succession in the EISB (Colter and Ebbern 1978; Jackson *et al.* 1986). The term OSF has been used in this review, as it remains nomenclature employed by the HNNWp and operators in reference to the target reservoirs, although studies covering relevant parts of the HSF are also considered.

Economic resource

The Lower to Middle Triassic SSG is one of the UK's most widespread sandstone reservoir rocks, subcropping offshore in the East Irish Sea, North Sea and Wessex basins and outcropping across the UK (Fig. 4a) (Ambrose *et al.* 2014; English *et al.* 2024). Forming the bedrock of many northern cities, including Manchester and Liverpool (Medici *et al.* 2019*a*), the SSG is considered a primary target for CCS projects across the UK (English *et al.* 2024).

The EISB's OSF is the lateral equivalent of the North Sea gas-producing Bunter Sandstone (Barnes *et al.* 1994; Wakefield *et al.* 2015), a formation also currently targeted for CCS (Quirk *et al.* 2022; Hollinsworth *et al.* 2024). Much of the understanding of the nature of the OSF in the offshore EISB derives from studies commissioned by the oil and gas industry (Stuart 1993; Cowan *et al.* 1999; Yaliz and Chapman 2003; Yaliz and Taylor 2003).

In 1974 South Morecambe Field became the first commercial natural gas discovery of the EISB (Colter and Ebbern 1978). Ultimate hydrocarbon recovery from the now mature EISB is an estimated 209 million barrels of oil equivalent (boe) and 8.3 trillion cubic feet (tcf) of gas, with the majority of production from the OSF (Gray 2013).

Hamilton Field, discovered in 1990 (English *et al.* 2024), has a top reservoir at approximately 690 m true vertical depth subsea (TVDSS), a gas–water contact (GWC) at 887 m TVDSS, and a gas initially in place (GIIP) of approximately 680 billion cubic feet (BCF). First gas was produced in February 1997 with a reported reservoir temperature of 30°C, and an initial reservoir pressure of 96.3 bar (Yaliz and Taylor 2003), dropping to 9.4–10.3 bar (Chedburn *et al.* 2022) as the field nears the end of hydrocarbon production, in preparation for imminent repurposing for CO_2 storage in Q4 2027 (OPRED 2025).

Hamilton North Field, discovered in 1991 (English *et al.* 2024), has a top reservoir at approximately 717 m TVDSS, a GWC at 887 m TVDSS and a GIIP of approximately 2300 BCF. Significant gas shows were recorded in the Andsell Mudstone Member seal (Seedhouse and Racey 1997), where pressure communication with the underlying OSF was detected.

Downloaded from https://www.lyellcollection.org by Imperial College of Science, Technology and Medicine on Mar 27, 2026

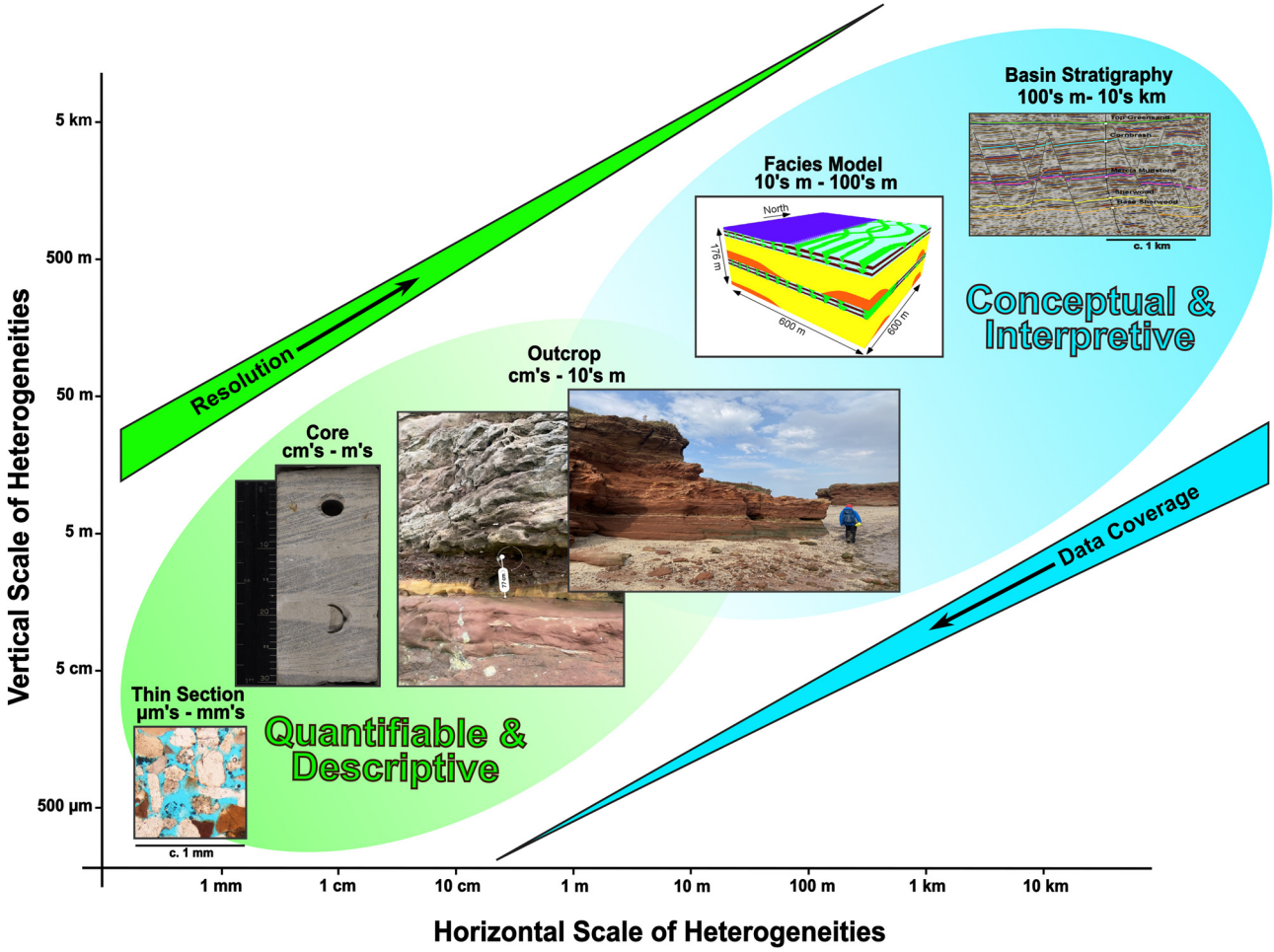


Fig. 2. Heterogeneities range from the microscopic pore scale of cements and pore throats, through lamination, cross-stratification, clay drapes, channel lags and stacked channel belts, up to the reservoir scale of basin-bounding faults and basin-wide marker horizons. Different data sources, at varying resolutions and with a range of data coverage, offer opportunities to quantify, interpret and model heterogeneities within a reservoir. High-resolution datasets enable quantifiable descriptions, whereas those with broader coverage require a more conceptual interpretive approach. A holistic methodology encompassing the wide range of scales covered is recommended in order to appropriately represent and model these heterogeneities. Images (left to right): pore-scale photomicrograph of aeolian sandstone from Hamilton North Field (well 110/13-5); core image of fluvial sandstone from Lennox Field (well 110/15-7); outcrop photographs from Little Hilbre and Hilbre Island (EISB); facies model image from Alshakri *et al.* (2023); and seismic image showing the Sherwood Sandstone Group (SSG) stratigraphy, Wytch Farm oilfield, Wessex Basin.

Lennox Field, discovered in 1992 (English *et al.* 2024), comprises three reservoir zones F1–F3, with F1 (wet gas) corresponding to the top reservoir at approximately 800 m TVDSS. Initial conditions indicate a pressure of 97 bar and a temperature of 31.6°C (Facchi *et al.* 2021). Lower units include F2 (106 bar, 29.4°C) and F3 (light oil with gas cap, 112 bar, 34.4°C), with the oil–water contact (OWC) at 970 m TVDSS, and a stock tank oil initial in place (STOIIP) of approximately 248 million barrels (MMbbl). The field is now significantly depleted, with abandonment pressure forecast at 5–10 bar, in preparation for CO_2 storage (BEIS 2020).

Geological setting

Tectonics and palaeogeography

The EISB is the largest, by area, in a string of NW–SE-oriented basins along the west coast of Britain, which includes the North Channel Basin, Solway Firth, East Irish Sea and Cheshire basins (Fig. 4a) (Jackson and Mulholland 1993; McKie and Williams 2009). The EISB overlies a region that acted as a locus for sediment accumulation since the Cambrian, with successive depocentres forming on the margins of the Iapetus Ocean throughout the Paleozoic (Jackson 1995; Woodcock 2012*a*). The NE–SW structural grain, imparted by Caledonian accretion and orogenic deformation (Woodcock 2012*b*; Pharaoh *et al.* 2018), was reactivated during the Mississippian, when NNW–SSE extension along NE–SW-trending faults generated subsiding half-graben that controlled sediment accommodation and depositional patterns (Jackson 1995; Williams *et al.* 2018). This period saw continuous marine to paralic deposition (Jackson *et al.* 1997; Davies *et al.* 2012), with deep-water Namurian shales forming the primary source rock for EISB hydrocarbon plays (see 'Economic resource' above) (Armstrong *et al.* 1997). The final phase of the Variscan orogeny, expressed as NNW–SSE-trending folds and thrusts (Warr 2012), imparted structural weaknesses that were reactivated during Mesozoic extensional episodes, forming the principal synsedimentary bounding faults of the EISB (Pharaoh *et al.* 2018).

Post-orogenic collapse gave way to a significant rifting phase (Hounslow *et al.* 2012). Extension across this string of basins peaked in the central EISB, with a maximum stretching factor (β_{max}) of 1.44 (Rowley and White 1998). During this period the EISB accumulated up to 5 km of infill comprising SSG sandstones and Mercia Mudstone Group (MMG) mudstones and evaporites (Pharaoh *et al.* 2018). Extensional tectonics are considered to

Downloaded from https://www.lyellcollection.org by Imperial College of Science, Technology and Medicine on Mar 27, 2026

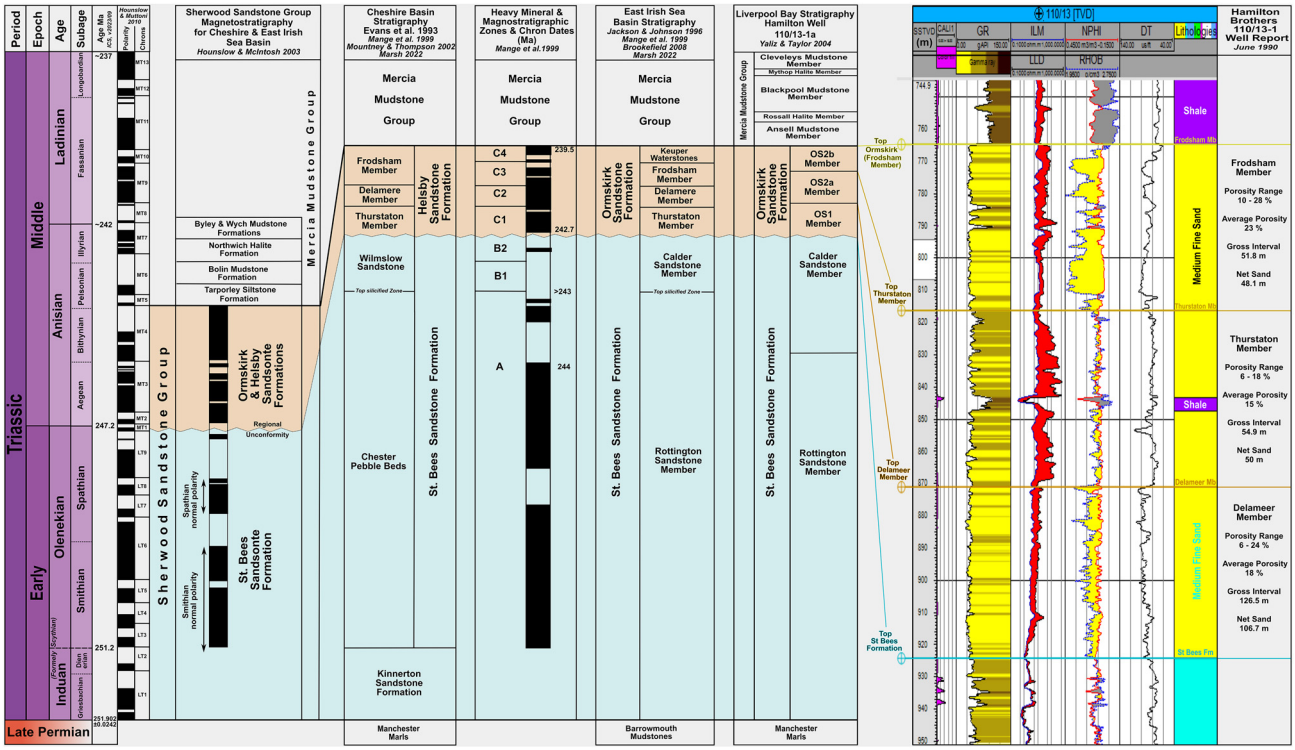


Fig. 3. Chronostratigraphic chart showing the Sherwood Sandstone Group (SSG) of the Cheshire and East Irish Sea basins. Due to the paucity of diagnostic marker fossils, workers have used magnetostratigraphy to define the stratigraphy of the St. Bees (blue zone) and Ormskirk Sandstone (OSF) (orange zone) formations. There is a clear discrepancy between the Mange *et al.* (1999) and Hounslow and McIntosh (2003) interpretations, with the former placing the base of the OSF at 242.7 Ma and the latter placing it at 247.2 Ma. Coupled with the stratigraphic chart is a set of wireline logs from the Hamilton Field discovery well (110/13-1a; Fig. 4), showing some of the log characteristics of the three OSF members.

have played a key role in the preferential preservation of aeolian deposits in the EISB (Herries and Cowan 1997). In contrast, aeolian deposits are entirely absent on the Eastern England Shelf Basin (Fig. 4a), where rates of tectonic subsidence were significantly lower (Wakefield *et al.* 2015).

At this time, Britain lay at a palaeolatitude of approximately 20° north of the equator, positioned within the supercontinent Pangaea (Fig. 5) (Ziegler 1990). Rifting that would ultimately lead to the opening of the Atlantic began with the development of a complex series of extensional basins separated by basement massifs and intra-basinal highs (Hounslow *et al.* 2012; Ambrose *et al.* 2014). Denudation of the Armorican Massif, situated in present-day northwestern France, contributed as a primary sediment source to the EISB (McKie and Williams 2009; Burgess *et al.* 2025). Fluvial transport carried sediment northwards via the Budleighensis river system (Wills 1955; Audley-Charles 1970). Provenance studies of SSG heavy mineral assemblages suggest that this fluvial system also drained more distant regions, including the French Massif Central and the Pyrenees (Fig. 5) (Morton *et al.* 2013). Additional sediment contributions came from more proximal UK topographic highs, such as the London–Brabant, Welsh massifs and the Pennine High (Medici *et al.* 2015; Wakefield *et al.* 2015; Burgess *et al.* 2025). Deposition of the SSG occurred in a series of interlinked basins, intermittently connected through fluvial processes, from the Wessex Basin to the East Irish Sea, Solway, Carlisle and Peel basins (Fig. 4a) (Ambrose *et al.* 2014).

Palaeoenvironment

The Lower Triassic (Induan–Olenekian) marks a transition in the EISB rock record from Upper Permian shallow-marine carbonate sedimentation (i.e. Kazanian–Tatarian, Zechstein Group), recorded in subsurface boreholes, to the continental red beds of the SSG, specifically the St Bees Sandstone Formation (Fig. 3) (Ambrose *et al.* 2014; Wakefield *et al.* 2015). The SSG was deposited in an arid to hyperarid continental setting (Brookfield 2008; Wakefield *et al.* 2015), although some authors suggest that the climate as having ranged from arid to semi-arid (Medici *et al.* 2015) or predominantly semi-arid (Yaliz and Taylor 2003).

Palaeoclimate models suggest a global surface temperature of 17.3°C, approximately 4°C higher than present-day (Peron *et al.* 2005), with these conditions continuing unabated for approximately 14 Myr throughout the Early and Middle Triassic (Fig. 3), a period of climatic stability largely due to Britain remaining entirely within the 15°–35° latitudinal desert belt (Fig. 5) (Ziegler 1990; Brookfield 2008). Deposition of the SSG occurred within interlinked, largely endorheic rift basins, infilled by dryland fluvial systems and terminating in playa lakes, sabkhas and aeolian dunes (McKie and Williams 2009). The Solway, Carlisle and Peel basins are considered terminal sites for this system (Figs 4a, 6) (Marsh *et al.* 2022).

In the Cheshire Basin the onset of the Late Triassic (Carnian) is marked by the Tarporley Siltstone Formation at the base of the MMG, where it has been interpreted as tidally influenced (Newell 2024). However, this formation is not present further north in the EISB, where the MMG is dominated by sabkha and ephemeral lake deposits, with no clear sedimentological evidence of open marine conditions (Seedhouse and Racey 1997; Scorgie *et al.* 2021). However, sulfur isotope data from early-stage evaporitic gypsum and anhydrite nodules in the OSF and lower MMG indicate $\delta^{34}S$ values consistent with Triassic marine sulfate, suggesting at the very least limited marine influence during early diagenesis (see 'Early-stage diagenetic heterogeneities' section below) (Greenwood and Habesch 1997).

Downloaded from https://www.lyellcollection.org by Imperial College of Science, Technology and Medicine on Mar 27, 2026

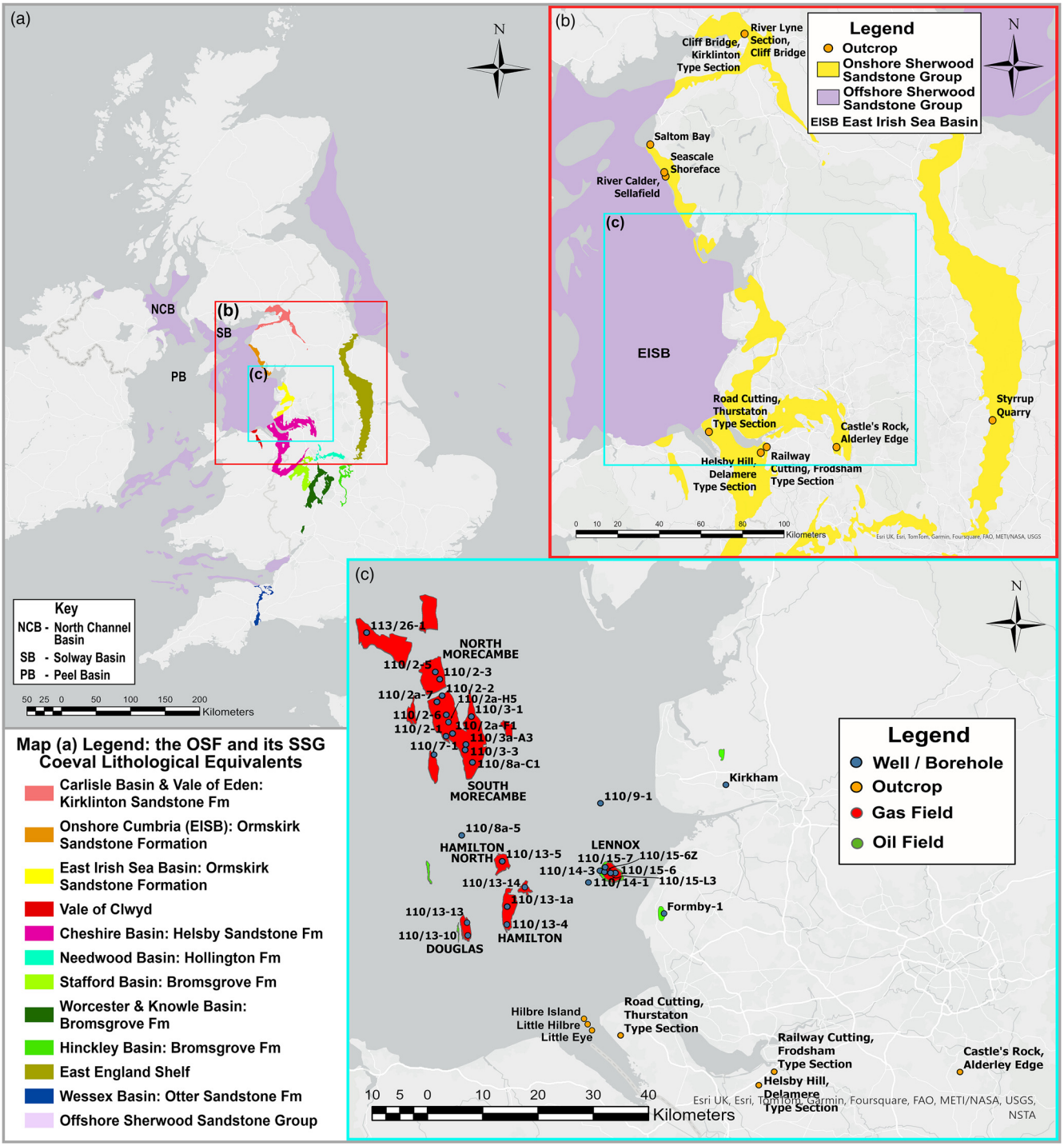


Fig. 4. (**a**) Onshore outcrops and offshore subcrops of the Sherwood Sandstone Group (SSG), showing distinct basins and their associated formation names prior to the 2014 British Geological Society review. All basins with a formation name listed in the map (a) legend now fall under the term Helsby Sandstone Formation, which includes the Ormskirk Sandstone Formation (OSF) in onshore Cumbria and both onshore and offshore areas of the East Irish Sea Basin (EISB). (**b**) Map showing the location of the onshore data points referenced in this paper. (**c**) Map of the EISB and Liverpool Bay area showing offshore wells, and onshore boreholes and outcrops cited in this paper in relation to the three HNNWp target reservoirs. Based on British Geological Survey data © UKRI 2024. All rights reserved. BGS Permit Number CP24/012. Source: basemap: Esri UK, Esri, TomTom, Garmin, FAO, NOAA and USGS.

Ormskirk Sandstone Formation

The SSG shows a clear geographical trend in depositional style across the UK, with fluvial-dominated successions in more proximal basins transitioning to more aeolian-influenced deposits in distal settings (Brookfield 2008; McKie and Williams 2009; Medici *et al.* 2019*a*). In the distal EISB, the OSF represents a mixed fluvial and aeolian system deposited under arid conditions with cyclical wetting and drying (Meadows 2006), and reflects the reduced fluvial discharge (McKie and Williams 2009). Recent outcrop-constrained provenance modelling highlights the complex, multi-source nature of sediment supply to the SSG (Burgess *et al.* 2025).

The base of the SSG in NW England corresponds to the base of the Triassic and often includes alluvial fan and debris flow conglomerates, which transition upwards into fluvially derived sandstones (English *et al.* 2024). In this region, the SSG is traditionally divided into three formations: St Bees, Calder and Ormskirk (Ambrose *et al.* 2014). However, offshore in the EISB, the Calder is classified as a member

Downloaded from https://www.lyellcollection.org by Imperial College of Science, Technology and Medicine on Mar 27, 2026

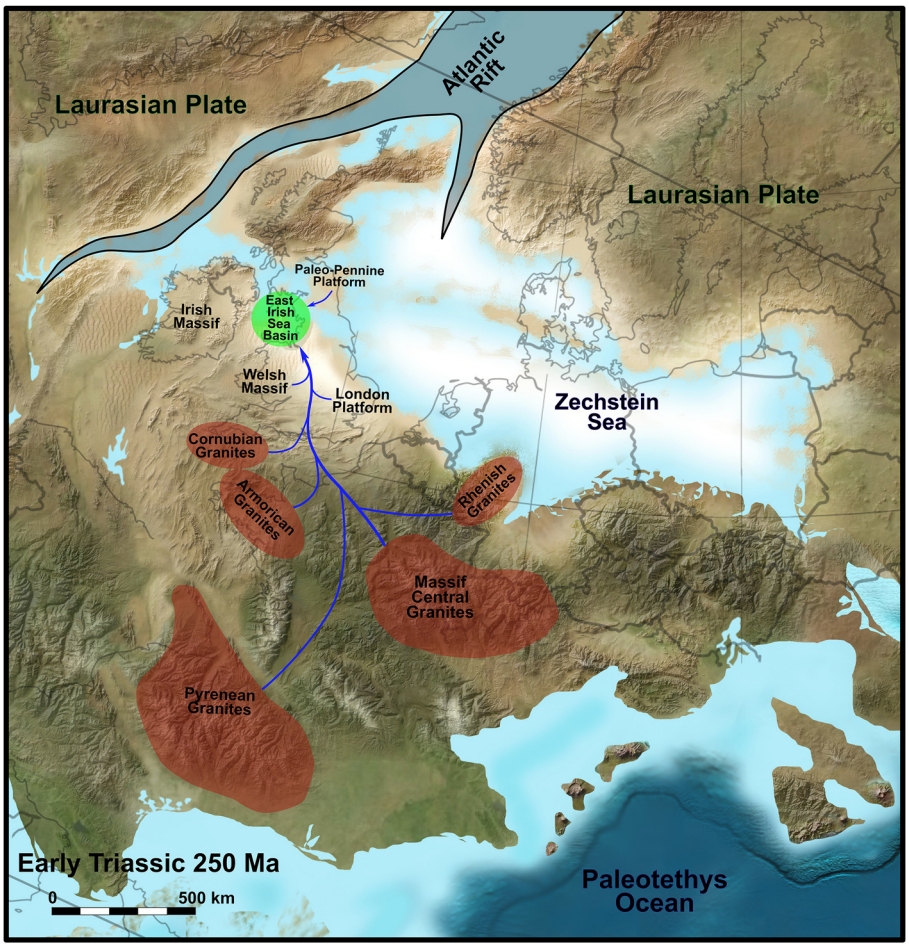


Fig. 5. Palaeogeographical reconstruction of the Budleighensis fluvial system during the Early Triassic (~250 Ma). At this time, Britain lay at a palaeolatitude of ~20° N, forming part of the supercontinent Pangaea. Although climatic conditions were arid, this fluvial system is interpreted to have had a sufficiently large catchment to have been perennial in nature. It drained into the East Irish Sea Basin (EISB) via the Cheshire Basin to the SE. According to heavy mineral provenance data (Morton *et al.* 2013), the system was sourced proximally by the Cornubian and Welsh massifs as well as the London Platform, and more distally by runoff from the Armorican Massif, the Massif Central, the Rhenish Massif and the Pyrenees. Additional input into the EISB also included material from the Palaeo-Pennine Platform to the NW (Burgess *et al.* 2025). Source: basemap used with permission from Deep Time Maps™.

within the St Bees Sandstone Formation (Jackson *et al.* 1997). The three formations are at their thinnest (1130–1270 m) at the eastern basin margin in the Sellafield area (Jones and Ambrose 1994), and thicken into the basin centre, where seismic data indicate a thickness of over 2000 m offshore (Jackson 1995).

The disconformity at the base of the OSF, dated at latest Anisian (242.7 Ma) by Mange *et al.* (1999) and earliest Anisian by Hounslow and McIntosh (2003) (Fig. 3), has been correlated with the Hardegsen disconformity of Northern Europe (Jackson 1995). However, its barely perceptible nature in the EISB (Meadows and Beach 1993*b*) suggests that the St Bees and Ormskirk formations comprise a relatively complete succession of Smithian to Anisian strata, consistent with magnetostratigraphic data (Fig. 3) (Hounslow and McIntosh 2003). In Liverpool Bay the base of the OSF is represented in geophysical logs by an increase in sonic velocity (typically representing increasing porosity) and a decrease in gamma radiation (representing a smaller proportion of K-bearing minerals) relative to the underlying Calder Sandstone Member (Fig. 3) (Jones and Ambrose 1994).

In the EISB the OSF has been subdivided into three units, OS1, OS2a and OS2b (Jackson *et al.* 1997), which are broadly equivalent to the Thurstaston, Delamere and Frodsham members of the Cheshire Basin, although notable differences in facies, thickness and stratigraphic completeness exist (Figs 3, 4) (Yaliz and Chapman 2003; Yaliz and Taylor 2003; Meadows 2006). Average thickness of these three units is 250 m (Bunce 2018; Williams *et al.* 2018). The shallower OS2a and OS2b units are dominated by perennial fluvial channels, lacustrine and minor aeolian deposits, while the deeper OS1 consists of thick wavy-bedded sabkha deposits interbedded with minor aeolian and fluvial deposits, arranged in drying-upward cycles (Herries and Cowan 1997). Morlet wavelet analysis of petrophysical data from well 110/8a-5 (Fig. 4c) shows broad agreement between the cyclicity observed in the drying-upward cycles and the Milankovitch cycles of 21, 41 and 100 kyr periodicity (Rivera *et al.* 2004).

QFL (quartz–feldspar–lithic fragments) point count analysis in Formby Field, at the eastern margin of the EISB, shows the OSF to be composed of predominantly sublithic or quartz arenites. Compositionally the grains comprise quartz, with minor amounts of K-feldspar and plagioclase, along with lithic fragments and dolomite lithic grains (Scorgie *et al.* 2021). An analysis of detrital mineralogy and bulk chemical composition of the OSF, using data from wells 110/2-6, 110/8a-5, 110/13-5 and 110/14-3 (Fig. 4c), identified two distinct sources of clastic material entering the EISB: metamorphosed Carboniferous material from the Variscan Armorican Massif to the south, and a distinct, feldspar-rich easterly source derived from a palaeo-Pennine escarpment (Fig. 6) (Meadows 2006).

Overlying the OSF, the MMG is composed of alternating red mudstones and halite, representing repeated evaporitic cycles, and reaches a maximum thickness of 3.2 km in the Keys Sub-Basin (Milroy *et al.* 2019). The OSF–MMG contact is diachronous, with halite–mudstone couplets becoming more laterally extensive but less numerous towards the south of the basin due to the progressive expansion of evaporitic conditions, which results in differing reservoir–seal pairings throughout the basin (Chedburn *et al.* 2022). In Liverpool Bay the Ansdell Mudstone Member of the Leyland Mudstone Formation overlies the OSF (Jackson *et al.* 1997).

Heterogeneities

Sedimentological heterogeneities in sandstones consist of variations in physical properties, composition and fabric, and can occur at multiple scales: from pore-scale variations (e.g. cements and grain contacts); through facies-scale features (e.g. bedding structures); to

Downloaded from https://www.lyellcollection.org by Imperial College of Science, Technology and Medicine on Mar 27, 2026

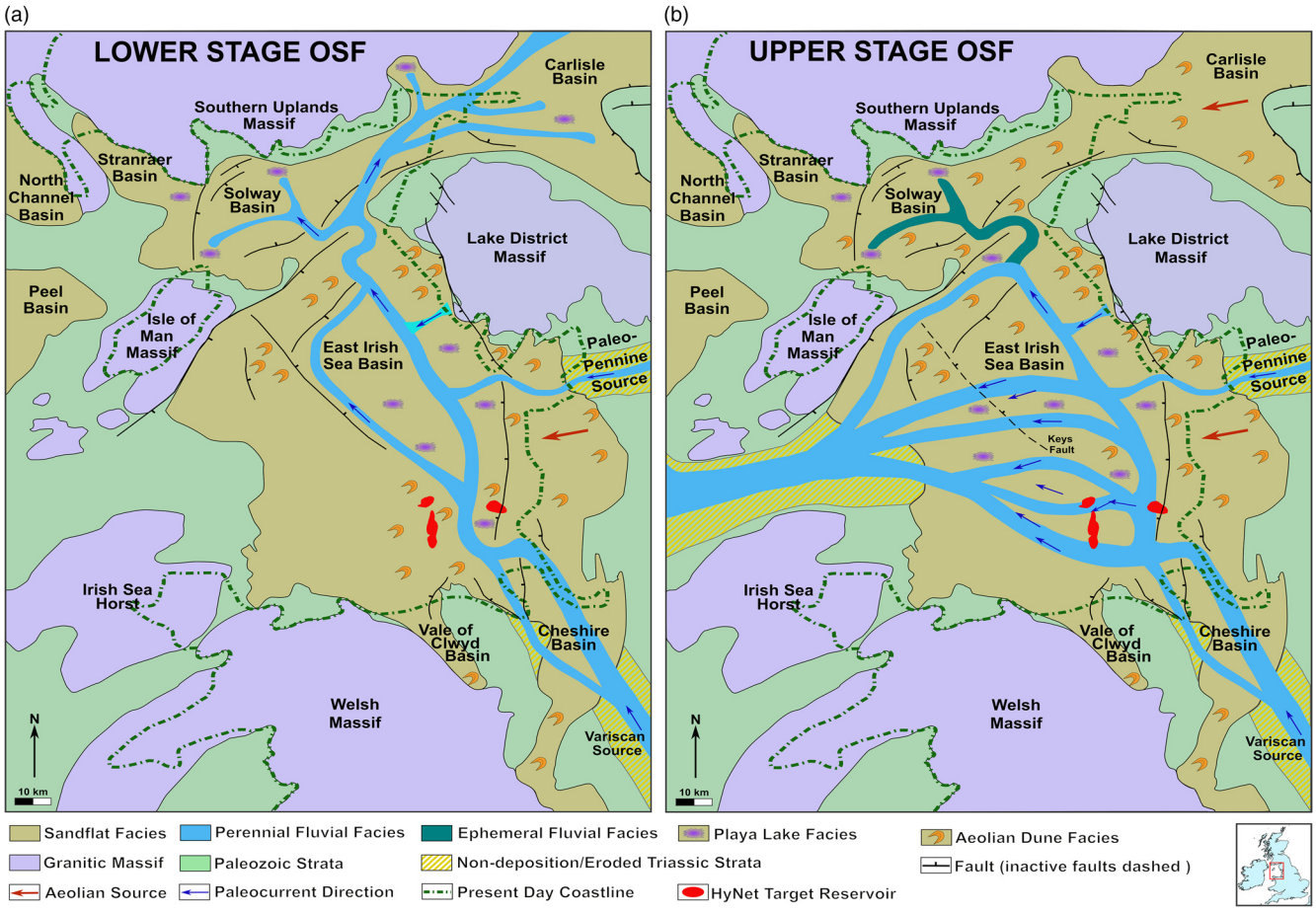


Fig. 6. Schematic palaeogeographical reconstructions for the East Irish Sea Basin (EISB) showing deposition of the Ormskirk Sandstone Formation (OSF), a mixed fluvial and aeolian system. This model places the Solway and Carlisle basins as the terminus of the endorheic Budleighensis fluvial system during the early stages of OSF deposition (**a**), as these two basins contain a higher proportion of mudstones compared to the EISB during the same interval. During later deposition of the OSF (**b**), a structural rotation (Cowan 1993) diverted the fluvial system westwards towards the Peel Basin. An abrupt change in facies from fluvial to aeolian in the Solway and Carlisle basins, coupled with palaeocurrent indicators from multiple wells in the EISB, provides evidence for this change. Movement on the Keys Fault (dashed in the right panel) is interpreted to have ceased during this interval. Source: modified from Marsh *et al.* (2022); and after Cowan (1993), Meadows and Beach (1993*b*), Herries and Cowan (1997), Bunce (2018) and Pharaoh *et al.* (2018).

reservoir-zone-scale architecture (e.g. stacked fluvial channel elements), reservoir-scale heterogeneities (e.g. intercalated fluvial, aeolian and heterolithic deposits); and up to basin-scale variability (e.g. transitions from marginal aeolian systems to more fluvially dominated basin-centre successions) (Weber 1982, 1986; Bloomfield *et al.* 2006; Morad *et al.* 2010; Alshakri *et al.* 2023).

Such heterogeneities are typically classified as primary depositional, arising from variations in sediment supply, transport mechanisms and depositional environments (Miall 1988), or as secondary diagenetic, which develop during post-depositional processes such as burial-related compaction, cementation and dissolution (Morad *et al.* 2000, 2010; Huggett 2005). Understanding these two types of heterogeneities is crucial for predicting fluid flow in subsurface siliciclastic reservoirs (Weber 1986).

This synthesis of heterogeneities documented in the OSF will first address pore-scale diagenetic heterogeneities, and as scale increases, will progress to larger-scale depositional heterogeneities observable in core and outcrop, and beyond (Fig. 2).

Diagenetic heterogeneities

Heterogeneities at the pore scale can exert a strong control on reservoir quality and often influence the distribution of porosity and permeability (Morad *et al.* 2010). Diagenesis is considered one of the primary controls on reservoir heterogeneity and quality (Morad *et al.* 2010; Griffiths *et al.* 2019; Li *et al.* 2020; Yeste *et al.* 2020).

Diagenetic processes are recognized to occur in three distinct phases:

(1) Early-stage diagenesis (eodiagenesis) refers to the interaction between porewater and detrital grain assemblages within the depositional system prior to burial (Worden and Burley 2003).
(2) Burial diagenesis (mesodiagenesis) results from mechanical and chemical compaction at depth, often destroying primary porosity and promoting cement growth (Schmidt and McDonald 1979).
(3) Uplift diagenesis (telodiagenesis) involves interaction with meteoric groundwater and may create secondary porosity or restore primary porosity (Fairbridge 1966; Schmidt and McDonald 1979). Of little significance in shales and mudstones, uplift diagenesis can play an important role in restoring reservoir quality to sandstones (Huggett 2005).

The diagenetic evolution of the OSF is summarized in Figure 7, which integrates mineral assemblages, burial history and temperature evolution through time to illustrate the multistage nature of diagenesis in the basin-centre succession.

Clay minerals in the OSF are depositionally uncommon but can be abundant locally due to diagenetic processes, resulting in significant spatial variation in abundance and origin. In the basin-margin Formby Field (Fig. 4c), where burial depths were shallow, clays have been interpreted to be of detrital origin (Scorgie *et al.*

Downloaded from https://www.lyellcollection.org by Imperial College of Science, Technology and Medicine on Mar 27, 2026

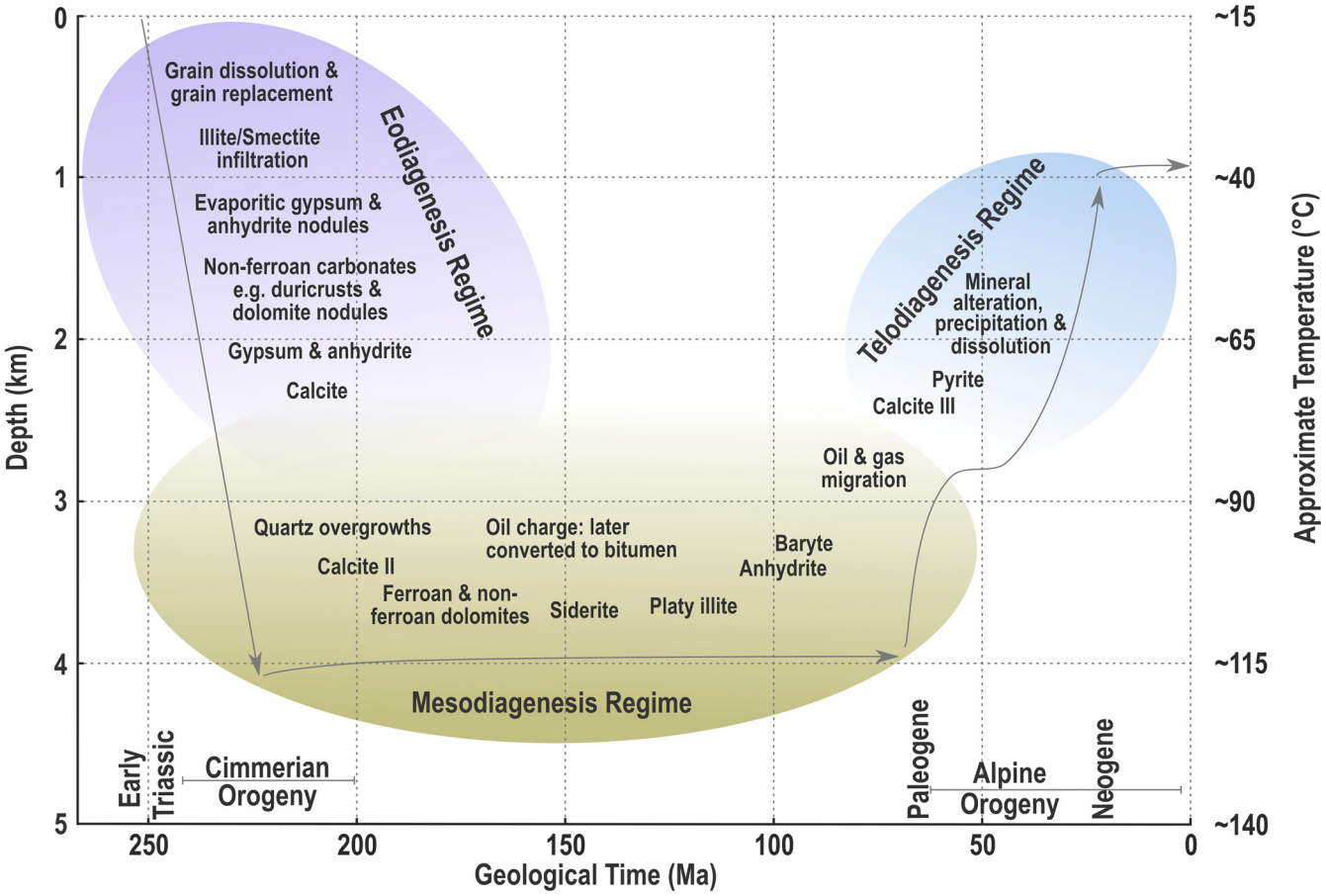


Fig. 7. Schematic diagenetic sequence for the EISB basin-centre Ormskirk Sandstone Formation (OSF), illustrating the mineral assemblages associated with the early (eodiagenetic), burial (mesodiagenetic) and uplift (telodiagenetic) regimes. The approximate burial curve shows burial to ~4 km, followed by minor uplift related to the Cimmerian Orogeny and later pulses of uplift linked to Alpine deformation throughout the Paleogene and Neogene, bringing the formation to its present depth of ~1 km. Eodiagenesis was characterized by grain dissolution, clay infiltration, and the precipitation of evaporitic gypsum and anhydrite nodules, non-ferroan carbonate and dolomite nodules, and calcite cement. Mesodiagenesis involved calcite II cementation nucleating around earlier caliche calcite, followed by quartz cementation, and subsequently ferroan and non-ferroan dolomite. Bitumen, recording an early phase of hydrocarbon migration, coated both detrital grains and earlier cements. Late-stage sulfate precipitation (baryte and anhydrite) predates migration of hydrocarbons presently found in the reservoirs. Telodiagenesis encompassed mineral alteration, dissolution and the precipitation of calcite III cement and pyrite during uplift and meteoric fluid ingress. The order of mineral formation shown is approximate, as several phases may have developed contemporaneously or overprinted earlier assemblages under varying pressure–temperature–fluid conditions. Source: based on data from: Knipe *et al.* (1993), Greenwood and Habesch (1997) and Worden and Burley (2003), Holford *et al.* (2005, 2009).

2021). In contrast, in basin-centre fields such as North and South Morecambe, Hamilton, Hamilton North, Lennox and Douglas (Fig. 4c), deeper burial and diagenetic fluid interactions have resulted in widespread development of diagenetic clays, particularly authigenic illite, as well as quartz overgrowths. These diagenetic features are especially prevalent in deeper reservoir sections, where they can significantly reduce reservoir quality (Bastin *et al.* 2003; Cowan and Boycott-Brown 2003; Yaliz and Chapman 2003; Yaliz and McKim 2003; Yaliz and Taylor 2003).

Early-stage diagenetic heterogeneities

Gross depositional environment plays a key role in eodiagenesis, with each environment imparting its own distinct diagenetic signature (Worden and Burley 2003). The type and availability of solutes is a major control on early diagenetic modification; the subsequent growth of cement reflects the chemical and mineralogical composition of the porewater (Curtis and Coleman 1985). According to Morad *et al.* (2000), early-stage diagenesis occurs at depths of $\lesssim$2 km and temperatures of $\lesssim$70°C (Fig. 7).

The OSF was deposited in an arid continental environment (see 'Palaeoenvironment' section) (Meadows 2006), which strongly influenced the three main diagenetic processes active during deposition: grain dissolution, grain replacement and authigenic mineral precipitation (Burley 1984). Preservation of textural changes in the OSF is best recorded in areas of shallow burial, such as basin margins in the Formby Field (Fig. 4c) (Scorgie *et al.* 2021). While sediments remained at shallow depths, partial geochemical equilibration between detrital grains and porewaters probably occurred under kinetically constrained conditions. Dissolution of unstable silicates released ions that contributed to the precipitation of early authigenic phases such as illite–smectite, K-feldspar, calcite, non-ferroan dolomite and hematite (Fig. 7) (Strong 1993; Worden and Burley 2003).

Burley (1984) conducted a study of textural changes of the OSF by logging 20 boreholes and analysing 525 samples from representative sections. Grain dissolution, preserved as relic outlines of original grains, created <4% porosity, and authigenic minerals and grains that replaced detrital grains included hematite, carbonates, clay minerals, as well as muscovite-to-kaolinite and altered biotite (Fig. 7). This process released significant quantities of potassium, iron, magnesium, calcium, sodium, aluminium and silicon into the porewaters. While these elements may have remained mobile under burial conditions, aluminium and silicon, due to their low solubility,

Downloaded from https://www.lyellcollection.org by Imperial College of Science, Technology and Medicine on Mar 27, 2026

were more probably sequestered into early-formed authigenic clay minerals such as kaolinite and smectite (Strong 1993; Worden and Burley 2003; Scorgie *et al.* 2021).

Point count analysis indicated that pore-lining authigenic clay cements comprise 1–7% of the OSF, and feldspar overgrowths 3% (Burley 1984). Although early work based on point count petrography described 'small incipient quartz overgrowths', typically <1% in volume (Burley 1984, p. 415), more recent analyses based on scanning electron microscopy (SEM) have not reported early quartz cementation in the Formby Field (Scorgie *et al.* 2021), suggesting such features may be rare, overprinted or less significant than previously thought. Authigenic carbonate cements comprise non-ferroan carbonates, with dolomite nodules frequently concentrated at the tops of fluvial units (Fig. 7) (Burley 1987). Early-stage evaporitic gypsum and anhydrite nodules at the millimetre to sub-centimetre scale have also been reported in the OSF and overlying MMG (Greenwood and Habesch 1997). While these are typically interpreted as early-stage features associated with near-surface processes, it is also possible that some carbonate precipitation continued during subsequent burial, a point further addressed in the section 'Burial diagenetic heterogeneities' below. Calcrete crusts (duricrusts) formed in response to near-surface water movement, including leaching, capillary rise, downward percolation and flow through, and may have developed either on exposed surfaces or at shallow subsurface water tables within porous and permeable sediment (Greenwood and Habesch 1997).

Clay minerals in cored and sampled material from well Formby-1 (Fig. 4c) are interpreted as depositional in origin, rather than diagenetic. This interpretation is supported by early-stage evaporitic dolomitic cementation, present in quantities of up to 11%, with calcite cements up to 10%, feldspar cements up to 3.5% and euhedral pyrite up to 1.5% (Scorgie *et al.* 2021). Minor compaction-related porosity loss is reported to have occurred in the OSF in the basin-margin Formby Field, with reservoir quality controlled by primary grain size, sorting and variable compaction, and only a small degree of influence attributed to carbonate cement and clay minerals (Scorgie *et al.* 2021).

Burial diagenetic heterogeneities

In the mesodiagenesis regime, structural and chemical factors typically control mechanical and chemical compaction, cementation and dissolution, all of which influence porosity, most commonly through its reduction, though localized dissolution may enhance and generate secondary porosity. With increasing burial, elevated pressure and temperature trigger reactions in porewater, resulting in heterogeneity derived from pressure dissolution and thermally activated cementation (Matter and Ramseyer 1985). According to Morad *et al.* (2000), shallow mesodiagenesis occurs at depths of 2–3 km and temperatures of 70–100°C, while deep mesodiagenesis occurs at depths >3 km and temperatures >100°C, extending up to the metamorphic window, which is at 200–250°C, with depth depending on geothermal gradient (Fig. 7).

On the margins of the EISB, including the Formby Field (Fig. 4c), the OSF was buried to depths <2000 m, with no evidence for mesodiagenesis reported (Scorgie *et al.* 2021). In contrast, burial history models indicated that in the basin centre the OSF reached depths of 3000–4250 m, before post-Jurassic uplift and erosion removed ~2000 m of overburden (Jackson *et al.* 1986; Burley 1987). This places the basin-centre OSF reservoirs firmly within the burial diagenesis window.

In intervals lacking early-stage cement frameworks, mechanical compaction during burial has been interpreted to have been the dominant driver of porosity loss, although the degree of reduction has not been quantified (Burley 1984, 1987). In contrast, where such frameworks were present, grain and nodule dissolution created secondary porosity, which was subsequently occluded by mesodiagenetic cements, particularly quartz overgrowths, ferroan dolomite and crystalline illite (Fig. 7) (Strong 1993; Greenwood and Habesch 1997).

Quartz cementation is strongly facies dependent, with point count analysis of 105 thin sections from five cored wells (110/13-13, 110/13-14, 110/14-1, 110/15-6Z and 110/15-7, Fig. 4c) indicating mean quartz cement abundances of up to 5.5% in fluvial facies, ~1.9% in sheetflood and ~1.5% in aeolian facies (Greenwood and Habesch 1997). A different study using a broader sample set reported similar trends, with modal quartz cement content of 8–12% in fluvial facies and <4% in sheetflood and aeolian deposits (Meadows and Beach 1993*a*). This disparity has been attributed to differences in grain morphology: fluvial sandstones contain angular to sub-angular low-sphericity grains, which present more surface area and nucleation sites for quartz overgrowths; by contrast, aeolian grains are typically well rounded with high sphericity, limiting cement development. In addition to grain morphology, the presence of detrital clays in fluvial and sheetflood deposits may have enhanced local silica availability through the smectite-to-illite transformation, further promoting quartz cementation (Meadows and Beach 1993*a*), which has been reported as occurring in several phases (Greenwood and Habesch 1997). These textural and mineralogical controls contributed to stratigraphic heterogeneity in cementation style and reservoir heterogeneity observed across multiple fields in the EISB. Quartz overgrowths (Fig. 8) were interpreted to have formed from basinal brines at temperatures between 89.6 and 158.1°C (mean 133.2°C), as determined by fluid microthermometry, with $\delta^{18}O$ values ranging from +13.4 to +22.1‰ SMOW (standard mean ocean water; mean +18.3‰) confirming precipitation from thermally evolved fluids (Fig. 7) (Greenwood and Habesch 1997). Interpretations were supported by cathodoluminescence microscopy and SEM imagery, which revealed zoning and overgrowth textures consistent with burial cementation. Cement distribution is heterogeneous and influenced by depositional facies, fluid flow, and potential inhibitors such as chlorite coatings and early hydrocarbon emplacement (Fig. 8) (Worden *et al.* 1998; Worden and Burley 2003). Overall, quartz cementation reflects the interplay of extrinsic controls (temperature, pressure, stress and burial duration) and intrinsic controls (grain surface area, clay coatings and grain type), consistent with regional diagenetic studies (Walderhaug 1996).

Carbonate cements, dominated by ferroan dolomites (Fig. 7), show similar burial timing and variable abundance. In fluvial facies, carbonate cement comprises approximately 4–6% of the rock volume, with slightly lower values in aeolian and sheetflood facies (Greenwood and Habesch 1997). Ferroan dolomite post-dates quartz, forms saddle-shaped crystals and precipitated from high-salinity evolved brines at temperatures of 97–144°C, supported by fluid inclusion and isotopic data (Greenwood and Habesch 1997).

Platy illite is present in secondary pores (Fig. 7) where it is locally associated with feldspar dissolution and evolved formation fluids (Stuart 1993; Greenwood and Habesch 1997). Although not volumetrically quantified, illite development appears spatially heterogeneous and is probably inhibited in hydrocarbon-bearing zones due to reduced water–rock interaction (Worden and Burley 2003). Paragenetic reconstruction places platy illite formation after quartz and non-ferroan dolomite but prior to anhydrite, baryte and hydrocarbon emplacement (Greenwood and Habesch 1997). This timing suggests illitization occurred during peak burial but may have been variably overprinted or suppressed in oil- or gas-saturated intervals.

Evidence from North Morecambe Field supports this interpretation: illite-cemented layers are stratigraphically concentrated in the deeper reservoir sections, which exhibit significantly reduced permeability compared to the gas-charged upper section where

Downloaded from https://www.lyellcollection.org by Imperial College of Science, Technology and Medicine on Mar 27, 2026

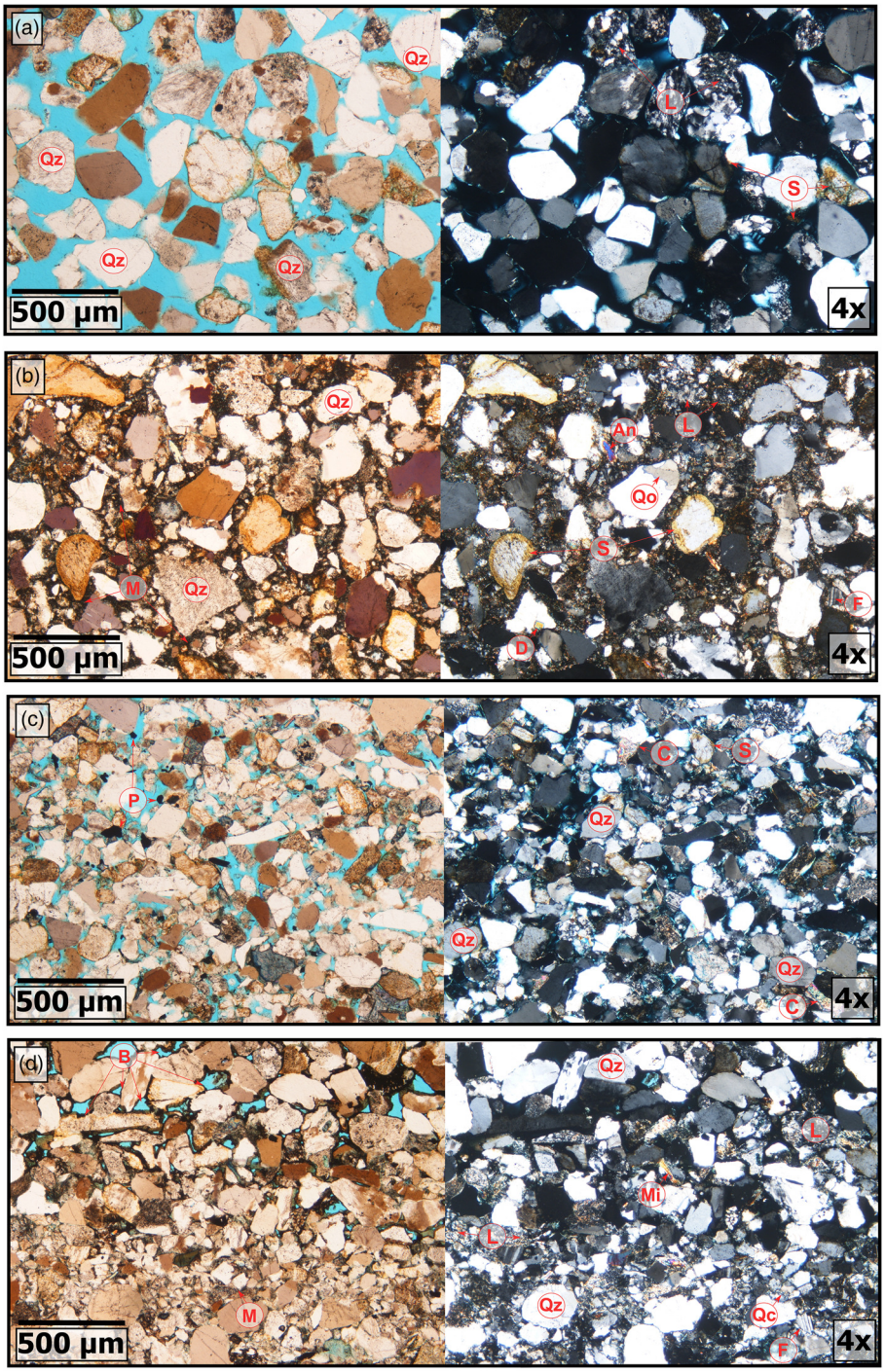


Fig. 8. Photomicrographs of distinct facies associations in normal (left) and cross-polarized (right) light. Thin sections have been impregnated with blue dyed resin, which indicates pore space. (**a**) Aeolian dune sandstone from Lennox Field, well 110/14-3 (Fig. 4c), showing good porosity and pore interconnectivity. Grains, composed of mainly two distinct populations of quartz (Qz) – one clean, one heavily altered – and a relatively high proportion of lithic fragments (L), are subrounded to well-rounded and well-sorted. Some minor smectite (S) and possible chlorite grain coating are also present. Also present, but not visible in this panel, were minor patches of calcite cementation and a very minor component of plagioclase feldspar grains. (**b**) Cemented sabkha deposit from Hamilton North Field, well 110/8a (Fig. 4c), displaying bimodal sorting, sub-angular to rounded grains of two distinct populations of quartz (Qz) grains (as per (a)) and very minor feldspar (F), and a relatively high proportion of lithics (L). Pore space is dominated by a micritic microcrystalline cement (M), with clustered anhydrite (An) and dolomite (D) crystal growth also recorded. Some minor illite/smectite (S) grain coating and quartz overgrowth (Qo) are present. (**c**) Aeolian sandsheet deposit from Lennox Field, well 110/14-3 (Fig. 4c), showing uncemented pore space, poorly sorted with minimal cementation and subrounded to angular grains, showing textural immaturity. Grain composition is principally quartz (Qz), with a minor component of pyrite (P) and other minor accessory phases such as rutile and mica. Minor calcite cement (C) and smectite/illite (S) overgrowths are also present. (**d**) Fluvial sandstone from Hamilton North Field, well 110/8a (Fig. 4c), poorly sorted with angular to sub-angular grains, comprising mainly quartz (Qz) with some lithic fragments (L) and minor feldspar (F) and mica (Mi). Note the upper half of the photomicrograph shows moderate porosity with relic bitumen staining (B) lining the pore space. In the lower half pore space is completely occluded by a combination of micritic microcrystalline cement (M) and quartz cement (Qc).

illite cementation is largely absent (Stuart 1993). In Lennox Field, analysis of wells 110/14-1, 110/15-7, 110/15-6Z and 110/15-6 (Fig. 4c) indicated a multiphase hydrocarbon charge history. The palaeo-GWC separates diagenetically altered, illite-cemented zones below from cleaner, less altered sandstones above, where early hydrocarbon emplacement may have inhibited further water-mediated diagenesis (Greenwood and Habesch 1997; Yaliz and Chapman 2003).

Uplift diagenetic heterogeneities

Although uplift-related diagenesis is volumetrically limited within the OSF, its localized effects, particularly in the water-leg zones and uncharged intervals, have implications for reservoir quality and fluid flow, and therefore warrant specific consideration. Uplift to shallow depths and subsequent mineral reactions with flowing, highly oxidized, often low-salinity meteoric water can result in mineral alteration, precipitation or dissolution (Fig. 7), producing secondary porosity and increasing heterogeneity in siliciclastic lithologies (Worden and Burley 2003). Vitrinite reflectance data and apatite fission track analysis (AFTA) demonstrated that inversion in the EISB resulted in approximately 3 km of uplift in basin-centre areas, across multiple phases. Uplift was significantly less around the basin margins, where pre-inversion burial limited the total amount of exhumation (Holford *et al.* 2005). Initial exhumation, linked to the Cimmerian orogeny, occurred during the Late Jurassic to Early Cretaceous, with subsequent phases during the Paleogene and late Paleogene–Neogene in response to the Alpine orogeny (Fig. 7) (Knipe *et al.* 1993; Holford *et al.* 2005). Mapping of

Downloaded from https://www.lyellcollection.org by Imperial College of Science, Technology and Medicine on Mar 27, 2026

erosional patterns in compacted shales, which exhibit anomalously high seismic velocities, supported the AFTA interpretation, and suggested that uplift removed between 1.3 and 3.3 km of overburden, with exhumation patterns being highly spatially variable (Holford *et al.* 2009).

The clearest petrographic evidence for uplift-related diagenesis in the Liverpool Bay reservoirs is the precipitation of non-ferroan calcite (calcite III) and pyrite (Fig. 7), which occur exclusively in the water legs of some fields (Greenwood and Habesch 1997). These late-stage cements post-date current hydrocarbon emplacement and are characterized by very low $\delta^{13}C$ values, consistent with a dominantly methane-derived carbon source. This geochemical signature, along with fluid inclusion T_h (homogenization temperature, i.e. minimum trapping temperature) measurements for the calcite and $\delta^{18}O$ values, suggest a change in porewater composition, possibly related to meteoric water influx during the Paleogene uplift. The precipitation of pyrite (Fig. 8) under these conditions has been attributed to anaerobic methane oxidation or thermochemical sulfate reduction during post-uplift fluid migration. The absence of these authigenic minerals from hydrocarbon-charged zones further supports the interpretation that uplift-driven, late-stage porewater flow and redox changes influenced authigenic mineral development in uncharged intervals (Greenwood and Habesch 1997).

Evidence from cored wells 110/2-6, 110/2a-7, 110/3a-A3 and 110/8a-C1 (Fig. 4c), located along the southern limb of South Morecambe Field, shows only limited uplift-related diagenesis. Stuart and Cowan (1991) described minor late-stage quartz and kaolinite cements interpreted to have formed during Cimmerian uplift-related fluid migration through high-permeability intervals. However, these phases represent a relatively minor diagenetic overprint and did not significantly affect reservoir quality, with cements from earlier burial phases remaining dominant.

Hydrocarbon alteration offers further evidence for uplift-related processes. In Lennox Field, Jurassic oil was partially biodegraded and converted to bitumen (Fig. 8) in the deeper sections, in zones vertically segregated below the present-day OWC. This transformation has been interpreted to have occurred during exhumation and post-burial fluid migration, the timing of which is consistent with an uplift-driven overprint that predated the current hydrocarbon charge (Yaliz *et al.* 2002).

While uplift-related diagenesis in the EISB is comparatively minor in volume and spatial extent, its effect is locally important. The best-supported signatures include meteoric-influenced carbonate and sulfide cements in the water legs, minor late-stage clay in permeable zones and uplift-related hydrocarbon degradation (Fig. 7).

Depositional heterogeneities

Depositional heterogeneities, which manifest at various scales in core and outcrop, influence reservoir volume and flow rates, whether the fluid is hydrocarbon or CO_2 (Morad *et al.* 2010). Three principal depositional environments have been recognized for the OSF: aeolian systems (see section 'Heterogeneities in aeolian dune and aeolian sandsheet facies associations'), interdune settings ('Heterogeneities in interdune sabkha, sandflat, sheetflood and playa lake facies associations') and braided fluvial channels ('Heterogeneities in fluvial facies associations') (Bushell 1986; Herries and Cowan 1997; Yaliz and Chapman 2003; Yaliz and Taylor 2003; Meadows 2006). In this paper, the term interdune encompasses sabkha, sandflat, sheetflood and playa lake deposits. These may be laterally associated with aeolian dune systems but are not necessarily aeolian in origin.

Recognized facies associations within the OSF include aeolian dunes and aeolian sandsheets, sabkha deposits, playa lake deposits, sheetflood deposits and fluvial sandstones (Figs 8–10) (Meadows and Beach 1993*a*, *b*; Jones and Ambrose 1994; Jackson 1995; Herries and Cowan 1997; Medici *et al.* 2019*b*; Scorgie *et al.* 2021; Chedburn *et al.* 2022). Each facies association is characterized by a distinct suite of depositional heterogeneities (Table 1).

Heterogeneities in aeolian dune and aeolian sandsheet facies associations

The NIREX 13B borehole, located on the northeastern margin of the EISB at Seascale (Fig. 4b), recovered 140.45 m of continuous aeolian sandstone core, comprising moderately to well-sorted, poorly cemented, red to brown, medium-grained sandstone (Barnes *et al.* 1994). Similar aeolian deposits have been recorded in cored well 110/15-7 from Lennox Field (Fig. 9a) (Burley 1987). While useful as a detailed reference profile, it should be noted that facies distributions in the Seascale area differ from those in the basin centre and southern margins, where aeolian deposits are more commonly interbedded with sabkha or fluvial deposits. Regional correlation indicates basin-wide lateral heterogeneity in the distribution of facies associations between South and North Morecambe fields (Fig. 4c), where lacustrine and sabkha deposits grade laterally into aeolian sandstones. These aeolian sandstone units thicken southwards to over 60 m (Cowan *et al.* 1999), forming part of the Liverpool Bay reservoirs targeted by the HNNWp.

Based on facies analysis of ten cored wells, 110/2-1, 110/2-2, 110/2-3, 110/2-5, 110/2-6 (Fig. 10), 110/3-1, 110/3-3, 110/7-1, 110/9-1 and 113/26-1 (Fig. 4c), from South Morecambe and surrounding fields in the central part of the EISB, Meadows and Beach (1993*a*) calculated that aeolian facies associations are volumetrically subordinate to other OSF facies associations in the EISB. However, due to their consistently high reservoir quality, they form an important component of any reservoir evaluation. Arithmetic mean porosity values in aeolian facies associations can exceed 15% with values of up to 30% recorded. Permeability generally ranges between 100 mD and 3 D with exceptional values of 10–11 D reported (Stuart and Cowan 1991; Meadows and Beach 1993*a*; Cowan *et al.* 1999).

The aeolian dune facies association is defined by rounded to well-rounded and well-sorted grains (Fig. 8), with secondary attributes including friability, high porosity, and an absence of mud or clay intraclasts (Table 1; Fig. 9a) (Cowan 1993). Heterogeneities in this facies association manifest as cross-lamination, featuring alternating finer- and coarser-grained foreset laminae and pinstripe lamination (Fig. 9b), with low-angle planar truncation surfaces separating individual sets.

Barnes *et al.* (1994) described outcrops on the shore at Seascale and along the River Calder at Sellafield (Fig. 4b) showing sets of gently dipping trough and planar cross-bedded, fine- to medium-grained sandstones with nearly planar erosional bounding surfaces. Cross-stratification occurs in stacked sets, with individual sets averaging 25 cm and ranging from 10 to 70 cm.

Three distinct types of laminations were identified (Jones and Ambrose 1994):

(1) Alternating laminae of well-sorted, fine- to medium-grained sandstone interpreted as grainfall, and subordinate, moderately to poorly sorted, medium- to coarse-grained sandstone interpreted as grainflow (Table 1; Fig. 9b). These represent interbedded dune-crest processes associated with grainfall accumulation and minor flow-related avalanching.
(2) Moderately well-sorted, medium- to coarse-grained sandstone forming foresets ~2 cm thick, interpreted as grainflow lamination. These foresets have sharp erosional bases and tops, and rarely display a fining-upward trend.
(3) Sharp-based pinstripe lamination (Table 1), characterized by alternating laminae of coarse- to very coarse-grained,

Downloaded from https://www.lyellcollection.org by Imperial College of Science, Technology and Medicine on Mar 27, 2026

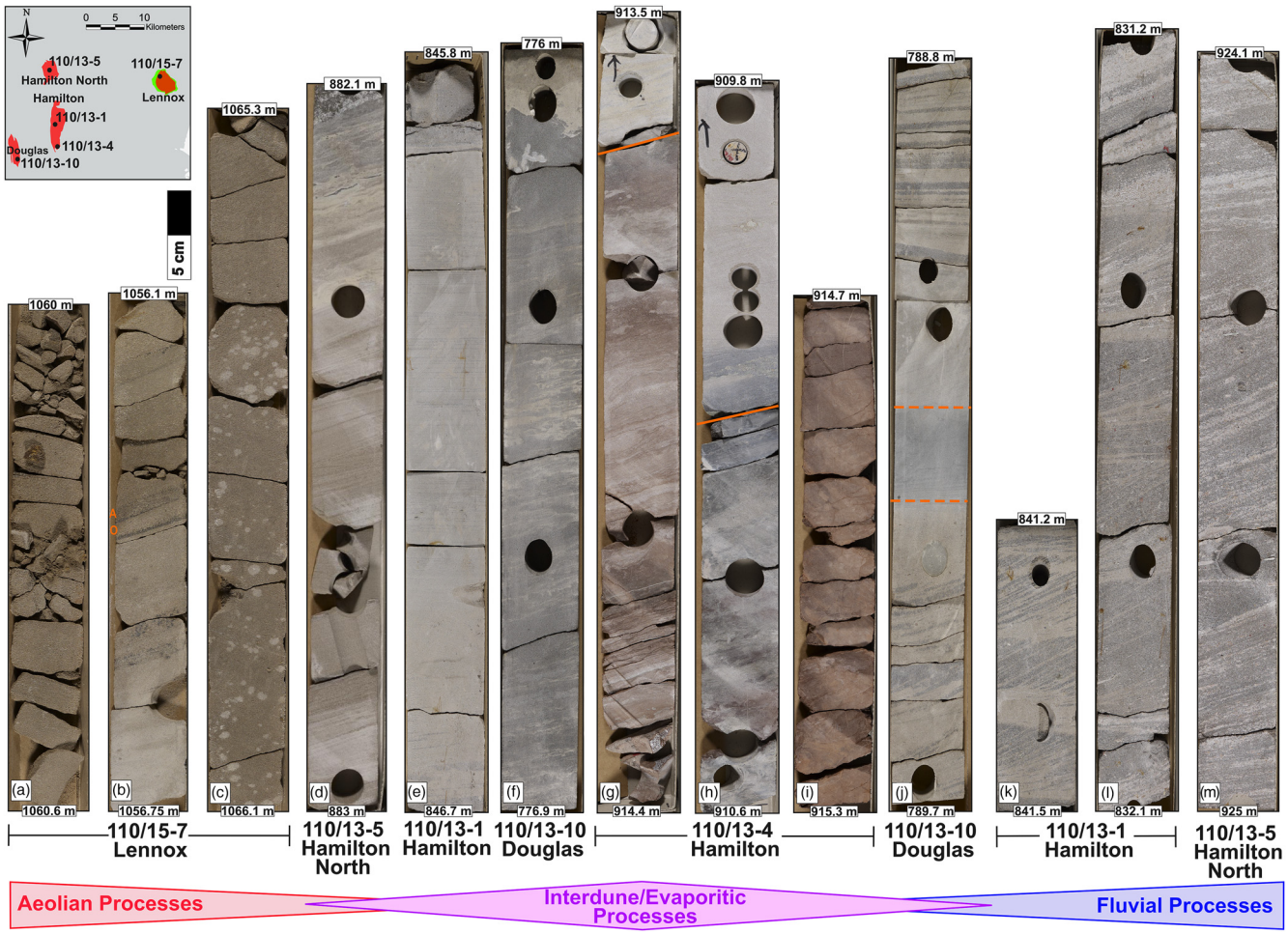


Fig. 9. Core images from the Hamilton, Hamilton North, Lennox and Douglas fields. (**a–d**) Aeolian dune facies association: (a) highly friable sandstone; (b) depositional textures such as grain flow (O) and grainfall (A) strata; (c) cemented, mottled textures; (d) a possible wetting-upward sequence with a gradual transition from aeolian dune to wavy-laminated sabkha/damp sandflat facies association. (**e**) Aeolian sandsheet facies association. Low-angle to flat cross-stratification, with bimodally sorted laminations. (**f**) Sabkha facies association, characterized by wavy laminations, possible dolomitic nodules ~12 cm from the top. (**g**) Sabkha and playa lake facies associations. Wavy laminations at the base (indicative of cyclical flooding and drying out) transition upwards to a silty interval, interpreted as playa lake deposits. An abrupt shift to pale sandstone-dominated deposits near the top (orange line) suggests unconfined sheetflood processes. (**h**) Playa lake facies association. Heterolithic playa margin deposits with discontinuous laminae transition upwards into fine-grained silty deposits displaying varve-like laminations, followed by an abrupt transition (orange line) into a package containing a basal granule lag, subtle cross-stratification and several intraclasts. (**i**) Sheetflood facies association. Reddish brown/ochre colour is indicative of subaerial oxidation, with dewatering structures and wavy laminations disrupted by evaporitic nodules, suggestive of low-energy overbank processes and episodic drying out. (**j**) Minor and abandoned fluvial channel facies associations. Fluvial channel sandstone with clay drapes at the base of the core transitions into a mudstone indicative of channel abandonment (dashed orange lines), followed by a return to cross-bedded fluvial deposits. (**k–m**) Major fluvial channel facies association: (k) stacked cross-bedded packages; widespread planar and trough cross bedding and lamination are seen in (k) and (l); (l) also features pale nodules of reworked dolomite. Contains British Geological Survey materials © UKRI 2024. Source: https://webapps.bgs.ac.uk/data/offshoreWells/wells.cfc?method=searchWells.

well-rounded and moderately sorted sandstone (up to 2 mm thick) and fine- to medium-grained, moderately sorted sandstone (1 mm thick), some displaying an upward-coarsening trend. These laminae are commonly interpreted as dune toesets, and may grade into aeolian sandsheet deposits, with upward-coarsening patterns attributed to wind ripple migration.

Aeolian dune sandstones are commonly preserved in cross-stratified sets, with regular deflation surfaces that are either planar or undulatory in geometry. The maximum recorded thickness for an individual unit is <3 m (Meadows and Beach 1993*a*). In the Kirklinton Sandstone Formation, a coeval lithological equivalent of the OSF in the Carlisle and Solway basins (Fig. 4a) (Holliday *et al.* 2004), trough cross-stratification in combination with very fine-grained sandstone observed at Cliff Bridge (Fig. 4b) suggested deposition within a three-dimensional, barchanoid-type linear dune field (Brookfield 2008). The uniformly fine-grained nature of the sandstones supports the interpretation that they were reworked from the underlying Triassic Annan Sandstone Formation, itself a coeval lithological equivalent of the St Bees Formation (Fig. 3) (Brookfield 2004).

In the basin centre, aeolian dune sandstones are commonly interbedded with aeolian sandsheets (Fig. 9e; Table 1). The aeolian sandsheet facies association was interpreted to have formed either by grain fall of saltating grains settling on a flat surface or by climbing ripples in a subcritical flow regime (Cowan 1993). Characteristically, it exhibits very low-angle to flat cross-stratification, with laminations displaying bimodal sorting (Meadows and Beach 1993*b*). In combination with aeolian dune deposits, this facies association typically accounts for <10% of the succession in core from the South and North Morecambe fields (Fig. 4c) (Cowan 1993).

Closer to the eastern basin margin, the OS2b Member (Fig. 3) in Lennox Field (Figs 1, 4c) is composed predominantly of aeolian

Downloaded from https://www.lyellcollection.org by Imperial College of Science, Technology and Medicine on Mar 27, 2026

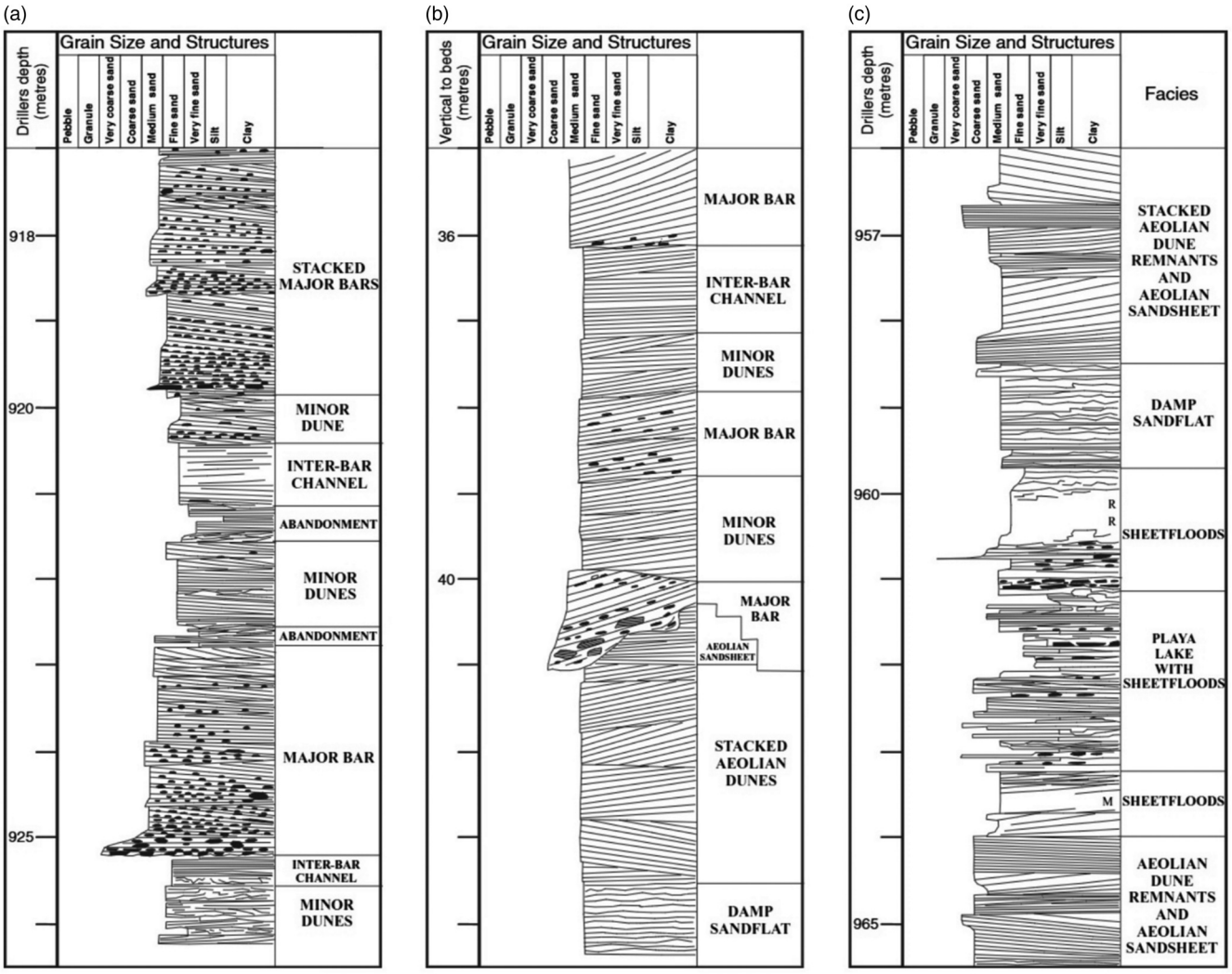


Fig. 10. Graphic sedimentary logs from: (**a**) well 110/2-6 (South Morecambe Field); (**b**) outcrop at Helsby Hill; and (**c**) well 110/13-5 (North Hamilton Field). Logs (a) and (c), from the East Irish Sea Basin, highlight significant variations in facies associations, reflecting changes in bedform type and grain size. Location of wells 110/2-6 and 110/13-5 in Figure 4c and Helsby Hill outcrop in Figure 4b, c. Source: reproduced from Meadows (2006).

dune and sandsheet deposits. However, due to lateral facies changes westwards across the field, these aeolian units are replaced by fluvial deposits (Yaliz and Chapman 2003). Aeolian dune deposits in Lennox Field range in thickness from 0.3 to 2 m per bed, with the thickest succession of interbedded aeolian dune and heterolithic sabkha sandstones recorded within the OS2b Member at approximately 79 m (Yaliz and Chapman 2003). Further west, in Hamilton and Hamilton North fields (Figs 1, 4c), a similar pattern is observed. The thickest continuous section of interbedded aeolian and heterolithic sabkha sandstones also occurs in the OS2b Member, measuring approximately 52 m thickness in Hamilton Field and 43 m in Hamilton North Field. In both fields, a thin fluvial sandstone unit (4.5–6 m thick) is present in the middle of these successions (Yaliz and Taylor 2003).

Porosity and permeability in the dominantly aeolian sandstones of the OS2b Member average 18% and 1 D in Lennox Field (Yaliz and Chapman 2003), 18.6% and 2.1 D in Hamilton Field, and 14.7% and 400 mD in Hamilton North Field (Yaliz and Taylor 2003).

Meadows and Beach (1993*a*) recorded OSF aeolian sandsheets, compositionally similar to aeolian dune deposits, that were locally interbedded with a sheetflood facies association at millimetre- to centimetre-scale, and with an aeolian dune facies association in thicker units of up to 1 m (Meadows and Beach 1993*a*), interpreting these bimodally sorted laminations within aeolian sandsheets as representing alternations of wet and dry depositional conditions (Fig. 10c).

In South Morecambe Field, Cowan *et al.* (1999) recorded laterally extensive aeolian sandsheets as having porosity values of up to 30% and permeability up to 10 D, although both parameters decrease with depth. Data from wells 110/2-6 and 110/3-3 (Figs 4c, 10) in South Morecambe Field indicate porosities in the aeolian facies associations ranging from 14 to 28%, with permeability ranging from 100 mD to 5 D (Marsh *et al.* 2022), although earlier work recorded permeability as high as 11 D (Stuart and Cowan 1991).

In block 110/13 (containing Douglas, Hamilton and Hamilton North fields) (Figs 1, 4c), aeolian sandsheets were reported to range in thicknesses from 15 to 45 cm (Yaliz and McKim 2003), with maximum sandsheet thickness rarely exceeding 1 m (Meadows and Beach 1993*b*). Data from development wells in South Morecambe Field show that some aeolian units can be correlated between wells over distances greater than 10 km, covering an area of more than 70 km^2 (Cowan 1993). This widespread preservation, despite the limited thickness of many of these units, is interpreted to result from early-stage carbonate or evaporite cementation (see 'Early-stage diagenetic heterogeneities' section above), which stabilized the sediment sufficiently to preserve architectural features, while still allowing significant reservoir quality to be retained (Stuart and Cowan 1991).

Downloaded from https://www.lyellcollection.org by Imperial College of Science, Technology and Medicine on Mar 27, 2026

Table 1. Summary of the most common facies present in the Ormskirk Sandstone Formation, including core or outcrop characteristics and associated heterogeneities observed within each facies

Facies association	Description	Associated depositional heterogeneities
Aeolian Dune	Typically, fine- to medium-grained, well-rounded and well-sorted sandstones with frosted grains, displaying trough cross-stratification and forming stacked dune successions.	**Grainfall and Grainflow Laminae**: alternating fine- and coarser-grained laminae introduce anisotropy in permeability. **Localized Slumping**: small-scale soft-sediment deformation zones create baffles.
Aeolian Sandsheet	Fine- to medium-grained, well-rounded and well-sorted sandstones with very low-angle to flat cross-stratification.	**Bimodal sorting**: lamina-scale bimodal sorting of sandstones and mudstones. **Interbedding**: occurs at millimetre scale with sheetflood fines and at decimetre scale with aeolian dunes.
Dry Interdune	Well-rounded, frosted, fine- to coarse-grained sandstones displaying low-angle and alternating parallel laminations of fine and coarse grains.	**Parallel Laminations**: contribute to permeability variations within otherwise homogeneous sandstones. **Textural Uniformity**: well-sorted but variable compaction results in permeability anisotropy.
Damp Interdune	Thinly laminated fine- to very fine-grained sandstones alternating with silty laminations, showing wavy bedding and minor convolutions.	**Adhesion Marks and Load Structures**: variable porosity. **Convoluted Layers**: dewatering structures create baffles. **Sparse Bioturbation**: contributes to localized permeability variation.
Wet Interdune	Predominantly claystone or siltstone with sand-filled desiccation cracks and mudstone laminations.	**Desiccation Cracks**: cracks filled with sand or mud modify flow-barrier continuity and flow paths. **Mudstone Lenses**: act as low-permeability baffles in porous zones.
Sabkha	Clay-rich sediments with evaporitic minerals (e.g. anhydrite, halite), fine-grained sandstones, fine laminae, wavy strata.	**Evaporite Cementation**: pervasive anhydrite, halite and calcite cements (due to environment-related early diagenesis) significantly reduce permeability (although an early diagenetic feature, this is closely tied to the sabkha depositional environment, and critical to the reservoir behaviour of sabkha facies). **Wavy strata and Mudstone Layers**: introduce fine-scale barriers and baffles in porosity and permeability due to cyclical wetting and drying.
Sheetflood	Fine- to medium-grained sandstones with granules and mudstone clasts.	**Grain-Size Fluctuations**: vertical permeability varies with alternating layers of granules and sand grains. **Erosional Surfaces**: lower boundaries and sharp upper contacts affect vertical and lateral flow.
Playa Lake	Thin beds of reddish-brown, laminated claystone and siltstone (typically ≤0.5 m, but locally up to 1.0 m), with lenses of thin cross- and parallel-laminated sandstone.	**Soft-Sediment Deformation**: load casts, pillow and flame structures disrupt bed continuity. **Desiccation Cracks**: sand-filled straight or ptygmatically folded cracks impact porosity and permeability profiles.
Abandoned Fluvial Channel	Massive claystone and siltstone (up to 1 m), forming lens-shaped bodies with sand-filled desiccation cracks.	**Desiccation Cracks**: sand-filled cracks may provide localized flow paths. **Load Structures**: modify the thickness and geometry of beds.
Minor Fluvial Channel	Narrow (≤2 m) sandstone units, interbedded with playa facies, displaying small-scale trough cross-stratification.	**Fining-Upward Patterns**: influence vertical permeability trends. **Mudstone Fragments**: rip-up clasts form permeability baffles. **Desiccation Cracks**: sand-filled, introduce localized permeability pathways.
Major Fluvial Channel	Thick (2–5 m), multistorey sandstone bodies with poorly sorted, cross-bedded sandstones in fining-upward successions.	**Basal Conglomerates**: basal brecciated and conglomeratic lags restrict fluid flow. **Cross-Stratification**: large trough and planar cross-beds produce directional anisotropy. **Mud Drapes and Soft-Sediment Deformation**: internal baffles and disrupted laminae continuity.

Based on observations at outcrop and data from: Cowan (1993), Meadows and Beach (1993*a*, *b*), Barnes *et al.* (1994), Jones and Ambrose (1994) and Herries and Cowan (1997).

Heterogeneities in interdune sabkha, sandflat, sheetflood and playa lake facies associations

To highlight the diversity of naming conventions present within the OSF literature, 'interdune' is used here as a broad lithographic descriptor encompassing a range of depositional environments, from sabkha to sheetflood (Fig. 9f–i). Jones and Ambrose (1994) have subdivided interdune deposits into dry, damp and wet interdune facies associations (Table 1).

Heterogeneities in wet to dry aeolian interdune facies associations, *sensu* Kocurek and Havholm (1993), also referred to as sandflat facies (*sensu* Meadows 2006), though not to be confused with aeolian sandsheet facies, as covered in the above section, are controlled primarily by fluctuations in the palaeo-water-table (Table 2). These heterogeneities manifest as:

(1) variations in grain size, representing changes in depositional energy (Fig. 8);
(2) the presence of evaporitic minerals, which may form zones of low permeability (see 'Diagenetic heterogeneities' section above); and
(3) sedimentary structures such as ripple cross-lamination, irregular or wavy laminations, and mud drapes (Fig. 9).

Reservoir quality can vary significantly depending on grain size variation, packing, and the presence or absence of evaporitic minerals and mud drapes (Meadows 2006).

The dry interdune facies association (Table 1) displays a wide range of grain sizes, from fine to coarse sand, although well-rounded, frosted, medium sand grains are most common. This variation reflects fluctuating energy conditions within the depositional environment. The defining characteristic of this very low-angle cross-stratified sandstone is its bimodal sorting at the lamina scale, comprising fine- to medium-to-coarse-grained sandstones in units up to 50 cm thick (Jones and Ambrose 1994).

Downloaded from https://www.lyellcollection.org by Imperial College of Science, Technology and Medicine on Mar 27, 2026

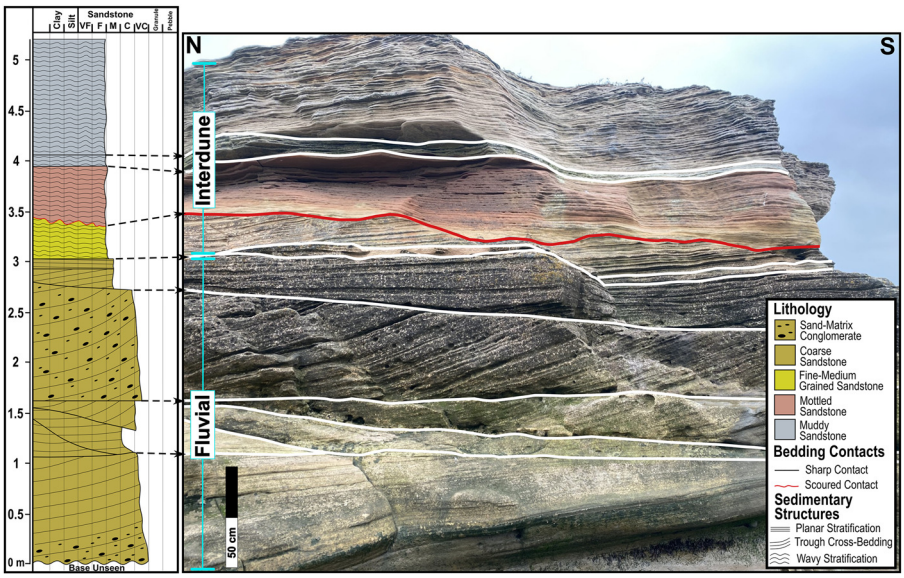


Fig. 11. Fluvial deposits in the lower half of the image display trough cross-stratification and are capped by red sabkha deposits ('aeolian sabkha' of Herries and Cowan 1997). These transition upwards to grey sabkha deposits characterized by distinct wavy strata ('damp sabkha' of Herries and Cowan 1997). White and yellow lines indicate higher and lower stratification order, respectively. Location: Little Hilbre Island, East Irish Sea Basin (Fig. 4c).

The damp interdune facies association (Table 1) is composed of very fine- to fine-grained sandstone with characteristic wavy strata (Figs 10b, c and 11), occasionally containing medium to coarse sand grains and rare silty laminae. These units can reach up to 1 m in thickness and are commonly interbedded with deposits of the aeolian dune facies association (Jones and Ambrose 1994), underscoring the heterogeneous and complex nature of OSF facies architecture.

The wet interdune facies association (Table 1), which comprises a minor component of interdune deposits, is most often found alongside the damp interdune facies association. It is characterized by thin laminae of siltstone or claystone, sand-filled desiccation cracks, upturned mudstone laminations and sandy load casts (Jones and Ambrose 1994).

Heterogeneities in the sabkha facies association (*sensu* Herries and Cowan 1997) include evaporitic accumulations of anhydrite and halite, which can result in localized zones of occluded porosity (Fig. 8). These minerals occur in depositional cycles that transition from siliciclastic to evaporitic mineralogy, formed in response to periodic wetting and drying, and introduce both vertical and lateral heterogeneity into the facies association. Commonly observed desiccation cracks, formed in response to these wetting and drying cycles, are locally infilled with mudstone, creating lateral compartmentalization and acting as baffles to fluid flow. Alternating laminae of siltstone and claystone within this facies association contribute to anisotropic permeability.

Finally, wavy strata (Fig. 11), previously also assigned to the damp interdune facies association, are interpreted to reflect surface moisture conditions: more continuous silty strata indicate damp sabkha conditions, whereas wavy laminae reflect a more evaporitic, aeolian influence. This distinction was classified by Herries and Cowan (1997) as 'aeolian sabkha' v. 'damp sabkha'.

Heterolithic playa lake and sheetflood facies associations, derived from unconfined fluvial processes and subsequent ponding, are typically poorly sorted due to the wide range of energy levels affecting deposition. A well-documented playa lake deposit, referred to as the 'Century Playa', has been recognized as being laterally correlatable across South Morecambe Field and the neighbouring central basin area (Meadows 2006). The presence of claystones and siltstones in fining-upward and coarsening-upward successions (Fig. 10c) is indicative of transgressive–regressive lacustrine cycles (Herries and Cowan 1997).

Deposits of the sheetflood facies association (Fig. 10c) have been interpreted as having formed under waning-flow conditions across broad floodplains by effectively unconfined fluvial processes (Bushell 1986). Closely associated with fluvial deposits and commonly no thicker than 2 m, the unconfined nature of sheetflood deposition tends to produce lateral heterogeneity, adversely affecting sandstone connectivity (Herries and Cowan 1997). Heterogeneities in these sheetflood sandstones include irregular wavy laminations (Table 1; Fig. 9i) of low-porosity, silty and argillaceous fine-grained sandstone interbedded with highly porous, moderately sorted, flood-reworked aeolian sandstone (Meadows and Beach 1993*a*). These deposits commonly exhibit soft-sediment deformation and bioturbation, which often obscure primary depositional structures. Where preserved, primary structures include planar laminations, current ripples and mud-draped wave ripples, features indicative of episodic slackwater conditions and deposition from suspension. Desiccation cracks are also present, suggesting intermittent drying of the sediment (Meadows and Beach 1993*b*).

The notion that the deposits displaying wavy laminations should be attributed to the sheetflood facies association and overbank fluvial processes (Meadows and Beach 1993*a*) was later challenged by Herries and Cowan (1997), who instead attributed these stratified wavy and crinkly siliciclastic deposits to algal and evaporitic processes characteristic of a sabkha environment (Table 1), arguing that the wavy strata in this facies reflects deposition on a damp surface influenced by water table fluctuations (Table 2). The continuity or disruption of these wavy strata was interpreted to relate to the degree of surface dampness, with more continuous strata being associated with damp sabkha conditions.

Heterogeneities in fluvial facies associations

The fluvial systems within the OSF span a spectrum from major perennial channels to minor abandoned channels (Table 1). End-member types, as well as intermediate examples such as minor ephemeral channels that show evidence of episodic drying out, each exhibit distinct heterogeneities (Herries and Cowan 1997).

This suite of fluvial facies associations, together with the sheetflood facies association (section above), comprises approximately 90% of the reservoir facies encountered within the EISB (Cowan 1993). The major fluvial channel facies association (Figs 9k–m and 10a, b) is linked to perennial braided systems, while the minor fluvial channel facies association (Fig. 9j) is linked to lower-energy systems, often ephemeral or, if perennial, consisting of smaller channels within a floodplain system.

The major fluvial channel facies association exhibits significant vertical heterogeneity due to a combination of grain sizes, distinct sorting patterns and the presence of fining-upward successions.

Downloaded from https://www.lyellcollection.org by Imperial College of Science, Technology and Medicine on Mar 27, 2026

Erosional bases within these successions are commonly lined by discontinuous conglomeratic lags (Thompson and Meadows 1997), typically composed of clay- to silt-grade material (Meadows and Beach 1993*b*) and containing a mixed assemblage of granule- to pebble-sized, rounded to angular clay clasts, dolomite nodules (Cowan 1993) and intraformational cemented sandstone clasts (Fig. 10a, b) (Meadows 2006).

Lateral grain-size variations are also common in fluvial deposits, contributing to the heterogeneous character of this facies association. These variations reflect the transition from coarser-grained bar deposits, often containing quartz and feldspar pebbles deposited during flood events, to moderately to well-sorted, medium-grained dune-form sandstones deposited under intermediate to low flow regimes. Pebbles are common in the fluvial channel deposits of the Cheshire Basin, becoming less frequent across the transition into the EISB. They are rare in the southern EISB and absent in the Morecambe fields and farther north. These fluvial deposits are locally interdigitated with finer-grained overbank deposits (Fig. 9i) (Meadows 2006).

The major fluvial channel facies association is characterized by large sets of cross-strata, abundant channel-base erosional surfaces and associated conglomeratic lags, and a multistorey, multilateral architecture (Fig. 10a). These channel-fill deposits comprise poorly sorted, fine- to coarse-grained, cross-stratified sandstone (Fig. 11) with angular to sub-angular sand grains. Both multistorey and multilateral bodies contain preserved single channel fills ranging from decimetres up to 2–5 m thick, with a stacked channel succession exceeding 20 m in thickness, in well 110/2-6 (Fig. 4c) (Meadows and Beach 1993*a*). An 80 m stacked succession, containing subordinate aeolian sandstones, was recorded in well 110/3a-A3 (Fig. 4c) (Herries and Cowan 1997).

Major fluvial channel fills are composed of simple and compound bars that represent distinct phases of the flow regime (Fig. 10a, b). Cross-set thicknesses decrease upward through a channel-fill succession, potentially reflecting a reduction in current velocity (Meadows and Beach 1993*a*). Interbedded with these dune- and bar-scale bedforms are laminated and current-rippled fine-grained sandstones (Fig. 10a), interpreted to represent periods of low-velocity flow. Preserved as part of a continuous succession, such intervals are not associated with abandonment mudstones, supporting the perennial flow within a channel system interpretation (Meadows 2006).

Sedimentary structures within the major fluvial channel facies association contribute a wide range of heterogeneities, including: grain size and sorting variations; compositional changes such as reworked dolomitic nodules forming basal lags; planar and trough cross-stratification; cross-lamination, climbing ripples and ripple-form sets; parallel lamination with primary current lineation; as well as imbrication and rare cross-stratification in breccias and conglomerates (Fig. 9k–m) (Jones and Ambrose 1994). Braided fluvial deposits have been interpreted in South Morecambe Field, intercalated with subordinate aeolian sandstones, resulting in pressure communication in Repeat Formation Tester (RFT) data (Cowan 1993).

Typically occurring at a smaller scale, the minor fluvial channel facies (Figs 9j, 10a) association shares many features with the major fluvial channel facies association, such as cross-stratification and fining-upward successions (Cowan 1993). However, the minor fluvial channel facies association occurs as more isolated deposits in intervals that often exhibit significant lateral heterogeneity between the fine-grained channel sandstones and overbank mudstones and siltstones (Meadows and Beach 1993*a*), reducing connectivity and contributing to reservoir compartmentalization.

The minor fluvial channel deposits are also interbedded with the abandoned fluvial channel facies association (Fig. 10a), which comprise mudstone-rich, fine-grained single-storey channel fill deposits recording channel abandonment and cessation of flow (Fig. 9j) that may display desiccation cracks and load structures. Desiccation cracks provide evidence that these fluvial systems dried out episodically (Jones and Ambrose 1994). Mud-draped foresets are common in cross-sets, reflecting a pattern of intermittent drying.

Individual minor fluvial channel fills, comprising single and compound bars, average 0.5 m in thickness, although a sequence of stacked minor channels up to 9 m thick was recorded in well 110/2-6 (Figs 4c, 10a) (Meadows and Beach 1993*b*). These stacked minor channel fills are typically arranged in a fining-upward then coarsening-upward succession, with associated abandoned channel fills (Fig. 9j) typically displaying very fine lamination, similar to varves, and occasional desiccation cracks, sand-infill structures and load casts (Herries and Cowan 1997).

Compositional heterogeneities in minor fluvial channel deposits also include the common presence of reworked aeolian sandstone and rare mudstone rip-up clasts. Additional depositional heterogeneities arise from the lateral interfingering of minor fluvial channel deposits with aeolian, playa lake and sheetflood deposits (Meadows and Beach 1993*b*).

Discussion

In this work, we explore the effect that diagenetic (see section 'Diagenetic heterogeneities') and depositional (section 'Depositional heterogeneities') heterogeneities in the OSF may have on the injection, migration and trapping of CO_2, given its planned role as a CCS reservoir. A thorough understanding of how these heterogeneities impact fluid flow, including their potential to both enhance and impede CO_2 trapping, is essential, as they directly govern key processes relevant to storage integrity, such as plume migration, trapping and pressure dissipation. Here the term 'plume' is used to describe the spatial extent and evolution of the injected CO_2 phase, irrespective of its local direction of movement, which may vary according to reservoir geometry, pressure gradients and density contrasts (Doughty and Oldenburg 2020; Worden 2024). Given their role in controlling groundwater movement in aquifers, and their documented impact on historical hydrocarbon production in the EISB (Yaliz and Chapman 2003; Medici *et al.* 2016), it follows that such heterogeneities will also affect future CO_2 storage within the same formation.

In both the Cheshire and East Irish Sea basins, groundwater flow in the OSF and St Bees Sandstone Formation (Fig. 3) has been shown to be affected by faults, fractures and deformation bands at shallow depths (≤180 m) (Medici *et al.* 2016; Griffiths *et al.* 2018). In particular, deformation bands, such as those documented in outcrop analogues to the OSF, may act as significant barriers or baffles to flow, particularly where grain fracturing and cementation has occurred (Griffiths *et al.* 2018). However, at greater depths, between 700 and 1000 m, the depth at which the three target reservoirs in Liverpool Bay are located (Section Economic resources), the transmissivity of tectonic features is significantly reduced as a result of overburden pressure, and matrix flow becomes dominant. At these depths, diagenetic heterogeneities such as quartz overgrowths and pore-occluding cements such as calcite or ferroan dolomite (Fig. 8), as well as depositional heterogeneities including bedding planes and low-permeability mudstone units (Fig. 9i), exert a greater influence. These features introduce anisotropy into fluid flow, reduce aquifer transmissivity and promote reservoir compartmentalization (Medici *et al.* 2019*a*).

Hydrocarbon recovery in the EISB has been impacted by such heterogeneities (Yaliz and Chapman 2003; Yaliz and Taylor 2003). Facies variability in Morecambe South Field significantly affected gas production: high-permeability zones, correlating with aeolian dune deposits (see section 'Heterogeneities in aeolian dune and aeolian sandsheet facies associations'), and lower permeability zones associated with fluvial deposits (section 'Heterogeneities in

Downloaded from https://www.lyellcollection.org by Imperial College of Science, Technology and Medicine on Mar 27, 2026

fluvial facies associations') created reservoir compartmentalization, complicating pressure management and recovery. Further reservoir compartmentalization resulted from playa lake (section 'Heterogeneities in interdune sabkha, sandflat, sheetflood and playa lake facies associations') and abandoned channel (section 'Heterogeneities in fluvial facies associations') mudstones, which acted as intraformational seals, reducing vertical connectivity. These heterogeneities led to uneven sweep efficiency in both North and South Morecambe Fields and required targeted infill drilling and advanced pressure management strategies (Medici *et al.* 2019*b*).

Medici *et al.* (2019*b*) also reported that diagenetic heterogeneities had a measurable impact on production. In North Morecambe Field, zones of calcite cementation within fluvial facies associations (section 'Early-stage diagenetic heterogeneities'), also present in the HNNWp target reservoirs (Yaliz and Chapman 2003; Yaliz and Taylor 2003), were found to reduce gas flow and create bottlenecks. Conversely, dissolution of calcite cement within aeolian facies associations (section 'Heterogeneities in aeolian dune and aeolian sandsheet facies associations') enhanced flow rates and improved recovery. The challenges encountered during hydrocarbon production therefore serve as valuable guidance for understanding the impact heterogeneities may have on CCS projects.

Before reviewing the mechanisms to trap CO_2 in the OSF reservoirs, and the role that sedimentological heterogeneities can play in this trapping, we first consider the CO_2 phases that are expected to be present during its injection and migration in the reservoirs. The properties of these CO_2 phases and of other fluids in the reservoirs differ from groundwater and water–oil–gas systems, and control aspects of multiphase fluid flow and the impact of heterogeneity on CO_2 trapping. In the Liverpool Bay OSF reservoirs, CO_2 will be injected in a superheated gas phase with a discharge temperature of ~40°C and wellhead pressures below the supercritical threshold, in order to avoid potential near-wellbore hydrate formation (BEIS 2020). As the CO_2 descends, it will cool due to frictional pressure loss and Joule–Thomas cooling, with bottom-hole temperatures expected to drop to ~22°C during initial injection. As storage progresses and both bottom-hole pressure and temperature exceed 74 bar and 31.1°C, respectively, CO_2 is expected to transition into a supercritical phase within the reservoir. Bottom-hole temperatures during late-stage injection are anticipated to reach ~55°C, and maximum pressures for Hamilton, Hamilton North and Lennox are anticipated to reach 96, 106 and 111 barg (i.e. bar gauge, relative to atmospheric pressure), respectively (BEIS 2020).

A reverse transition from supercritical back to gas phase could occur late in the injection process, particularly if the CO_2 plume enters cooler or shallower reservoir zones during shut-in, subsequent pressure decline or the longer-term post-injection containment period. This is plausible given that Hamilton, Hamilton North and Lennox reservoirs lie at depths of ~700–1000 m (see section 'Economic resources'), near the lower threshold for maintaining supercritical conditions (Rochelle *et al.* 1999; Bachu 2000). Such a phase change could lead to local volumetric expansion (IPCC 2005) and transient pressure redistribution within the reservoir, potentially inducing leakage along structural or stratigraphic discontinuities. Similar short-term pressure perturbations near injection zones have been observed in modelling studies of saline aquifer systems (Onoja and Shariatipour 2018). Specific CO_2 phase modelling would validate this potential scenario for the HNNWp fields. Injected CO_2 will remain less dense than brine and is still expected to rise within the water leg, particularly during early- and mid-stage injection (BEIS 2020). In oil-bearing fields such as Lennox, where residual oil may persist near the OWC, the relative density of supercritical CO_2 (~500–800 kg m^{-3}) compared to oil (~800–950 kg m^{-3}) adds to the complexity of plume evolution and the efficiency of residual trapping.

CO_2 trapping mechanisms

Four principal trapping mechanisms are commonly recognized for CO_2 injected into geological formations: structural, residual (capillary), solubility and mineralization (Benson *et al.* 2005; Massarweh and Abushaikha 2024). Each contributes to secure long-term storage of CO_2 to varying degrees over time (IPCC 2005). These mechanisms have traditionally been framed around saline aquifer systems, and recent work highlights that trapping behaviour in depleted gas fields can differ significantly due to differences in pressure conditions, fluid configurations and storage efficiency (Worden 2024). Nonetheless, the canonical mechanisms remain a useful framework for assessing CO_2 behaviour in the OSF.

Pore-scale parameters such as porosity and permeability, traditionally used to assess reservoir quality for hydrocarbon production, are also critical for evaluating the suitability of a depleted reservoir for CO_2 storage (Payton *et al.* 2023). CO_2 is stored most efficiently in its supercritical phase (Kim *et al.* 2023), which occurs above 31.1°C and 7.38 MPa. In the EISB fields, this phase is expected to develop progressively during late-stage injection as reservoir pressure rises toward ~100 barg, and temperatures rise above the critical threshold (~40–50°C), consistent with HyNet flow-assurance modelling (BEIS 2020). Given that the kinetic diameter of a CO_2 molecule is approximately 0.5 nm smaller than that of CH_4 (Sayed Siamak Ashraf *et al.* 2010), coupled with its distinct capillary entry pressures and wetting behaviour (Payton *et al.* 2022), CO_2 exhibits different flow and trapping dynamics compared with natural gas.

Structural trapping

Structural trapping refers to the physical confinement of CO_2 by an impermeable cap rock layer and is analogous to the structural and stratigraphic trapping mechanisms defined in the hydrocarbon industry. Depleted hydrocarbon fields, such as the Liverpool Bay reservoirs (Section Economic resources), are considered attractive CCS targets due to their proven geological containment and potentially reusable infrastructure (Bump *et al.* 2022).

In such settings, structural trapping is typically the dominant mechanism during the early stages of CO_2 injection. Because these fields are depleted, residual CH_4 remains at low saturation, generally confined to attic regions beneath the caprock, while formation water occupies most of the pore space. The distribution of these fluids, and their relative densities, is a key control on CO_2 migration.

While buoyancy is an important control on CO_2 movement in most storage systems (Krishnamurthy *et al.* 2022), the behaviour of injected CO_2 in depleted gas reservoirs remains the subject of ongoing discussion. Some conceptual models suggest that, because CO_2 is denser than residual methane, it will accumulate toward the base of the structure and act as a cushion to the remaining gas (Worden 2024). In contrast, reservoir-scale simulations indicate that buoyancy flow remains a dominant control on plume evolution, with injected CO_2 migrating upward and updip, displacing residual methane into attic zones (Doughty and Oldenburg 2020). The actual behaviour in the EISB fields will depend on local pressure, fluid saturation and water content, with both end-member models providing valuable boundary conditions for predicting plume migration and trapping behaviour.

Containment in depleted gas fields, therefore, depends primarily on cap rock integrity, with structural architecture remaining critical to long-term storage performance. Monitoring strategies should be designed to capture the direction and extent of CO_2 movement under the prevailing phase relationships during injection and storage.

Downloaded from https://www.lyellcollection.org by Imperial College of Science, Technology and Medicine on Mar 27, 2026

Residual trapping and capillary pinning

Residual trapping occurs when, during imbibition, capillary forces strand the non-wetting gas phase within pore bodies and throats, limiting plume mobility over decadal timescales (Ghanbari *et al.* 2020). In depleted gas reservoirs, free-phase CH_4 typically persists at low overall saturation, confined to attic regions beneath the caprock, while most of the pore space is water-filled and may contain some dissolved methane. Under these conditions, CO_2 is denser than CH_4 but less dense than water, so post-injection behaviour is governed by buoyancy relative to water combined with imbibition-driven trapping.

Although reservoir pressure is lower than in undepleted systems, two-phase flow between CO_2 and formation water still occurs, and relative-permeability and capillary-pressure relationships therefore remain relevant. The assumption that low pressure eliminates these effects applies only to an idealized dry-gas system and not to water-bearing depleted fields such as those of the EISB. Numerical simulations of CO_2 injection into a depleted gas reservoir (Doughty and Oldenburg 2020) explicitly include hysteretic relative-permeability and capillary-pressure functions and demonstrate that omitting these leads to unrealistic plume evolution. After injection ceases, gas saturation declines in deeper reservoir zones and increases in shallower zones as water imbibes and CO_2 migrates upward and updip; reproducing this behaviour requires a hysteretic residual gas-saturation model. These results indicate that residual and capillary trapping mechanisms can remain operative under depleted-pressure conditions.

The efficiency of residual trapping depends strongly on fluid phase and miscibility. In localized gas-rich attic zones where CO_2 and CH_4 are fully miscible, capillary discontinuities may be limited and residual trapping less effective (Worden 2024). Where CO_2 remains in a supercritical or gas phase immiscible with residual methane, as assumed in many field-scale models, plume-scale behaviour is controlled by CO_2–H_2O capillary interactions. Residual methane may also contribute to seal integrity by forming a low-density buffer beneath the caprock, reducing the risk of CO_2 breakthrough (Bump *et al.* 2022). Overall, the available modelling and experimental evidence suggests that, under realistic phase and saturation conditions, residual and capillary trapping remain relevant processes in water-bearing depleted gas reservoirs such as those of the EISB.

Variations in capillary entry pressure may significantly influence the migration and trapping of both hydrocarbons and CO_2 in porous media at scales larger than individual pores (Gershenzon *et al.* 2016; Ghanbari *et al.* 2020; Krishnamurthy *et al.* 2022; Zhang *et al.* 2025). These variations govern fluid movement through pore throats and can immobilize supercritical and gaseous CO_2 via capillary forces, particularly where heterogeneities characterized by variations in pore-throat size are present (e.g. subtle grain-size contrasts associated with lamination, bedding and cross-stratification; see sections 'Heterogeneities in aeolian dune and aeolian sandsheet facies associations' and 'Heterogeneities in fluvial facies associations'), which can form local capillary barriers (capillary pinning *sensu* Gershenzon *et al.* 2016). Capillary trapping operates through several mechanisms, including snap-off, where non-wetting CO_2 becomes disconnected within pore bodies during drainage, and pinning, which immobilizes the CO_2 front at pore throats due to contrasts in entry pressure. Such capillary-entry heterogeneity at lamination or bedding scales can pin advancing CO_2 fronts, further immobilizing CO_2 pockets (Zhang *et al.* 2025); characterizing these facies-scale contrasts is therefore critical for predicting long-term plume behaviour in depleted gas reservoirs.

The presence of multiple fluid types and phases in the OSF reservoirs of depleted Liverpool Bay oil and gas fields complicates the actions and effects of capillary forces, and their interaction with geological heterogeneity to immobilize CO_2 by residual trapping and capillary pinning. Irreducible water saturation (S_{wirr}) refers to the fraction of pore space occupied by water that cannot be displaced by non-wetting fluids, including both hydrocarbons and CO_2. It plays a significant role in multiphase flow and trapping mechanisms in both saline aquifers and depleted gas fields, influencing relative permeability and plume migration dynamics (Krevor *et al.* 2011; Jackson and Krevor 2020). S_{wirr} is influenced by depositional and diagenetic heterogeneities such as grain size and sorting (section 'Depositional heterogeneities') and cement and clay content (section 'Diagenetic heterogeneities'), as well as by structural heterogeneities, which lie beyond the scope of this discussion (Park *et al.* 2019). In depleted oil and gas fields, particularly where residual hydrocarbons are present, the interaction between injected CO_2 and *in situ* fluids is governed by capillary pressure and phase relationships. As Ghanbari *et al.* (2020) have demonstrated, gas mixing and capillary discontinuities critically affect plume behaviour and storage performance, meaning S_{wirr} continues to influence CO_2 injectivity, distribution and residual trapping. Therefore, characterizing S_{wirr} distribution remains a valuable tool for improving CO_2 injection strategy and understanding storage security in both saline aquifers and depleted oil and gas reservoirs.

Wettability, the tendency of a fluid to adhere to grain surfaces, in the presence of another immiscible fluid, strongly influences capillary pressure relationships and thus CO_2 trapping efficiency (Baker 1995; Li and Fan 2015). While wettability effects are most extensively studied in oil-bearing systems, their relevance in depleted gas fields, particularly under low-pressure gas-phase CO_2 injection conditions such as those planned for the Liverpool Bay reservoirs (BEIS 2020), is more limited. This is primarily because interfacial tensions are much lower in the gas phase than in the supercritical phase, which in turn reduces capillary pressure gradients and the influence of wettability on pore-scale displacement and trapping (Worden 2024). Additionally, the mobility and compressibility of gas-phase CO_2 weakens viscous and capillary contrasts, limiting the effectiveness of wettability-driven residual trapping mechanisms. Nevertheless, in fields such as Lennox, where an oil leg is present (see section 'Economic resources'), oil-wet conditions may persist locally and influence CO_2–brine–rock interactions during injection. Li and Fan (2015) demonstrated that contact angles vary significantly between water- and oil-wet systems and depend on the phase state of CO_2, with a supercritical phase amplifying wettability effects. While these effects are diminished under gas-phase conditions, they may still exert a subtle control on CO_2 plume behaviour injectivity where residual hydrocarbons remain (Li and Fan 2015). The predominance of quartz- and feldspar-rich, water-wet sandstones in the Liverpool Bay reservoirs (see section 'Ormskirk Sandstone Formation') suggests that, overall, favourable wettability conditions for CO_2 containment are likely in most Liverpool Bay reservoir intervals.

Solubility trapping

Solubility trapping, which operates over decadal to centennial timescales, occurs when CO_2 molecules dissolve in formation water, forming carbonic acid. This acid enhances fluid–rock interaction and reduces plume mobility by diminishing buoyancy-driven migration. Both hydrocarbons and CO_2 can dissolve in formation water, whether brine or fresh, and in the case of CO_2, dissolution increases overall trapping security (Ghanbari *et al.* 2020). However, the extent of solubility trapping in depleted gas fields may be limited compared to saline aquifers. In hydrocarbon-bearing systems, pre-existing gas saturation and altered-water–rock interactions may reduce the efficiency of CO_2 dissolution (Worden 2024). Additionally, elevated levels of residual methane at the time of CO_2 injection may further reduce solubility trapping efficiency (Bump *et al.* 2022).

Downloaded from https://www.lyellcollection.org by Imperial College of Science, Technology and Medicine on Mar 27, 2026

Mineralization trapping

Mineralization trapping involves precipitation of carbonate minerals from CO_2-charged fluids over centennial to millennial timescales (Khandoozi *et al.* 2023; Kim *et al.* 2023). In the OSF, detrital feldspars are dominated by K-feldspars with only minor sodic plagioclase and no Ca-rich (anorthic) component (Burley 1984, 1987), meaning Ca^{2+} release and calcite formation are limited. Recent work from the basin margins of the EISB confirms this mineralogy and identifies only minor ferroan carbonates and pyrite (Scorgie *et al.* 2021), which may act as local sources for Fe^{2+} to support limited siderite or ankerite precipitation under reducing conditions. Overall, mineralization is probably a minor, spatially restricted process relative to structural, residual and solubility trapping in the EISB reservoirs.

Implications of diagenetic and pore-scale heterogeneities for CO_2 trapping

Diagenetic processes have significantly contributed to heterogeneity in the OSF (see section 'Diagenetic heterogeneities'). In the basin-centre fields targeted by the HNNWp, mechanical compaction and burial-stage quartz cementation are the dominant controls on porosity and permeability, with additional heterogeneity arising from early-stage grain dissolution and minor late-stage cementation. Authigenic illite, formed primarily during burial (Fig. 7), is present throughout the reservoir but tends to be most abundant in the water legs (Fig. 12), where its presence reduces pore throat size and permeability. By contrast, uplift-related diagenetic features, such as non-ferroan calcite precipitated from meteoric fluids and authigenic pyrite formed during subsequent reducing conditions (Figs 7, 8), are generally confined to structurally elevated zones where exposure to meteoric fluids occurred. Together, these features contribute to stratigraphic and facies-controlled barriers to flow, influencing residual trapping efficiency through permeability contrasts and anisotropic fluid behaviour (Morad *et al.* 2010; Luo *et al.* 2022; Hossain *et al.* 2024). In previously oil-charged zones, such as in Lennox Field, the presence of clay minerals and carbonate cements may further influence CO_2 residual trapping dynamics by promoting mixed CO_2–water wettability conditions. This mixed-wet behaviour arises when minerals such as illite and calcite have undergone surface alteration during prior hydrocarbon charging, leading to partial oil-wet characteristics that persist after depletion and may modify CO_2–brine contact angles during injection (Garfi *et al.* 2020).

In the Liverpool Bay reservoirs, the overall volume of diagenetic clays is modest, but their distribution and impact are stratigraphically controlled (see section 'Burial diagenetic heterogeneities'). Authigenic illite, formed during burial, occurs preferentially in the deeper reservoir sections, especially below the palaeo-GWC, where it significantly reduces permeability (Stuart 1993; Yaliz and Taylor 2003). In contrast, the upper reservoir zones, particularly in aeolian and gas-charged intervals, show minimal illite development and preserve high reservoir quality (Fig. 12). The only early-stage cements occurring in sufficient quantities to significantly reduce porosity and permeability are non-ferroan carbonates (Fig. 7), including calcite and dolomitic nodules (see section 'Early-stage diagenetic heterogeneities'). These affect 10–15% of the fluvial sandstones and 0–5% of the aeolian sandstones (Yaliz and Chapman 2003). In fluvial OSF deposits, calcitic nodules and duricrusts may create isolated localized patches of reduced permeability.

In addition to these early-stage cements, laterally variable sabkha and sheetflood interdune heteroliths (see section 'Heterogeneities in interdune sabkha, sandflat, sheetflood and playa lake facies associations') often exhibit burial-stage dolomite and anhydrite cementation (up to 15%) (Figs 7, 8), which can significantly restrict vertical permeability (Yaliz and McKim 2003). These heteroliths, typically only 1.5–3 m thick, are laterally variable and may act as vertical barriers depending on the continuity of cemented intervals. While anhydrite is not volumetrically widespread in the OSF, its occurrence in sabkha heteroliths is consistent with burial diagenesis (Greenwood and Habesch 1997). Cheshire Basin analogues show similar behaviour (Mountney and Thompson 2002; Cosgrove *et al.* 2025).

Gas production data provide direct evidence of the permeability-reducing effects of authigenic illite in the OSF. Illite typically occurs as platy, pore-lining or bridging crystals that reduce pore-throat diameter and increase flow tortuosity. In South Morecambe Field, fluvial sandstones within the illite-cemented deeper reservoir zones exhibit permeabilities two to three orders of magnitude lower than those in the overlying illite-free intervals (Fig. 12) (Stuart and Cowan 1991). In contrast, authigenic illite is much less common, and locally absent, in the southern EISB, particularly in the Liverpool Bay fields, reflecting basin-wide differences in burial history and diagenetic conditions (Meadows 2006). Aeolian sandstones exhibit much weaker permeability contrasts between reservoir intervals, highlighting a facies-dependent control on permeability (Cowan 1993). This contrast probably reflects the higher proportions of feldspar and lithic fragments in fluvial sandstones (Fig. 8d), which provide additional chemical precursors (notably K^+, Al^{3+} and Fe^{2+} sources) for illite formation during burial. In contrast, the quartz-dominated and well-sorted aeolian facies (Fig. 8a) lack these reactive components, limiting authigenic clay development (Greenwood and Habesch 1997). These inter-facies variations in clay content and resulting flow properties may influence the preferential migration and trapping behaviour of CO_2 during injection and post-injection phases.

Further evidence for this pattern of diagenetic control on permeability comes from analogue studies outside the EISB. A minipermeameter study in the Cheshire Basin showed that mean permeabilities across six lithofacies of the Helsby and Wilmslow Sandstone formations varied by an order of magnitude, with clay content exerting a strong control, while calcite cement had a negligible effect due to its low abundance, partial dissolution and discontinuous distribution (Bloomfield *et al.* 2006). More recent work using core plug and minipermeameter measurements from the Endurance CO_2 storage site in the Bunter Sandstone Formation (see section 'Economic resources') demonstrated that grain size and cement distribution can produce up to three orders of magnitude variation in permeability (Hossain *et al.* 2024). These findings suggest that similar heterogeneities in the OSF could significantly influence anisotropic CO_2 fluid flow during injection and migration.

In sections of the OSF that reached significant burial depths during the Mesozoic, diagenetic cements such as quartz overgrowths (Fig. 8b) and ferroan dolomite formed through pressure dissolution and precipitation (see section 'Burial diagenetic heterogeneities'). The resulting spatial variations in cementation reflect differences in depositional facies, with quartz overgrowths and ferroan carbonate cementation most developed in fluvial facies associations, where grain morphology and detrital clay content promoted nucleation. In contrast, aeolian dune and sandsheet facies associations exhibit lower cement abundance and preserve higher porosity (Figs 8a, c and 12). During uplift, limited teleogenetic overprinting occurred, most notably the precipitation of non-ferroan calcite, postulated to have derived from thermochemical sulfate reduction involving methane, as evidenced by low $\delta^{13}C$ values and the associated presence of authigenic pyrite (Greenwood and Habesch 1997) (Fig. 7 and 'Uplift diagenetic heterogeneities' section). Illite, by contrast, is interpreted as a burial-phase mineral and not a product of meteoric overprinting (see 'Burial diagenetic heterogeneities').

Pore-scale heterogeneities, including variations in wettability, pore-throat geometry and capillary entry pressure, can further influence CO_2 migration and trapping. Such features may disrupt

Downloaded from https://www.lyellcollection.org by Imperial College of Science, Technology and Medicine on Mar 27, 2026

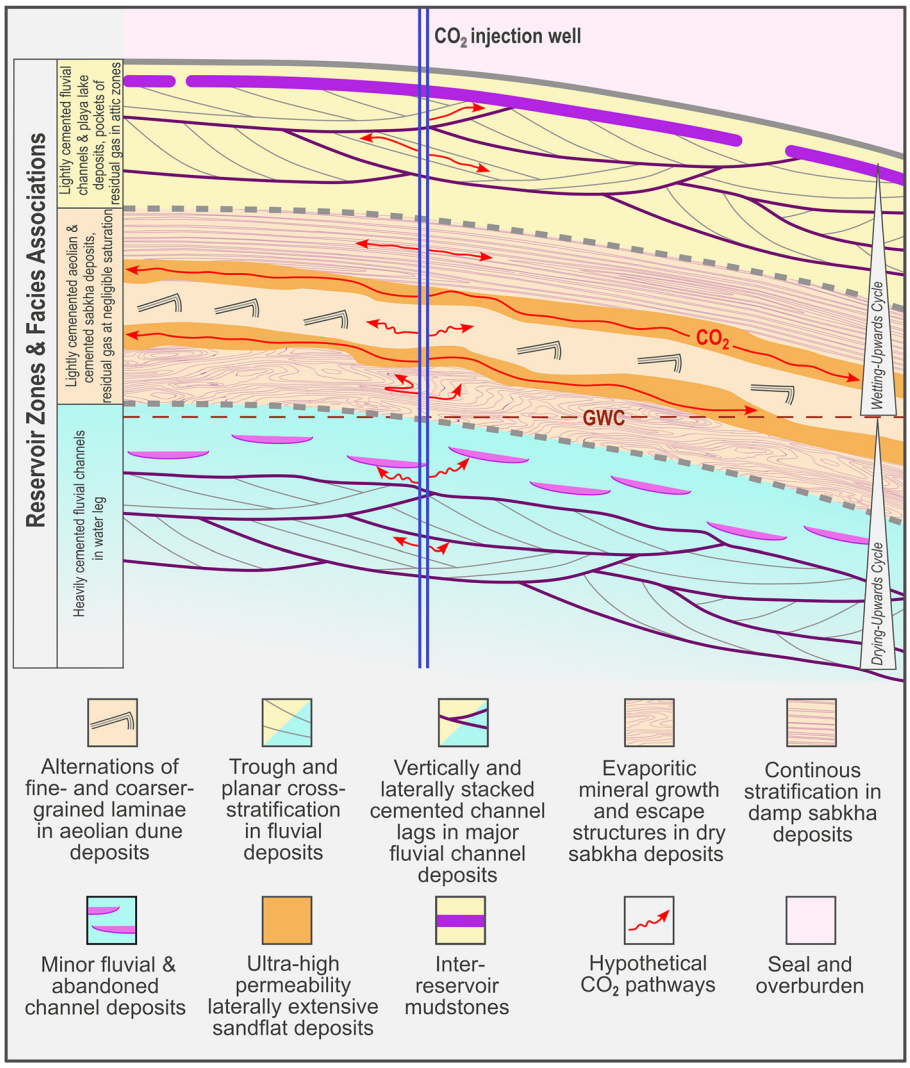


Fig. 12. Idealized schematic diagram of the reservoir architecture of a mixed aeolian–fluvial system (analogous to the Ormskirk Sandstone Formation, characterized by drying-upward and wetting-upward cycles; *sensu* Meadows 2006), showing the hypothetical responses of distinct facies associations to CO_2 injection. The model represents a simplified cross-section through a depleted gas reservoir, highlighting contrasts between high-permeability aeolian dune and sandsheet deposits, moderate-permeability fluvial channel deposits, and low-permeability sabkha and interdune heteroliths. Below the gas–water contact (GWC), reservoir zones may be heavily cemented; pore-space occlusion inhibits CO_2 migration and increases flow tortuosity. Zones of greater-than-residual CO_2 saturation may occur below capillary barriers (e.g. abandoned channel deposits) due to capillary pinning, and in the water leg, brine may imbibe into pores during post-injection equilibration, resulting in isolated CO_2 ganglia, or 'snap off' (*sensu* Zhang *et al.* 2025). Evaporitic mineral growth and escape structures in dry sabkha deposits that obscure primary bedding may result in relatively higher vertical permeability compared with the more laterally continuous stratification in damp sabkha deposits (Herries and Cowan 1997). Small-scale textural variations within aeolian dune deposits can influence fluid migration and create localized anisotropic flow (Newell and Shariatipour 2016). High-permeability, laterally extensive aeolian sandflat deposits are likely to control the lateral migration rate of injected CO_2 plumes (Meadows 2006; Newell and Shariatipour 2016; Alshakri *et al.* 2023). Erosionally based, coarse-grained fluvial channel elements exhibit the highest porosity and permeability relative to other fluvial architectural elements and are therefore likely to act as primary flow conduits within this facies association (Meadows and Beach 1993*a*). Within these fluvial deposits, intergranular porosity aligned with bedding surfaces may promote enhanced horizontal flow, although the vertical and lateral stacking of channel elements may locally restrict connectivity (Wakefield *et al.* 2015). Cemented channel lags within fluvial sections can act as barriers or baffles to vertical fluid flow (Newell and Shariatipour 2016), while laterally extensive playa-lake mudstones may also compartmentalize the reservoir and act as inter-reservoir barriers to vertical CO_2 migration (Alshakri *et al.* 2023).

large-scale buoyancy-driven flow, leading to localized plume immobilization and enhancing residual trapping efficiency (Fig. 12) (Ghanbari *et al.* 2020; Krishnamurthy *et al.* 2022).

Implications of depositional heterogeneities for CO_2 trapping

Within the wide range of facies present in the OSF, depositional processes influencing grain size, composition and textural maturity are the main controls on reservoir quality (see section 'Depositional heterogeneities') (Yaliz and Chapman 2003; Yaliz and Taylor 2003). Depositional heterogeneities critically affect CO_2 injection and storage by influencing porosity and permeability, and by introducing variations in scale, geometry, continuity, spatial distribution and rock properties at multiple scales, thereby significantly impacting fluid flow within a reservoir (Alshakri *et al.* 2023). This section examines the influence of depositional heterogeneities across multiple scales on CO_2 trapping and migration, drawing on hydrocarbon production data from the Liverpool Bay fields as direct evidence of reservoir dynamics.

Downloaded from https://www.lyellcollection.org by Imperial College of Science, Technology and Medicine on Mar 27, 2026

Pore- and facies-scale heterogeneities: grain size variation, lamina-scale and sedimentary structures

In South and North Morecambe fields, gas recovery from an interval of fluvial, sabkha and subordinate aeolian facies associations was highly sensitive to permeability anisotropy (i.e. k_v/k_h ratio), with flow particularly restricted in zones overprinted by illite cementation (see section 'Diagenetic heterogeneities') (Thomas *et al.* 1996). This illustrates how small-scale depositional heterogeneity, when compounded by diagenetic modification, can strongly influence flow architecture.

Aeolian sandstones, though typically well-sorted and highly permeable, contain small-scale cross-stratification and more subtle textural features including grainflow/grainfall laminae (Fig. 9b) and pinstripe lamination (see section 'Heterogeneities in aeolian dune and aeolian sandsheet facies associations') that influence fluid migration (Weber 1982; Goggin *et al.* 1988; Swanson *et al.* 2006; Newell and Shariatipour 2016; Alshakri *et al.* 2023). These features can create localized anistropic fluid flow (Fig. 12). In Auk Field (North Sea) permeability was higher in grainflow strata and lower in wind-rippled intervals, with cements and clay mineral accumulations in laminated zones restricting flow (Prosser and Maskall 1993).

Desiccation cracks, wavy lamination (Figs 9f–i and 11) and localized evaporite cementation (see section 'Implications of diagenetic and pore-scale heterogeneities for CO_2 trapping') within sabkha and interdune heteroliths ('Heterogeneities in interdune sabkha, sandflat, sheetflood and playa lake facies associations') compartmentalize the reservoir at fine scales. In the damp sabkha facies association, relatively continuous stratification tends to inhibit vertical fluid migration and promote lateral flow, whereas in the dry sabkha facies association, evaporitic crystal growth and disruption of primary bedding may enhance vertical permeability (i.e. higher k_v/k_h) and local connectivity (Fig. 12) (Herries and Cowan 1997). These contrasts illustrate how subtle textural differences within similar depositional environments can strongly influence flow anisotropy and potential CO_2 plume evolution.

Fluvial facies associations, comprising the majority of deposits in the OSF (Cowan 1993), exhibit small-scale sedimentological heterogeneities linked to grain size and sorting (see section 'Heterogeneities in fluvial facies associations'; Figs 8d, 9j–m, 10 and 11), which influence fluid flow. Outcrop and subsurface analogues from the Bunter Sandstone Formation show that lamina-scale variation, particularly in grain size, lamination style and clay content, can drive up to two orders of magnitude variation in effective permeability (Hossain *et al.* 2024). Facies-scale (0.01–10 m^3) models constructed using sketch-based modelling methods (Fig. 13) (Jacquemyn *et al.* 2021) demonstrate that effective permeability correlates most strongly with the proportion of clay-poor sandstone (Hossain *et al.* 2024).

Reservoir-zone-scale heterogeneities: facies associations and architectural elements

The OSF contains laterally extensive aeolian sandsheets (see section 'Heterogeneities in aeolian dune and aeolian sandsheet facies associations'), which form high-permeability carrier beds within a complex reservoir architecture (Figs 8c, 9e and 12) (Cowan 1993; Cowan *et al.* 1999). This stratigraphic compartmentalization is comparable to that observed in the SSG at Wytch Farm (Wessex Basin), where clean sandstone bodies are interbedded with flow barriers and baffles (Hogg *et al.* 1999). Similar aeolian deposits are present in the Frogmouth Unit, within the predominantly fluvial Delamere Member of the Cheshire Basin HSF, and extend laterally for hundreds of metres (Mountney and Thompson 2002).

The low-angle, wavy laminations characteristic of heterolithic sabkha and sheetflood facies associations in the OSF (Figs 8b and 9f, g, i; see section 'Heterogeneities in interdune sabkha, sandflat, sheetflood and playa lake facies associations') are interpreted to reflect a range of processes, including aeolian sand adhering to episodically damp surfaces (Table 2), subaqueous reworking of former aeolian ripples during episodic unconfined high-energy sheetflood events, subaerial modification of previously subaqueous ripples, evaporite precipitation and algal growth (Hummel and Kocurek 1984; Cowan 1993; Meadows and Beach 1993*a*; Jones and Ambrose 1994; Herries and Cowan 1997; Thompson and Meadows 1997; Mountney and Thompson 2002; Meadows 2006; Cosgrove *et al.* 2025). Cored intervals of this facies have been correlated over kilometres across Block 110/13 (Hamilton and Hamilton North fields) (Yaliz and McKim 2003), and over several hundred metres in Block 110/15 (Lennox Field) (Yaliz and Chapman 2003).

Lateral correlation of these facies between cored wells typically assumes that heterolithic sabkha deposits are non-climbing, implying limited vertical connectivity. However, as Mountney and Thompson (2002) proposed, reinterpreting dry interdune units as climbing interdune sandstones would increase both vertical and lateral connectivity of sandstone bodies (Table 2) and thereby enhance fluid migration (Rubin and Hunter 1982).

Variations in the angle of climb influence the geometry and connectivity of interdune deposits. Higher angles promote vertical stacking and enhance vertical connectivity across stratigraphic levels, while lower angles produce thinner, laterally extensive units that reduce vertical flow (Fig. 12). These trends reflect palaeo-water-table dynamics during deposition (Mountney and Thompson 2002) (Table 2). Recognizing such patterns aids prediction of vertically restricted flow zones that enhance capillary pinning or complicate plume migration.

In fluvial OSF units, depositional architecture, particularly facies association extent, stacking and interfingering, strongly influence fluid flow (Fig. 12). Much of the current understanding of these units is derived from core data, particularly from the Sellafield area in West Cumbria (Barnes *et al.* 1994), where outcrop is limited or absent. However, fluvial outcrops do occur along the southern margin of the EISB in the Wirral region, although these are commonly interbedded with aeolian facies associations (Meadows 2006). Erosional lags in OSF channel bases can reach 30 cm in thickness (Fig. 10a) and laterally extend for tens to hundreds of metres (Herries and Cowan 1997). Where cemented, these features act as baffles or barriers to vertical fluid flow (Fig. 12; see section 'Early-stage diagenetic heterogeneities') (Newell 2006; Alshakri *et al.* 2023).

Depositional fabrics such as cross-stratification (Fig. 11) can enhance effective permeability parallel to bedding, a factor that affects reservoir quality and influences fluid migration (Weber 1982). Channel-base scours and associated lags can adversely affect effective vertical permeability (k_{ve}). Pebble and mudclast lags, locally cemented by quartz and carbonate (both dolomite and calcite) within a sandstone matrix, can act as baffles and barriers to vertical fluid flow (Strong 1993; Barnes *et al.* 1994). The vertical and lateral stacking of major fluvial channels into multilateral, multistorey bodies (Figs 11, 12) creates complex reservoir architectures, leading to compartmentalization and affecting connectivity and fluid flow pathways (Jones *et al.* 1995; Alshakri *et al.* 2023).

In South Morecambe Field, cored sections from wells 110/2a-F1, 110/2a-7 and 110/2a-H5 (Fig. 4c) contain transverse bars with internal stratification, including upward-fining sequences, with well-developed planar and trough cross-stratification (Figs 10 and 11) (Stuart and Cowan 1991). At a slightly larger scale, in the same wells, stacked fluvial channel-fill deposits with sharp erosional bases are interpreted to cut down into thin aeolian units (Cowan 1993). These sedimentary structures may create anisotropic flow patterns, enhancing permeability parallel to bedding while restricting vertical fluid migration (Fig. 12).

Downloaded from https://www.lyellcollection.org by Imperial College of Science, Technology and Medicine on Mar 27, 2026

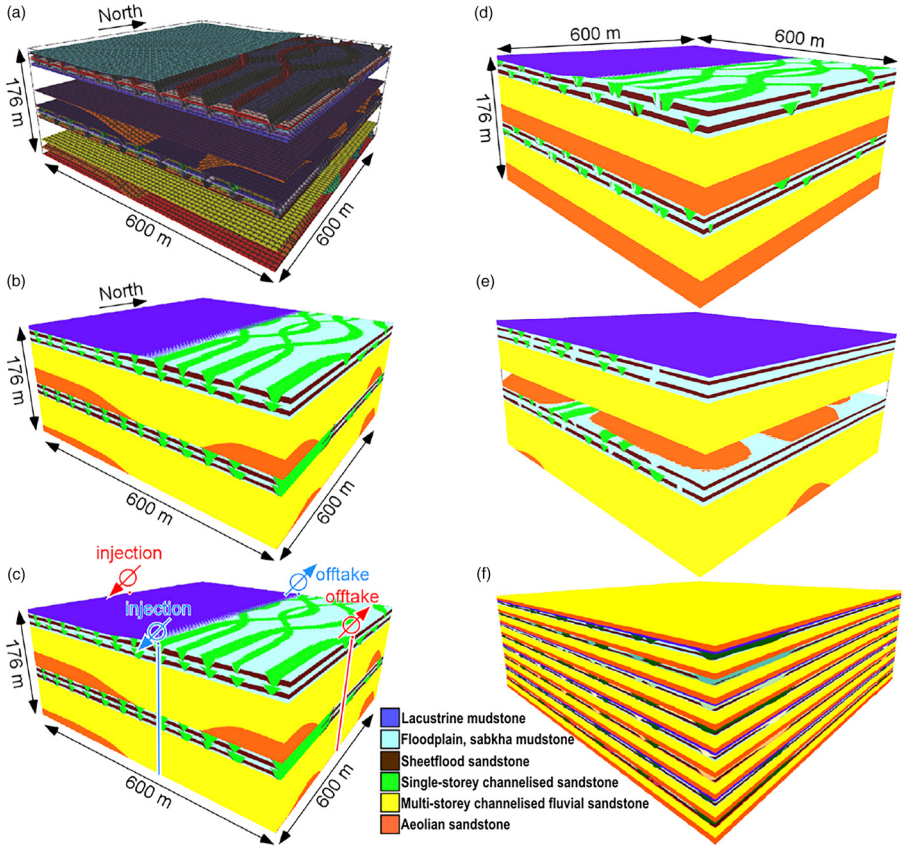


Fig. 13. Sketch-based stratigraphic models illustrating how sedimentological heterogeneity influences CO_2 flow behaviour in mixed fluvial–aeolian systems, based on Sherwood Sandstone Group analogues. (**a**–**c**) Representative model outputs showing: (a) geologically realistic sketch-generated surfaces; (b) surface-bounded depositional domains; and (c) well placements used to simulate south–north (blue) and west–east (red) tracer flows. (**d**–**f**) Selected models displaying contrasting heterogeneity configurations: (d) Model 28 – thick facies association layers, laterally continuous aeolian sandsheets, discontinuous lacustrine mudstones, poorly connected fluvial bodies and discontinuous heterolithic layers; (f) Model 15 – thick facies association layers, laterally discontinuous aeolian sandstone lenses and laterally continuous mudstone sheets with a few well-connected fluvial units and discontinuous sheetflood sandbodies; (f) Model 15 – thin layer cake facies association layers with laterally continuous aeolian sandsheet and lacustrine mudstone layers with numerous poorly connected fluvial units. All models were generated using the sketch-based modelling workflow of Jacquemyn *et al.* (2021). This approach enables rapid construction of stratigraphic architectures and screening of how different heterogeneity impacts flow scenarios in carbon capture and storage-relevant reservoirs. Source: from Alshakri *et al.* (2023).

In SSG fluvial sandstones at Styrrup Quarry (Eastern Shelf Basin; Fig. 4a), erosionally based channel elements with coarse-grained sandstones and pebble lags exhibit the highest porosity and permeability relative to other fluvial architectural elements, acting as primary flow conduits within fluvial facies associations (Wakefield *et al.* 2015). Similar architectures are present in the Liverpool Bay OSF fields (Fig. 10a) (Yaliz and Chapman 2003; Yaliz and Taylor 2003), where vertically stacked channel elements may enhance k_{ve}, though cemented lags along erosional channel bases can locally restrict vertical flow (Fig. 12).

Lateral- and downstream-accreting architectural elements, composed of cross-bedded sandstones arranged in dipping barform strata (Fig. 10a), may exhibit relatively high effective horizontal permeability (k_{he}), though this can be disrupted by bed truncations at element boundaries (Wakefield *et al.* 2015). Enhanced horizontal flow is attributed to the lateral continuity of low-angle cosets (up to 40 m wide, 2.6 m thick), medium to coarse grain size, upward-fining trends and intergranular porosity aligned with depositional surfaces. Based on observations from Styrrup Quarry, the absence of interbedded mudstones or palaeosols, along with clean, conformable erosive bounding surfaces, limits disruption to fluid flow between stacked elements (Wakefield *et al.* 2015). A recent outcrop study of the Lower Triassic Buntsandstein Group in the Upper Rhine Graben demonstrated that permeability was higher in lower flow-regime trough cross-bedded sandstones compared to upper flow-regime low-angle cross-bedded sandstones (Bofill *et al.* 2025).

Table 2. Summary of the effects of palaeo-water-table fluctuations during deposition on interdune geometry and connectivity

Palaeo-water-table behaviour	Effect on interdune geometry	Impact on connectivity
Steady rise	Climbing, vertically stacked interdune deposits	Good vertical and moderate lateral connectivity
Fluctuating	Episodic interdune deposits of variable thickness	Patchy vertical and lateral connectivity
Static high	Laterally extensive, thin interdune deposits	Poor vertical, good lateral connectivity
Falling	Deflated or erosional interdune deposits	Very poor or fragmented connectivity

Source: based on Mountney and Thompson (2002).

Downloaded from https://www.lyellcollection.org by Imperial College of Science, Technology and Medicine on Mar 27, 2026

Table 3. Summary of reservoir quality in the Ormskirk Sandstone Formation by facies association, based on data from wells in the South Morecambe Field (Fig. 4a)

Facies associations	Porosity (%)	Permeability (mD)	Gas recovery potential	Notes
Major Fluvial Channel, Minor Fluvial Channel	12–18%	100 to >1000 mD	Moderate to high	Low to moderate cement content
Abandoned Fluvial Channel, Sheetflood	Commonly >10%	<0.1 to ~1 mD	Very low to none	Fine-grained, high illite content, quartz overgrowth
Damp Interdune, Wet Interdune, Sabkha, Playa Lake	~4–22%	Similar range to fluvial sandstones	Low to moderate (variable)	Highly variable permeability: reworked aeolian intervals have relatively high permeability, other clay-rich intervals low permeability
Aeolian Dune, Aeolian Sandsheet, Dry Interdune	14–26%	100 to >3000 mD	High	Some aeolian units so friable that core-analysis unreliable

Source: based on Meadows and Beach (1993*a*) and Cowan *et al.* (1999).

Reservoir-scale and basin-scale heterogeneities

Reservoir- and basin-scale heterogeneities govern CO_2 plume migration, pressure dissipation and long-term containment efficiency, key factors in the design and monitoring of CCS operations. Understanding heterogeneities at this scale in the Liverpool Bay reservoirs is essential for predicting injection behaviour and plume migration, and ensuring secure long-term storage.

Hydrocarbon production data indicate that the distribution and lateral continuity of reservoir-scale aeolian sandstone bodies (Fig. 10b, c) is the primary control on horizontal fluid migration within the OSF. In South Morecambe Field, approximately 50% of production from well 110/2a-7 (Fig. 4c) originated from a 6 m thick aeolian dune unit within a 200 m hydrocarbon column (Cowan 1993). These units exert disproportionate control on flow behaviour and are likely to act as preferential CO_2 migration pathways (Fig. 12). Production data suggest these thin aeolian units are laterally extensive, with some correlated across 70 km^2 and between wells up to 10 km apart (see section 'Heterogeneities in aeolian dune and aeolian sandsheet facies associations'). RFT data from well 110/2a-H5 (Fig. 4c) showed that a thin, high-permeability aeolian layer experienced rapid pressure depletion and maintained pressure communication across the field (Cowan 1993). Such units may have enabled early water breakthrough during production and could similarly promote preferential lateral CO_2 plume migration (Fig. 12).

Interpreting the dominant aeolian dune and related cross-stratification types in the OSF has important implications for predicting reservoir connectivity and plume migration pathways. While ancient aeolian deposits are often interpreted as barchanoid dunes, modern desert systems frequently host more complex forms, such as linear, star or reversing dunes, with multidirectional permeability anisotropy (Fryberger *et al.* 2021). In the OSF, limited high-resolution subsurface data introduce uncertainty regarding cross-stratification geometry and continuity of aeolian dune sandstones. Misinterpreting these forms during drill stem testing or modelling could lead to overestimating lateral connectivity, particularly in fields such as Hamilton and Hamilton North, where thin, high-permeability aeolian sandstones dominated production in reservoir Zones I and III (Yaliz and Taylor 2003).

Heterolithic sandstones analogous to those of the OSF (see section 'Heterogeneities in interdune sabkha, sandflat, sheetflood and playa lake facies associations') have been documented to extend laterally over 1.5 km in coastal sabkha deposits of the Jurassic Page Sandstone, Utah (Taggart *et al.* 2010), with composite stratigraphic sections of sheetflood deposits (Fig. 9i) up to 300 m thick. In the Permian Cutler Group (Utah), similar deposits reach 5 m in thickness and span up to 300 m between pinchouts (Jordan and Mountney 2010). Reinterpreted as damp interdune architectural elements (Hême de Lacotte and Mountney 2022), such heteroliths may significantly reduce vertical permeability and enhance reservoir anisotropy (Fig. 12).

Gas production data from wells 110/2-1, 110/2-2, 110/2-3, 110/2-5, 110/2-6, 110/3-1, 110/3-3, 110/7-1, 110/9-1 and 113/26-1 (Fig. 4c) in the OSF of North and South Morecambe fields demonstrate that porosity and permeability variability within fluvial sandstone intervals significantly influenced production performance (Table 3). Reservoir zones composed of major and minor fluvial channel sandstones exhibited high permeability (100–1000 mD) and porosity ranging from 12 to 18%, serving as the primary conduits for gas flow within this facies association (Fig. 12). In contrast, finer-grained abandoned fluvial channel (Fig. 9j), sheetflood (Fig. 9i) and sabkha (Fig. 9f, g) deposits displayed lower permeability, which adversely affected gas flow and recovery efficiency (Meadows and Beach 1993*a*). This reservoir-scale compartmentalization is further compounded by diagenetic modification, particularly the development of authigenic quartz cement, arguably the most significant pore-occluding cement in the OSF (see sections 'Burial diagenetic heterogeneities' and 'Implications of diagenetic and pore-scale heterogeneities for CO_2 trapping'), and burial-stage illite. These low-permeability zones acted as flow barriers, compartmentalizing the reservoir, lowering production rates and causing localized overpressure. Such barriers may restrict CO_2 migration and contribute to stratigraphic compartmentalization and reduced sweep efficiency during storage (Fig. 12).

Similar variability in gas flow was not observed in Hamilton and Hamilton North fields. Pressure monitoring across wells in both reservoirs showed uniform depletion, with no evidence of significant stratigraphic compartmentalization, probably due to the simple horst block structure, high net:gross ratio, limited diagenetic overprint and laterally continuous facies architecture (Yaliz and Taylor 2003). In contrast, Lennox Field exhibits significant interbedding of fluvial and thin aeolian sandstones, similar to the reservoir architecture of South Morecambe Field, and experienced notable water encroachment during production (Yaliz and Chapman 2003). This suggests that high-permeability carrier beds may strongly influence CO_2 migration pathways (Fig. 12).

Integrating multi-scale heterogeneities into predictive models is essential for understanding plume behaviour and optimzing CO_2 storage strategies. A sketch-based reservoir modelling workflow developed by Jacquemyn *et al.* (2021) enables geoscientists to construct geologically realistic 3D representations of facies- and reservoir-scale complexity. As illustrated in Figure 13, this approach allows the simulation of contrasting heterogeneity scenarios, demonstrating how variations in aeolian sandsheet continuity, mudstone extent and fluvial sandbody connectivity influence CO_2 migration pathways and breakthrough times. This approach provides transferable insight into how sedimentological heterogeneity governs flow behaviour and storage performance in CCS reservoirs beyond the Liverpool Bay OSF.

Downloaded from https://www.lyellcollection.org by Imperial College of Science, Technology and Medicine on Mar 27, 2026

Conclusions

The OSF is a complex reservoir interval that, as demonstrated in this contribution, contains a diverse suite of sedimentological heterogeneities arising from both diagenetic and depositional processes. These heterogeneities occur across a wide range of scales within all OSF facies associations, from pore-throat-blocking illite at the pore scale, to thin laminae at the facies scale, and to stacked architectural elements spanning hundreds of metres in width and tens of metres in thickness at the reservoir-zone scale. At the reservoir scale, the intercalation of aeolian sandstones, fluvial sandstones, and sabkha or overbank heteroliths defines laterally extensive flow zones within the reservoir.

The findings from this review highlight the importance of interactions between distinct sedimentological processes, such as the aeolian reworking of fluvial deposits, the fluvial reworking of aeolian sands, particularly within minor channel fills, and cyclical changes in the palaeo-water table, in generating a complex facies architecture that exhibits repeating heterogeneity patterns throughout the OSF. The presence or absence of early-stage evaporitic cements (e.g. gypsum and anhydrite) within sabkha deposits can locally occlude pore space, while the dominant porosity-reducing cements are burial-stage quartz overgrowths and carbonate cements. These are volumetrically significant in fluvial facies associations but less common in the aeolian and interdune deposits. Burial-related compaction and cementation reduced primary porosity in zones lacking early-stage cement frameworks and represent a key control on reservoir quality in the Liverpool Bay fields. Late-stage, uplift-related cements and authigenic minerals (e.g. non-ferroan calcite and pyrite), confined to the water-legs and absent from hydrocarbon-charged intervals, suggest that hydrocarbon charge inhibited their development by excluding reactive fluids or altering redox conditions. Collectively, these features record a multi-stage geological evolution, from primary deposition and early diagenetic modification, through burial-related porosity reduction, to late-stage uplift and meteoric overprinting.

To assess the significance of these heterogeneities for CO_2 injection and migration within the Hamilton, Hamilton North and Lennox reservoirs, the following points merit consideration:

- Early-stage diagenesis: dissolution of labile detrital grains (e.g. feldspar) led to the precipitation of grain coatings and patchy cementation, and coupled with calcite cementation these early cements provided a local framework during burial, resisting compaction and helping to preserve primary porosity, particularly in aeolian dune, aeolian sandsheet and dry interdune facies associations.
- Burial-stage processes: mechanical compaction and the precipitation of quartz overgrowths, illite, calcite and non-ferroan dolomite significantly reduced porosity and permeability, especially in fluvial facies associations. These effects reflect both the higher abundance of labile grains and clays in fluvial sediments and the limited development of early-stage cement frameworks that could otherwise have inhibited compaction.
- Hydrocarbon influence: sandstones lacking a hydrocarbon charge were more susceptible to late-stage uplift-related pore occlusion, including precipitation of non-ferroan calcite and pyrite, which reduced porosity and permeability. Charged zones were protected from this overprinting and typically retain higher reservoir quality.
- Aeolian facies association distribution: aeolian sandstones occur mainly along basin margins, particularly the southern, eastern and northeastern sectors, reflecting palaeotopographic highs and local fluvial diversion. In the basin centre, aeolian units are thinner, often reworked and typically interbedded with other facies, but can still be laterally extensive. Even subtle heterogeneities in this facies association (e.g. grainfall and grainflow laminae) can exert a significant control on permeability.
- Reservoir architecture: the complex interbedding of aeolian, sabkha/interdune and fluvial facies associations results in enhanced lateral and vertical facies heterogeneity at the reservoir scale. Extremely high-porosity and high-permeability aeolian sandstones (up to 30% porosity and 10 D) will probably act as preferential conduits for CO_2 migration, dictating the direction and rate of lateral plume migration within the Liverpool Bay reservoirs.
- Facies stacking patterns: complex stacking of vertically amalgamated, erosively based channels and laterally extensive barform-accretion packages generates strong permeability anisotropy. Architectural- and bedform-scale features combine to inhibit vertical flow and enhance lateral connectivity, contributing to reservoir compartmentalization.

Scientific editing by Gene Rankey

Acknowledgements The authors thank Neil Meadows, Richard Worden and Gene Rankey for their critical reviews and editorial assessments, which greatly improved the manuscript. Neil Meadows (Redrock International Limited) also provided valuable advice and the loan of thin sections that greatly supported this study. Margaret Collinson, Kevin de Souza, Christina Manning and Jerry Morris (Royal Holloway, University of London) are gratefully acknowledged for their assistance with microscopy. Thanks also to Frank Lehane (Royal Holloway, University of London) for his IT support, and to Amaia and Enara Breeze for their instruction in the use of *Procreate*. We also thank SLB for provision of *Petrel* seismic and well interpretation software via an academic software donation.

Author contributions **DB**: conceptualization (lead), investigation (equal), methodology (lead), visualization (lead), writing – original draft (lead), writing – review & editing (lead); **NS**: supervision (supporting), writing – review & editing (supporting); **GJH**: writing – review & editing (supporting); **DC**: investigation (equal), supervision (lead), writing – review & editing (supporting)

Funding This work was funded by the Natural Environment Research Council and the ARIES Doctoral Training Partnership (NE/S007334/1).

Competing interests The authors declare that they have no known competing financial interests or personal relationships that could have appeared to influence the work reported in this paper.

Data availability Data sharing is not applicable to this article as no datasets were generated or analysed during the current study.

References

Alshakri, J., Hampson, G.J. *et al.* 2023. A screening assessment of the impact of sedimentological heterogeneity on CO_2 migration and stratigraphic-baffling potential: Sherwood and Bunter sandstones, UK. *Geological Society, London, Special Publications*, **528**, 245–266, https://doi.org/10.1144/SP528-2022-34

Ambrose, K., Hough, E., Smith, N.J.P. and Warrington, G. 2014. *Lithostratigraphy of the Sherwood Sandstone Group of England, Wales and South-West Scotland*. British Geological Survey, Nottingham, UK, https://nora.nerc.ac.uk/id/eprint/507530

Armstrong, J.P., Smith, J., D'Elia, V.A.A. and Trueblood, S.P. 1997. The occurrence and correlation of oils and Namurian source rocks in the Liverpool Bay–North Wales area. *Geological Society, London, Special Publications*, **124**, 195–211, https://doi.org/10.1144/GSL.SP.1997.124.01.12

Audley-Charles, M.G. 1970. Stratigraphical correlation of the Triassic rocks of the British Isles. *Quarterly Journal of the Geological Society, London*, **126**, 19–46, https://doi.org/10.1144/gsjgs.126.1.0019

Bachu, S. 2000. Sequestration of CO_2 in geological media: criteria and approach for site selection in response to climate change. *Energy Conversion and Management*, **41**, 953–970, https://doi.org/10.1016/S0196-8904(99)00149-1

Baker, L.E. 1995. Three-phase relative permeability of water-wet, intermediate-wet and oil-wet sandstone. *Geological Society, London, Special Publications*, **84**, 51–61, https://doi.org/10.1144/GSL.SP.1995.084.01.06

Downloaded from https://www.lyellcollection.org by Imperial College of Science, Technology and Medicine on Mar 27, 2026

Barnes, R.P., Ambrose, K., Holliday, D.W. and Jones, N.S. 1994. Lithostratigraphical subdivision of the Triassic Sherwood Sandstone Group in west Cumbria. *Proceedings of the Yorkshire Geological Society*, **50**, 51–60, https://doi.org/10.1144/pygs.50.1.51

Bastin, J.C., Boycott-Brown, T., Sims, A. and Woodhouse, R. 2003. The South Morecambe Gas Field, Blocks 110/2a, 110/3a, 110/7a and 110/8a, East Irish Sea. *Geological Society, London, Memoirs*, **20**, 107–118, https://doi.org/10.1144/GSL.MEM.2003.020.01.09

BEIS 2020. *HyNet CCUS Pre-FEED Flow Assurance Report*. Progressive Energy Ltd, on behalf of the HyNet Consortium, https://assets.publishing.service.gov.uk/media/629535dad3bf7f036ebf58cd/HyNet_CCUS_Pre-FEED_KKD_WP5_HYN01-03_Rev_03_Flow_Assurance_Report.pdf

Benson, S., Cook, P. *et al.* 2005. *IPCC Special Report on Carbon Dioxide Capture and Storage*. IPCC, Geneva, Switzerland, 195–276.

Bloomfield, J.P., Moreau, M.F. and Newell, A.J. 2006. Characterization of permeability distributions in six lithofacies from the Helsby and Wilmslow sandstone formations of the Cheshire Basin, UK. *Geological Society, London, Special Publications*, **263**, 83–101, https://doi.org/10.1144/GSL.SP.2006.263.01.04

Bofill, L., Bozetti, G. *et al.* 2025. Sedimentary control on permeability heterogeneity: the middle Buntsandstein continental sandstones (Lower Triassic, eastern France). *Marine and Petroleum Geology*, **173**, 107261, https://doi.org/10.1016/j.marpetgeo.2024.107261

Brookfield, M.E. 2004. The enigma of fine-grained alluvial basin fills: the Permo-Triassic (Cumbrian Coastal and Sherwood Sandstone Groups) of the Solway Basin, NW England and SW Scotland. *International Journal of Earth Sciences: Geologische Rundschau*, **93**, 282–296, https://doi.org/10.1007/s00531-004-0381-z

Brookfield, M.E. 2008. Palaeoenvironments and palaeotectonics of the arid to hyperarid intracontinental latest Permian-late Triassic Solway basin (U.K.). *Sedimentary Geology*, **210**, 27–47, https://doi.org/10.1016/j.sedgeo.2008.06.003

Bump, A., Bakhshian, S., Hovorka, S., Rhodes, J. and Neades, S. 2022. Criteria for depleted reservoirs to be developed for CO_2 storage. 16th International Conference on Greenhouse Gas Control Technologies, 23–24 Ocober, Lyon. SSRN Electronic Journal, https://doi.org/10.2139/ssrn.4286409

Bunce, J. 2018. The history of exploration and development of the Liverpool Bay fields and the east Irish Sea basin. *Geological Society, London, Special Publications*, **465**, 95–118, https://doi.org/10.1144/SP465.6

Burgess, P.M., Dobromylskyj, E. and Lovell-Kennedy, J. 2025. Probably proximal pebbles? An outcrop-constrained quantitative analysis of clast transport distances in the lower Triassic Sherwood Sandstone Group, UK. *Journal of the Geological Society, London*, **182**, https://doi.org/10.1144/jgs2024-155

Burley, S.D. 1984. Patterns of diagenesis in the Sherwood Sandstone group (Triassic), United Kingdom. *Clay Minerals*, **19**, 403–440, https://doi.org/10.1180/claymin.1984.019.3.11

Burley, S.D. 1987. *Diagenetic Modelling in the Triassic Sherwood Sandstone Group of England and Its Offshore Equivalents, United Kingdom Continental Shelf*. PhD thesis, University of Hull, https://hull-repository.worktribe.com/output/4209690/diagenetic-modelling-in-the-triassic-sherwood-sandstone-group-of-england-and-its-offshore-equivalents-united-kingdom-continental-shelf

Bushell, T.P. 1986. Reservoir geology of the Morecambe Field. *Geological Society, London, Special Publications*, **23**, 189–208, https://doi.org/10.1144/GSL.SP.1986.023.01.12

Chedburn, L., Underhill, J.R., Head, S. and Jamieson, R. 2022. The critical evaluation of carbon dioxide subsurface storage sites; geological challenges in the depleted fields of Liverpool Bay. *AAPG Bulletin*, **106**, 1753–1789, https://doi.org/10.1306/07062221120

Chiarella, D., Longhitano, S.G., Spalluto, L. and Martinius, A.W. 2025. Hierarchies of stratigraphic discontinuity surfaces in siliciclastic, carbonate and mixed siliciclastic-bioclastic tidalites: implications for fluid migration in reservoir quality assessment. *The Depositional Record*, **11**, 373–402, https://doi.org/10.1002/dep2.307

Colter, V.S. and Ebbern, J. 1978. The petrography and reservoir properties of some Triassic sandstones of the Northern Irish Sea Basin. *Journal of the Geological Society, London*, **135**, 57–62, https://doi.org/10.1144/gsjgs.135.1.0057

Cosgrove, G.I.E., Alkathery, M., Al-Masrahy, M., Colombera, L., Mountney, N.P. and Thompson, D.B. 2025. Quantitative sedimentological analysis of the aeolian–fluvial Triassic Sherwood Sandstone Group, Cheshire Basin, UK. *Sedimentology*, **72**, 1233–1274, https://doi.org/10.1111/sed.70000

Cowan, G. 1993. Identification and significance of aeolian deposits within the dominantly fluvial Sherwood Sandstone Group of the East Irish Sea Basin UK. *Geological Society, London, Special Publications*, **73**, 231–245, https://doi.org/10.1144/GSL.SP.1993.073.01.14

Cowan, G. and Boycott-Brown, T. 2003. The North Morecambe Field, Block 110/2a, East Irish Sea. *Geological Society, London, Memoirs*, **20**, 97–105, https://doi.org/10.1144/GSL.MEM.2003.020.01.08

Cowan, G., Burley, S.D. *et al.* 1999. Oil and gas migration in the Sherwood Sandstone of the East Irish Sea Basin. *Geological Society, London, Petroleum Geology Conference Series*, **5**, 1383–1398, https://doi.org/10.1144/0051383

Coward, M.P. 1995. Structural and tectonic setting of the Permo-Triassic basins of northwest Europe. *Geological Society, London, Special Publications*, **91**, 7–39, https://doi.org/10.1144/GSL.SP.1995.091.01.02

Curtis, C.D. and Coleman, M.L. 1985. Controls on the precipitation of early diagenetic calcite, dolomite and siderite concretions in complex depositional sequences. *SEPM Special Publications*, **38**, 23–33, https://doi.org/10.2110/pec.86.38.0023

Davies, S.J., Guion, P.D. and Gutteridge, P. 2012. Carboniferous sedimentation and volcanism on the Laurussian Margin. *In:* Woodcock, N. and Strachan, R. (eds) *Geological History of Britain and Ireland*, **2**. John Wiley & Sons, Ltd, Chichester, 231–273, https://doi.org/10.1002/9781118274064.ch14

Doughty, C. and Oldenburg, C.M. 2020. CO_2 plume evolution in a depleted natural gas reservoir: modeling of conformance uncertainty reduction over time. *International Journal of Greenhouse Gas Control*, **97**, 103026, https://doi.org/10.1016/j.ijggc.2020.103026

English, K.L., English, J.M., Moscardini, R., Haughton, P.D.W., Raine, R.J. and Cooper, M. 2024. Review of Triassic Sherwood Sandstone Group reservoirs of Ireland and Great Britain and their future role in geoenergy applications. *Geoenergy*, **2**, https://doi.org/10.1144/geoenergy2023-042

ENI UK Limited 2024. *Summary of Project Human Rights Risk Assessment: HyNet CO_2 Transport and Storage Company*. Eni UK Limited, London, https://www.eni.com/content/dam/enicom/documents/eng/actions/global-activities/united-kingdom/Liverpool-HRRA-Summary-Report.pdf

Facchi, G.L.D., Atena, R., Brignoli, M., Elgendy, A.M.S., Geloni, C., Di Lullo, A.G. and Baffi, S. 2021. Liverpool Bay Area CCS Project: integrated reservoir study for a successful CO2 storage planning. OMC Med Energy Conference and Exhibition, Ravenna, September. OMC-2021-241. OMC-2021-241.

Fairbridge, R.W. 1966. Diagenetic phases. *Bulletin of the American Association of Petroleum Geologists*, **50**, 612–613.

Fryberger, S.A., Hern, C.Y. and Jones, N. 2021. Modern and ancient analogues for complex eolian reservoirs. AAPG Datapages/Search and Discovery Article 51401, 7 August 7, https://www.searchanddiscovery.com/documents/2017/51401fryberger/ndx_fryberger.pdf

Garfi, G., John, C.M., Lin, Q., Berg, S. and Krevor, S. 2020. Fluid surface coverage showing the controls of rock mineralogy on the wetting state. *Geophysical Research Letters*, **47**, 1–9, https://doi.org/10.1029/2019GL086380

Gershenzon, N.I., Ritzi, R.W., Jr, Dominic, D.F., Mehnert, E. and Okwen, R.T. 2016. Comparison of CO_2 trapping in highly heterogeneous reservoirs with Brooks-Corey and van Genuchten type capillary pressure curves. *Advances in Water Resources*, **96**, 225–236, https://doi.org/10.1016/j.advwatres.2016.07.022

Ghanbari, S., Mackay, E.J., Heinemann, N., Alcalde, J., James, A. and Allen, M.J. 2020. Impact of CO_2 mixing with trapped hydrocarbons on CO_2 storage capacity and security: a case study from the Captain aquifer (North Sea). *Applied Energy*, **278**, 1–13, https://doi.org/10.1016/j.apenergy.2020.115634

Goggin, D.J., Chandler, M.A., Kocurek, G. and Lake, L.W. 1988. Patterns of permeability in eolian deposits: Page Sandstone (Jurassic), Northeastern Arizona. *SPE Formation Evaluation*, **3**, 297–306, https://doi.org/10.2118/14893-PA

Gray, J. 2013. *Petroleum Prospectivity of the Principal Sedimentary Basins on the United Kingdom Continental Shelf*. Department of Energy and Climate Change, London, https://assets.publishing.service.gov.uk/media/5a7dfb8b40f0b62302688671/UKCS_offshore_2013.pdf

Greenwood, P.J. and Habesch, S.M. 1997. Diagenesis of the Sherwood Sandstone Group in the southern East Irish Sea Basin (Blocks 110/13, 110/14 and 110/15): constraints from preliminary isotopic and fluid inclusion studies. *Geological Society, London, Special Publications*, **124**, 353–371, https://doi.org/10.1144/GSL.SP.1997.124.01.24

Griffiths, J., Faulkner, D.R., Edwards, A.P. and Worden, R.H. 2018. Deformation band development as a function of intrinsic host-rock properties in Triassic Sherwood Sandstone. *Geological Society, London, Special Publications*, **435**, 161–176, https://doi.org/10.1144/SP435.11

Griffiths, J., Worden, R.H., Wooldridge, L.J., Utley, J.E.P. and Duller, R.A. 2019. Compositional variation in modern estuarine sands; predicting major controls on sandstone reservoir quality. *AAPG Bulletin*, **103**, 797–833, https://doi.org/10.1306/09181818025

Hannis, S., Lu, J., Chadwick, A., Hovorka, S., Kirk, K., Romanak, K. and Pearce, J. 2017. CO_2 storage in depleted or depleting oil and gas fields: what can we learn from existing projects? *Energy Procedia*, **114**, 5680–5690, https://doi.org/10.1016/j.egypro.2017.03.1707

Hême de Lacotte, V.J.P. and Mountney, N.P. 2022. A classification scheme for sedimentary architectures arising from aeolian-fluvial system interactions: Permian examples from southeast Utah, USA. *Aeolian Research*, **58**, https://doi.org/10.1016/j.aeolia.2022.100815

Herries, R.D. and Cowan, G. 1997. Challenging the 'sheetflood' myth: the role of water-table-controlled sabkha deposits in redefining the depositional model for the Ormskirk Sandstone Formation (Lower Triassic), East Irish Sea Basin. *Geological Society, London, Special Publications*, **124**, 253–276, https://doi.org/10.1144/GSL.SP.1997.124.01.16

Hogg, A.J.C., Evans, I.J., Harrison, P.F., Meling, T., Smith, G.S., Thompson, S.D. and Watts, G.F.T. 1999. Reservoir management of the Wytch Farm Oil Field, Dorset, UK: providing options for growth into later field life. *Geological Society, London, Petroleum Geology Conference Series*, **5**, 1157–1172, https://doi.org/10.1144/0051157

Holford, S.P., Turner, J.P. and Green, P.F. 2005. Reconstructing the Mesozoic–Cenozoic exhumation history of the Irish Sea basin system using apatite fission track analysis and vitrinite reflectance data. *Geological Society, London, Petroleum Geology Conference Series*, **6**, 1095–1107, https://doi.org/10.1144/0061095

Downloaded from https://www.lyellcollection.org by Imperial College of Science, Technology and Medicine on Mar 27, 2026

Holford, S.P., Turner, J.P., Green, P.F. and Hillis, R.R. 2009. Signature of cryptic sedimentary basin inversion revealed by shale compaction data in the Irish Sea, western British Isles. *Tectonics (Washington, D.C.)*, **28**, TC4011, https://doi.org/10.1029/2008TC002359

Holliday, D.W., Holloway, S., McMillan, A.A., Jones, N.S., Warrington, G. and Akhurst, M.C. 2004. The evolution of the Carlisle Basin, NW England and SW Scotland. *Proceedings of the Yorkshire Geological Society*, **55**, 1–19, https://doi.org/10.1144/pygs.55.1.1

Hollinsworth, A.D., De Jonge-Anderson, I., Underhill, J.R. and Jamieson, R.J. 2024. Impact of reservoir quality on the carbon storage potential of the Bunter Sandstone Formation, southern North Sea. *Geoenergy*, **2**, https://doi.org/10.1144/geoenergy2023-037

Hossain, S., Hampson, J.H., Jacquemyn, C., Jackson, M.D. and Chiarella, D. 2024. Permeability characterisation of sedimentological facies in the Bunter Sandstone Formation, Endurance CO_2 storage site, offshore UK. *International Journal of Greenhouse Gas Control*, **135**, https://doi.org/10.1016/j.ijggc.2024.104140

Hounslow, M.W. and McIntosh, G. 2003. Magnetostratigraphy of the Sherwood Sandstone Group (Lower and Middle Triassic), south Devon, UK: detailed correlation of the marine and non-marine Anisian. *Palaeogeography, Palaeoclimatology, Palaeoecology*, **193**, 325–348, https://doi.org/10.1016/S0031-0182(03)00235-9

Hounslow, M.W. and Muttoni, G. 2010. The geomagnetic polarity timescale for the Triassic: linkage to stage boundary definitions. *Geological Society, London, Special Publications*, **334**, 61–102, https://doi.org/10.1144/SP334.4

Hounslow, M.W., McKie, T. and Ruffell, A.H. 2012. Permian to late Triassic post-orogenic collapse and rifting, arid deserts, evaporating seas and mass extinctions. *In:*Woodcock, N. and Strachan, R. (eds) *Geological History of Britain and Ireland*, **2**. John Wiley & Sons, Chichester, 299–321, https://doi.org/10.1002/9781118274064.ch16

Huggett, J.M. 2004. Sedimentary rocks. Clays and their diagenesis. *In:* Selley, R.C., Cocks, L.R. and Plimer, I. (eds) *Encyclopedia of Geology*. 2nd edn. Elsevier Ltd, 62–70, https://doi.org/10.1016/B0-12-369396-9/00311-7

Hummel, G. and Kocurek, G. 1984. Interdune areas of the back-island dune field, North Padre Island, Texas. *Sedimentary Geology*, **39**, 1–26, https://doi.org/10.1016/0037-0738(84)90022-8

IPCC 2005. *Special Report on Carbon Dioxide Capture and Storage*. IPCC, Cambridge, 431, https://www.ipcc.ch/site/assets/uploads/2018/03/srccs_wholereport-1.pdf

Jackson, D.I. 1995. *The Geology of the Irish Sea United Kingdom Offshore Regional Report*. British Geological Survey, London.

Jackson, S.J. and Krevor, S. 2020. Small-scale capillary heterogeneity linked to rapid plume migration during CO_2 storage. *Geophysical Research Letters*, **47**, https://doi.org/10.1029/2020GL088616

Jackson, D.I. and Mulholland, P. 1993. Tectonic and stratigraphic aspects of the East Irish Sea Basin and adjacent areas: contrasts in their post-Carboniferous structural styles. *Geological Society, London, Petroleum Geology Conference Series*, **4**, 791–808, https://doi.org/10.1144/0040791

Jackson, D.I., Mulholland, P., Jones, S.M. and Warrington, G. 1986. The geological framework of the East Irish Sea Basin. *In:*Brooks, J. and Glennie, K.W. (eds) Petroleum Geology of North West Europe: Proceedings of the 3rd Conference on Petroleum Geology of North West Europe, 1986, Barbican, London. Graham & Trotman, 191–203, https://www.researchgate.net/publication/297202748_The_geological_framework_of_the_East_Irish_Sea_Basin

Jackson, D.I., Johnson, H. and Smith, N.J.P. 1997. Stratigraphical relationships and a revised lithostratigraphical nomenclature for the Carboniferous, Permian and Triassic rocks of the offshore East Irish Sea Basin. *Geological Society, London, Special Publications*, **124**, 11–32, https://doi.org/10.1144/GSL.SP.1997.124.01.02

Jackson, W.A., Hampson, G.J. *et al.* 2022. A screening assessment of the impact of sedimentological heterogeneity on CO_2 migration and stratigraphic-baffling potential: Johansen and Cook formations, Northern Lights project, offshore Norway. *International Journal of Greenhouse Gas Control*, **120**, 103762, https://doi.org/10.1016/j.ijggc.2022.103762

Jacquemyn, C., Pataki, M.E.H. *et al.* 2021. Sketch-based interface and modelling of stratigraphy and structure in three dimensions. *Journal of the Geological Society, London*, **178**, https://doi.org/10.1144/jgs2020-187

Jones, N.S. and Ambrose, K. 1994. Triassic sandy braidplain and aeolian sedimentation in the Sherwood Sandstone Group of the Sellafield area, West Cumbria. *Proceedings of the Yorkshire Geological Society*, **50**, 61–76, https://doi.org/10.1144/pygs.50.1.61

Jones, A., Doyle, J., Jacobsen, T. and Kjønsvik, D. 1995. Which sub-seismic heterogeneities influence waterflood performance? A case study of a low net-to-gross fluvial reservoir. *Geological Society, London, Special Publications*, **84**, 5–18, https://doi.org/10.1144/GSL.SP.1995.084.01.02

Jordan, O.D. and Mountney, N.P. 2010. Styles of interaction between aeolian, fluvial and shallow marine environments in the Pennsylvanian to Permian lower Cutler beds, south-east Utah, USA. *Sedimentology*, **57**, 1357–1385, https://doi.org/10.1111/j.1365-3091.2010.01148.x

Jordan, D.W. and Pryor, W.A. 1992. Hierarchical levels of heterogeneity in a Mississippi River Meander Belt and application to reservoir systems: geologic note 1. *AAPG Bulletin*, **76**, 1601–1624, https://doi.org/10.1306/BDFF8A6A-1718-11D7-8645000102C1865D

Khandoozi, S., Hazlett, R. and Fustic, M. 2023. A critical review of CO_2 mineral trapping in sedimentary reservoirs – from theory to application: pertinent parameters, acceleration methods and evaluation workflow. *Earth-Science Reviews*, **244**, 104515, https://doi.org/10.1016/j.earscirev.2023.104515

Kim, K., Kim, D., Na, Y., Song, Y. and Wang, J. 2023. A review of carbon mineralization mechanism during geological CO_2 storage. *Heliyon*, **9**, e23135, https://doi.org/10.1016/j.heliyon.2023.e23135

Knipe, R.J., Cowan, G. and Balendran, V.S. 1993. The tectonic history of the East Irish Sea Basin with reference to the Morecambe Fields. *Geological Society, London, Petroleum Geology Conference Series*, **4**, 857–866, https://doi.org/10.1144/0040857

Kocurek, G. and Havholm, K.G. 1993. Eolian sequence stratigraphy – a conceptual framework. *AAPG Memoirs*, **58**, 393–410, https://doi.org/10.1306/M58581

Krevor, S.C.M., Pini, R., Li, B. and Benson, S.M. 2011. Capillary heterogeneity trapping of CO_2 in a sandstone rock at reservoir conditions. *Geophysical Research Letters*, **38**, https://doi.org/10.1029/2011GL048239

Krishnamurthy, P.G., DiCarlo, D. and Meckel, T. 2022. Geologic heterogeneity controls on trapping and migration of CO_2. *Geophysical Research Letters*, **49**, https://doi.org/10.1029/2022GL099104

Lasseter, T.J., Waggoner, J.R. and Lake, L.W. 1986. Reservoir heterogeneities and their influence on ultimate recovery. *In:* Lake, L.W. and Carroll, H.B. (eds) *Reservoir Characterization Technical Conference*. Academic Press, Orlando, 545–559.

Li, X. and Fan, X. 2015. Effect of CO_2 phase on contact angle in oil-wet and water-wet pores. *International Journal of Greenhouse Gas Control*, **36**, 106–113, https://doi.org/10.1016/j.ijggc.2015.02.017

Li, M., Guo, Y., Li, Z. and Wang, H. 2020. The diagenetic controls of the reservoir heterogeneity in the tight sand gas reservoirs of the Zizhou Area in China's east Ordos Basin: implications for reservoir quality predictions. *Marine and Petroleum Geology*, **112**, 104088, https://doi.org/10.1016/j.marpetgeo.2019.104088

Luo, J., Hou, Z., Feng, G., Liao, J., Haris, M. and Xiong, Y. 2022. Effect of reservoir heterogeneity on CO_2 flooding in tight oil reservoirs. *Energies (Basel)*, **15**, 3015, https://doi.org/10.3390/en15093015

Mange, M., Turner, P., Ince, D., Pugh, J. and Wright, D. 1999. A new perspective on the zonation and correlation of barren strata: an integrated heavy mineral and palaeomagnetic study of the Sherwood Sandstone Group, East Irish Sea Basin and surrounding areas. *Journal of Petroleum Geology*, **22**, 325–348, https://doi.org/10.1111/j.1747-5457.1999.tb00990.x

Marsh, J.R., Jones, S.J., Meadows, N.S. and Gluyas, J.G. 2022. Petrographic and diagenetic investigation of the distal Triassic 'Budleighensis' fluvial system in the Solway and Carlisle Basins for potential CO_2 storage. *Petroleum Geoscience*, **28**, https://doi.org/10.1144/petgeo2021-065

Massarweh, O. and Abushaikha, A.S. 2024. CO_2 sequestration in subsurface geological formations: a review of trapping mechanisms and monitoring techniques. *Earth-Science Reviews*, **253**, 104793, https://doi.org/10.1016/j.earscirev.2024.104793

Matter, A. and Ramseyer, K. 1985. Cathodoluminescence microscopy as a tool for provenance studies of sandstones. *In*: Zuffa, G.G. (ed.) *Provenance of Arenites*. NATO ASI Series, **148**. Springer, https://doi.org/10.1007/978-94-017-2809-6_9

McKie, T. and Williams, B.P.J. 2009. Triassic palaeogeography and fluvial dispersal across the northwest European basins. *Geological Journal*, **44**, 711–741, https://doi.org/10.1002/gj.1201

Meadows, N.S. 2006. The correlation and sequence architecture of the Ormskirk Sandstone Formation in the Triassic Sherwood Sandstone Group of the East Irish Sea Basin, NW England. *Geological Journal*, **41**, 93–122, https://doi.org/10.1002/gj.1034

Meadows, N.S. and Beach, A. 1993*a*. Controls on reservoir quality in the Triassic Sherwood Sandstone of the Irish Sea. *Geological Society, London, Petroleum Geology Conference Series*, **4**, 823–833, https://doi.org/10.1144/0040823

Meadows, N.S. and Beach, A. 1993*b*. Structural and climatic controls on facies distribution in a mixed fluvial and aeolian reservoir: the Triassic Sherwood Sandstone in the Irish Sea. *Geological Society, London, Special Publications*, **73**, 247–264, https://doi.org/10.1144/GSL.SP.1993.073.01.15

Medici, G., Boulesteix, K., Mountney, N.P., West, L.J. and Odling, N.E. 2015. Palaeoenvironment of braided fluvial systems in different tectonic realms of the Triassic Sherwood Sandstone Group, UK. *Sedimentary Geology*, **329**, 188–210, https://doi.org/10.1016/j.sedgeo.2015.09.012

Medici, G., West, L.J. and Mountney, N.P. 2016. Characterizing flow pathways in a sandstone aquifer: tectonic vs sedimentary heterogeneities. *Journal of Contaminant Hydrology*, **194**, 36–58, https://doi.org/10.1016/j.jconhyd.2016.09.008

Medici, G., West, L., Mountney, N.P. and Welch, M. 2019*a*. Permeability of rock discontinuities and faults in the Triassic Sherwood Sandstone Group (UK): insights for management of fluvio-aeolian aquifers worldwide. *Hydrogeology Journal*, **27**, 2835–2855, https://doi.org/10.1007/s10040-019-02035-7

Medici, G., West, L.J., Mountney, N.P. and Ruffell, A. 2019*b*. Sedimentary flow heterogeneities in the Triassic U.K. Sherwood Sandstone Group: insights for hydrocarbon exploration. *Geological Journal*, **54**, 1361–1378, https://doi.org/10.1002/gj.3233

Miall, A.D. 1988. Reservoir heterogeneities in fluvial sandstones; lessons from outcrop studies. *AAPG Bulletin*, **72**, 682–697, https://doi.org/10.1306/703C8F01-1707-11D7-8645000102C1865D

Downloaded from https://www.lyellcollection.org by Imperial College of Science, Technology and Medicine on Mar 27, 2026

Milroy, P., Wright, V.P., Simms, M.J. and Reijmer, J. 2019. Dryland continental mudstones: deciphering environmental changes in problematic mudstones from the Upper Triassic (Carnian to Norian) Mercia Mudstone Group, south-west Britain. *Sedimentology*, **66**, 2557–2589, https://doi.org/10.1111/sed.12626

Morad, S., Ketzer, J.M. and De Ros, L.F. 2000. Spatial and temporal distribution of diagenetic alterations in siliciclastic rocks: implications for mass transfer in sedimentary basins. *Sedimentology*, **47**, 95–120, https://doi.org/10.1046/j.1365-3091.2000.00007.x

Morad, S., Al-Ramadan, K., Ketzer, J.M. and De Ros, L.F. 2010. The impact of diagenesis on the heterogeneity of sandstone reservoirs: a review of the role of depositional fades and sequence stratigraphy. *AAPG Bulletin*, **94**, 1267–1309, https://doi.org/10.1306/04211009178

Morrow, N.R. 1971. Small-scale packing heterogeneities in porous sedimentary rocks. *AAPG Bulletin*, **55**, 514–522, https://doi.org/10.1306/5D25CF6F-16C1-11D7-8645000102C1865D

Morton, A., Hounslow, M.W. and Frei, D. 2013. Heavy-mineral, mineral-chemical and zircon-age constraints on the provenance of Triassic sandstones from the Devon coast, southern Britain. *Geologos*, **19**, 67–85, https://doi.org/10.2478/logos-2013-0005

Mountney, N.P. and Thompson, D.B. 2002. Stratigraphic evolution and preservation of aeolian dune and damp/wet interdune strata: an example from the Triassic Helsby Sandstone Formation, Cheshire Basin, UK. *Sedimentology*, **49**, 805–833, https://doi.org/10.1046/j.1365-3091.2002.00472.x

Needham, T. and Morgan, R. 1997. The East Irish Sea and adjacent basins; new faults or old? *Journal of the Geological Society, London*, **154**, 145–150, https://doi.org/10.1144/gsjgs.154.1.0145

Newell, A. 2006. Calcrete as a source of heterogeneity in Triassic fluvial sandstone aquifers (Otter Sandstone Formation, SW England). *Fluid Flow and Solute Movement in Sandstones: The Onshore UK Permo-Triassic Red Bed Sequence*. Geological Society, London, **263**, 119–127.

Newell, A. 2024. *UK Stratigraphical Framework Series: Mercia Mudstone Group*. British Geological Survey, Nottingham, UK, https://nora.nerc.ac.uk/id/eprint/539122/1/OR24046.pdf

Newell, A.J. and Shariatipour, S.M. 2016. Linking outcrop analogue with flow simulation to reduce uncertainty in sub-surface carbon capture and storage: an example from the Sherwood Sandstone Group of the Wessex Basin, UK. *Geological Society, London, Special Publications*, **436**, 231–246, https://doi.org/10.1144/SP436.2

Onoja, M.U. and Shariatipour, S.M. 2018. The impact of gradational contact at the reservoir-seal interface on geological CO_2 storage capacity and security. *International Journal of Greenhouse Gas Control*, **72**, 1–13, https://doi.org/10.1016/j.ijggc.2018.03.007

Onoja, M.U., Williams, J.D.O., Vosper, H. and Shariatipour, S.M. 2019. Effect of sedimentary heterogeneities in the sealing formation on predictive analysis of geological CO_2 storage. *International Journal of Greenhouse Gas Control*, **82**, 229–243, https://doi.org/10.1016/j.ijggc.2019.01.013

OPRED 2025. *HyNet Carbon Dioxide Transportation and Storage Project – Offshore: Regulation 14 EIA Decision Document*. UK Government, London, https://assets.publishing.service.gov.uk/media/6808dd020324470d6a394f00/ES_2022_009_Liverpool_Bay_CCS_Ltd._HYNET_Regulation_14_EIA_Decision_Document.pdf

Park, Y.-C., Kim, S., Lee, J.H. and Shinn, Y.J. 2019. Effect of reducing irreducible water saturation in a near-well region on CO_2 injectivity and storage capacity. *International Journal of Greenhouse Gas Control*, **86**, 134–145, https://doi.org/10.1016/j.ijggc.2019.04.014

Payton, R.L., Sun, Y., Chiarella, D. and Kingdon, A. 2022. Pore scale numerical modelling of geological carbon storage through mineral trapping using true pore geometries. *Transport in Porous Media*, **141**, 667–693, https://doi.org/10.1007/s11242-021-01741-9

Payton, R.L., Chiarella, D. and Kingdon, A. 2023. Using legacy core material to assess subsurface carbon storage reservoir potentiality. *Geological Society, London, Special Publications*, **527**, 387–397, https://doi.org/10.1144/SP527-2022-18

Peron, S., Bourquin, S., Fluteau, F. and Guillocheau, F. 2005. Paleoenvironment reconstructions and climate simulations of the Early Triassic; impact of the water and sediment supply on the preservation of fluvial systems. *Geodinamica Acta*, **18**, 431–446, https://doi.org/10.3166/ga.18.431-446

Pharaoh, T.C., Gent, C.M.A. *et al.* 2018. An overlooked play? Structure, stratigraphy and hydrocarbon prospectivity of the Carboniferous in the East Irish Sea–North Channel basin complex. *Geological Society, London, Special Publications*, **471**, 281–316, https://doi.org/10.1144/SP471.7

Prosser, D.J. and Maskall, R. 1993. Permeability variation within aeolian sandstone: a case study using core cut sub-parallel to slipface bedding, the Auk Field, Central North Sea, UK. *Geological Society, London, Special Publications*, **73**, 377–397, https://doi.org/10.1144/GSL.SP.1993.073.01.22

Quirk, D.G., Underhill, J.R., Gluyas, J.G., Howe, M.J., Wilson, H.A.M. and Anderson, S. 2022. A low-carbon future for The North Sea Basin. *Geological Society, London, Special Publications*, **494**, 197–213, https://doi.org/10.1144/SP494-2020-236

Ringrose, P.S., Furre, A.-K. *et al.* 2021. Storage of carbon dioxide in saline aquifers: physicochemical processes, key constraints, and scale-up potential. *Annual Review of Chemical and Biomolecular Engineering*, **12**, 471–494, https://doi.org/10.1146/annurev-chembioeng-093020-091447

Rivera, N.A., Ray, S., Jensen, J.L., Chan, A.K. and Ayers, W.B. 2004. Detection of cyclic patterns using wavelets: an example study in the Ormskirk Sandstone, Irish Sea. *Mathematical Geology*, **36**, 529–543, https://doi.org/10.1023/B:MATG.0000037735.34280.42

Rochelle, C.A., Pearce, J.M. and Holloway, S. 1999. The underground sequestration of carbon dioxide: containment by chemical reactions in the deep geosphere. *Geological Society, London, Special Publications*, **157**, 117–129, https://doi.org/10.1144/GSL.SP.1999.157.01.09

Rockström, J., Gupta, J. *et al.* 2023. Safe and just Earth system boundaries. *Nature*, **619**, https://doi.org/10.1038/s41586-023-06083-8

Rowley, E. and White, N. 1998. Inverse modelling of extension and denudation in the East Irish Sea and surrounding areas. *Earth and Planetary Science Letters*, **161**, 57–71, https://doi.org/10.1016/S0012-821X(98)00137-X

Rubin, D.M. and Hunter, R.E. 1982. Bedform climbing in theory and nature. *Sedimentology*, **29**, 121–138, https://doi.org/10.1111/j.1365-3091.1982.tb01714.x

Sayed Siamak Ashraf, T., Shohreh, F., Sayed Jalal, H. and Peyman, E. 2010. Comparative study of carbon dioxide and methane adsorption by synthesized fine particles of SAPO-34 molecular sieve. *Iranian Journal of Chemistry & Chemical Engineering*, **29**, 37–45, https://doi.org/10.30492/ijcce.2010.6511

Schmidt, V. and McDonald, D.A. 1979. *Secondary Reservoir Porosity in the Course of Sandstone Diagenesis*. AAPG, Tulsa, OK, https://doi.org/10.1306/CE12404

Scorgie, J.C., Worden, R.H., Utley, J.E.P. and Roche, I.P. 2021. Reservoir quality and diagenesis of Triassic sandstones and siltstones from arid fluvial and playa margin environments; a study of one of the UK's earliest producing oilfields. *Marine and Petroleum Geology*, **131**, 105–154, https://doi.org/10.1016/j.marpetgeo.2021.105154

Seedhouse, J.K. and Racey, A. 1997. Sealing capacity of the Mercia Mudstone Group in the East Irish Sea Basin: implications for petroleum exploration. *Journal of Petroleum Geology*, **20**, 261–286, https://doi.org/10.1111/j.1747-5457.1997.tb00636.x

Strong, G.E. 1993. Diagenesis of Triassic Sherwood Sandstone Group rocks, Preston, Lancashire, UK: a possible evaporitic cement precursor to secondary porosity? *Geological Society, London, Special Publications*, **73**, 279–289, https://doi.org/10.1144/GSL.SP.1993.073.01.17

Stuart, I.A. 1993. The geology of the North Morecambe Gas Field, East Irish Sea Basin. *Geological Society, London, Petroleum Geology Conference Series*, **4**, 883–895, https://doi.org/10.1144/0040883

Stuart, I.A. and Cowan, G. 1991. The South Morecambe Field, Blocks 110/2a, 110/3a, 110/8a, UK East Irish Sea. *Geological Society, London, Memoirs*, **14**, 527–541, https://doi.org/10.1144/GSL.MEM.1991.014.01.66

Swanson, S.K., Bahr, J.M., Bradbury, K.R. and Anderson, K.M. 2006. Evidence for preferential flow through sandstone aquifers in Southern Wisconsin. *Sedimentary Geology*, **184**, 331–342, https://doi.org/10.1016/j.sedgeo.2005.11.008

Taggart, S., Hampson, G.J. and Jackson, M.D. 2010. High-resolution stratigraphic architecture and lithological heterogeneity within marginal aeolian reservoir analogues. *Sedimentology*, **57**, 1246–1279.

Thomas, S., Corbett, P. and Jensen, J. 1996. Permeability and permeability anisotropy characterisation in the near wellbore: a numerical model using the probe permeameter and micro-resistivity image data. SPWLA 37th Annual Logging Symposium, 16–19 June 1996, New Orleans. One Petro, https://onepetro.org/SPWLAALS/proceedings-abstract/SPWLA-1996/SPWLA-1996/SPWLA-1996-JJJ/19559

Thompson, D.B. 1970. The stratigraphy of the so-called Keuper Sandstone Formation (Scythian–?Anisian) in the Permo–Triassic Cheshire Basin. *Quarterly Journal of the Geological Society, London*, **126**, 151–181, https://doi.org/10.1144/gsjgs.126.1.0151

Thompson, J. and Meadows, N.S. 1997. Clastic sabkhas and diachroneity at the top of the Sherwood Sandstone Group: East Irish Sea Basin. *Geological Society, London, Special Publications*, **124**, 237–251, ttps://doi.org/10.1144/GSL.SP.1997.124.01.15

Wakefield, O.J.W., Hough, E. and Peatfield, A.W. 2015. Architectural analysis of a Triassic fluvial system; the Sherwood Sandstone of the East Midlands Shelf, UK. *Sedimentary Geology*, **327**, 1–13, https://doi.org/10.1016/j.sedgeo.2015.07.006

Walderhaug, O. 1996. Kinetic modeling of quartz cementation and porosity loss in deeply buried sandstone reservoirs. *AAPG Bulletin*, **80**, 731–745.

Warr, L.N. 2012. *The Variscan Orogeny: The Welding of Pangaea*. John Wiley & Sons, Chichester, 274–298, https://doi.org/10.1002/9781118274064.ch15

Warrington, G., Audley-Charles, M.G. *et al.* 1980. *A Correlation of Triassic Rocks in the British Isles. Special Report; No. 13*. The Geological Society of London, London.

Weber, K.J. 1982. Influence of common sedimentary structures on fluid flow in reservoir models. *Journal of Petroleum Technology*, **34**, 665–672, https://doi.org/10.2118/9247-PA

Weber, K.J. 1986. How heterogeneity affects oil recovery. *In:* Lake, L.W. and Carroll, H.B. (eds) *Reservoir Characterization*. Academic Press, Orlando, 487–544, https://doi.org/10.1016/B978-0-12-434065-7.50021-6

Williams, J.D.O., Jin, M., Bentham, M., Pickup, G.E., Hannis, S.D. and Mackay, E.J. 2013. Modelling carbon dioxide storage within closed structures in the UK Bunter Sandstone Formation. *International Journal of Greenhouse Gas Control*, **18**, 38–50, https://doi.org/10.1016/j.ijggc.2013.06.015

Williams, J.D.O., Gent, C.M.A., Fellgett, M.W. and Gamboa, D. 2018. Impact of in situ stress and fault reactivation on seal integrity in the East Irish Sea Basin,

Downloaded from https://www.lyellcollection.org by Imperial College of Science, Technology and Medicine on Mar 27, 2026

UK. *Marine and Petroleum Geology*, **92**, 685–696, https://doi.org/10.1016/j.marpetgeo.2017.11.030

Wills, L.J. 1955. *Concealed Coalfields: A Palaeogeographical Study of the Stratigraphy and Tectonics of Mid-England in Relation to Coal Reserves*. Blackie, Glasgow.

Woodcock, N.H. 2012*a*. The Cambrian and earliest Ordovician Quiescent margin of Gondwana. *In:* Woodcock, N. and Strachan, R. (eds) *Geological History of Britain and Ireland*, **1**. John Wiley & Sons, Chichester, 150–161, https://doi.org/10.1002/9781118274064.ch9

Woodcock, N.H. 2012*b*. Late Ordovician to Silurian evolution of Eastern Avalonia during Iapetus Closure. *In:*Woodcock, N. and Strachan, R. (eds) *Geological History of Britain and Ireland*, **1**. John Wiley & Sons, Ltd, Chichester, UK, 177–191, https://doi.org/10.1002/9781118274064.ch11

Worden, R.H. 2024. Carbon dioxide capture and storage (CCS) in saline aquifers versus depleted gas fields. *Geosciences (Basel)*, **14**, 146, https://doi.org/10.3390/geosciences14060146

Worden, R.H. and Burley, S.D. 2003. Sandstone diagenesis: the evolution of sand to stone. *In:*Burley, S.D. and Worden, R.H. (eds) *Sandstone Diagenesis: Recent and Ancient*, **24**. John Wiley & Sons, Chichester, 1–44, https://doi.org/10.1002/9781444304459.ch

Worden, R.H., Oxtoby, N.H. and Smalley, P.C. 1998. Can oil emplacement prevent quartz cementation in sandstones? *Petroleum Geoscience*, **4**, 129–137, https://doi.org/10.1144/petgeo.4.2.129

Yaliz, A. and Chapman, T. 2003. The Lennox Oil and Gas Field, Block 110/15, East Irish Sea. *Geological Society, London, Memoirs*, **20**, 87–96, https://doi.org/10.1144/GSL.MEM.2003.020.01.07

Yaliz, A. and McKim, N. 2003. The Douglas Oil Fields, Block 110/13b, East Irish Sea. *Geological Society, London, Memoirs*, **20**, 61–75, https://doi.org/10.1144/GSL.MEM.2003.020.01.05

Yaliz, A. and Taylor, P. 2003. The Hamilton and Hamilton North Gas Fields, Block 110/13a, East Irish Sea. *Geological Society, London, Memoirs*, **20**, 77–86, https://doi.org/10.1144/GSL.MEM.2003.020.01.06

Yaliz, A., Chapman, T. and Downie, J. 2002. Case study of a quad-lateral horizontal well in the Lennox Field: a Triassic Oil-Rim Reservoir. SPE/DOE Improved Oil Recovery Symposium, 13–17 April 2002, Tulsa, 1091–1107, https://doi.org/10.2118/75249-MS

Yeste, L.M., Varela, A.N., Viseras, C., McDougall, N.D., García-García, F. and Bristow, C. 2020. Reservoir architecture and heterogeneity distribution in floodplain sandstones: key features in outcrop, core and wireline logs. *Sedimentology*, **67**, 3355–3388, https://doi.org/10.1111/sed.12747

Zhang, Q., Geiger, S. *et al.* 2025. Capillary pinning in sedimentary rocks for CO_2 storage: mechanisms, terminology and state-of-the-art. *International Journal of Greenhouse Gas Control*, **144**, 104385, https://doi.org/10.1016/j.ijggc.2025.104385

Ziegler, P.A. 1990. *Geological Atlas of Western and Central Europe*. Shell Internationale Petroleum Maatschappij and Geological Society, The Hague.